University of Trier

Department IV – Mathematics

Numerical Analysis

Numerical Modelling of the Human Menstrual Cycle applied to Ovulation Prediction

---

A thesis submitted to the faculty of mathematics of the University of Trier
in partial fulfillment of the requirements for the degree of
Master of Science in Applied Mathematics

Jo Andrea Brueggemann

Berlin, 9th of April 2013

Prof. Dr. Ekkehard Sachs
Department of Mathematics
University of Trier
D-54286 Trier

Dr. Susanna Röblitz
Konrad-Zuse-Zentrum für
Informationstechnik Berlin
D-14195 Berlin

Abstract

In this Master Thesis, the modelling process and the required biological background to adequately describe the hormonal dynamics of the human menstrual cycle are presented. The aim of this Master thesis project is to establish a mathematical routine that enables prediction of potentially fertile time windows.
A system of four parameter dependent ordinary differential equations coupled with two algebraic equations is built, accounting for the main kinetic drivers of the human menstrual cycle – basal body temperature, estradiol, progesterone, luteinizing and follicle stimulating hormone.

The key parameters are identified using a nonlinear least squares approach to match the model to individual data. Aiming to solve the optimality problem arising, the Newton and Gauss-Newton method are examined and their local convergence theory is outlined. By the nature of the application, a globalised Gauss-Newton method seems more convenient. An adaptive trust region approach to determine the step lengths is chosen, which together with an linearly-implicit Euler extrapolation for the given differential algebraic equation system makes parameter estimation possible.

The simulation results are discussed particularly in view of limitations and problems arising through the modelling approach.

Contents

1. Introduction

A major task in mathematical medicine and systems biology consists of the study of bio-chemical mechanisms happening in some real biological context. Aiming at building a fruitful fusion of biology, computer science, mathematics and engineering sciences, the human female body can tried to be assessed in the same complex way. Controlling reproduction, adjusting therapy treatments to the individual patient or the adequate prediction of fertile phases are only a few of the numerous features and possible applications of such a model.

The female menstrual cycle regulates the hormonal balance of follicular growth in the ovaries, such that after ovulation, reproduction is enabled.
The basic dynamics happening in the framework of the human menstrual cycle involve the pituitary and the ovaries. Controlled by the endocrine system, the menstrual cycle can be divided into follicular, ovulatory and luteal phases. Equivalently, one may refer to preovulatory, ovulatory and postovulatory phases (Weschler (2006), p. 373). Commonly, menstrual cycles are counted from the first day of bleeding, which will be adapted in the following.

Particularly, the dynamics during the preovulatory phase are mainly driven by rising levels of follicle stimulating hormone (FSH) and luteinizing hormone (LH). Both being produced by the anterior pituitary, LH and FSH are responsible for early-stage development of the follicles in the ovary. Competing for dominance, only one of all growing follicles will continue to mature and later contains the egg. The maturing process of the dominant follicle increases the level of estradiol, the main estrogen involved in the menstrual cycle (Adlercreutz/ Lehtinen/ Kairento (1980), p. 400).
Rising levels of estradiol concentration during the follicular phase suppress the production of LH. Close to maturity of the follicle, the response of luteinizing hormone (LH) to estradiol (E_2) reverses. When E_2 reaches a specific threshold, namely the preovulatory E_2 peak, estradiol starts to positively stimulate LH production. By the time LH surges to its peak, the egg continues to grow averagely for another $12-24$ hours until it reaches its maximum diameter. Once the egg has maximally matured, it is released from the ovary. Ovulation, often featured by the characteristic *Mittelschmerz* (i.e. mid cycle pain) at mid cycle, happens around 36 hours after the total E_2 peak and consequently around $12-24$ hours after LH peak, following Selgrade/ Schlosser (2000) (p. 875) and the World Health Organisation (1983).
The postovulatory or luteal phase begins with the growing of the corpus luteum, being the solid body formed in the ovary after an egg has been released at ovulation. The corpus luteum causes a significant rise in heat-producing steroid hormone progesterone (P_4), produced in the ovaries. Progesterone is mainly involved into the implantation processus of the released egg and support of early pregnancy, high P_4 concentrations in the endocrine system result in a surge of the woman's basal body temperature (BBT). BBT measures the lowest body temperature attained after rest and can keep rising until three days after ovulation (Weschler (2006), p. 361/362) before it drops again in case of non-pregnancy.
Progesterone levels are furthermore triggered by the pituitary hormones LH and FSH after ovulation, transforming the remainders of the dominant follicle into the corpus luteum. LH peak is assumed to last for $16-20$ hours at which time progesterone starts to rise (Johansson/ Wide (1969)). Once P_4 levels are high, LH and FSH are suppressed while BBT rises with a certain

delay compared to P_4. Quickly decreasing levels of LH and FSH result in the corpus luteum's atrophy, which itself monotonically increases P_4 concentration in the blood for a duration of around 14 days after ovulation. While high (plasma) P_4 concentration indicates the formation of the corpus luteum, P_4 concentration falls rapidly from plateau level at the onset of menstrual bleeding (Johansson (1969)). Effectively, withdrawal of P_4 triggers the beginning of the next cycle and hence menstruation.
Though cycle length may vary significantly from woman to woman (Carter/ Blight (1981), p. 744), Weschler (2006) notes that mostly follicular phases vary for every individual woman while luteal phase remains consistent over all cycles (p. 47/380).

Computerised fertility monitors have become widely available over the past decades which are per definition electronic devices enabling the woman to determine fertile and infertile periods of her menstrual cycle. Aiming at either pregnancy achievement or avoidance, most of the electronic devices on the market seem to work inefficient compared to standard Natural Family Planning (NFP) methods according to Freundl/ Godehardt/ Frank-Herrmann/ Koubenec/ Gnoth (2003).

The start-up company *Clue*, Berlin[1], intends to link a fertility monitor to a smart phone through an *App* which enables the woman to collect basal body temperature data and estradiol levels. The latter should be measurable through an assay utilizing saliva, which currently *Clue* and the *Fraunhofer Institute for Biomedical Engineering Potsdam-Golm* are developing.

The project crucial to this thesis is the development of a model implemented with an efficient algorithm such that increases in estrogen levels, specifically estradiol, and in basal body temperature can be detected and used for the prediction of potentially fertile periods.
The main idea is that in future, BBT and estradiol values will be made available through the *Clue App*. Emphasis should also be put on the fact that by the possibility to store BBT and estradiol values for numerous cycles over time on a web database, any prior information of an individual woman could be used to individualise and hence enhance prediction of fertile periods to support pregnancy achievement.

The final objective of this work is to propose a simplified, qualitative and adequate model for a very complex process taking place in the female body. The temporal and endocrinological characteristics of the human menstrual cycle are worked out in section 2. At the end of this section, a reduced model of four differential equations coupled with two algebraic equations is proposed.
The subsequent sections are directed by the outline about *Inverse problems in Systems Biology* given by Engl/Flamm/Kügler/ Lu /Müller/ Schuster (2009) (pp. 3–12). Developing a model by common guidelines to adequately mathematically describe a biological process measured by some experimental data (chapter 2), chapter 3 will provide the mathematical theory applicable for parameter estimation formulated as nonlinear least squares problem. The algorithmic approach to parameter identification is outlined in chapter 4, where the methods and algorithms used for simulation are described. Subsequently, simulation results are used to evaluate and validate the proposed model as far as possible in section 5. A conclusion critically reviewing the model and obtained results is given in section 6.

[1] Clue. Showing women when they can get pregnant, on their phone. (www.helloclue.com)

2. A Model for the Human Menstrual Cycle

The objective of the human menstrual cycle is basically the hormonal regulation of follicular growth and the maturation of the egg in the ovaries. Leading to ovulation around mid cycle, reproduction is enabled. If fertilisation does not happen during the woman's potentially fertile period, the beginning of the new cycle is induced.

Apart from cycle length and the different phases of the menstrual cycle, the endocrinological network and its complex dynamics need to be understood to accurately describe a woman's cycle.
The main drivers of hormonal regulation are identified as estradiol (E_2), progesterone (P_4), luteinizing hormone (LH) and follicle stimulating hormone (FSH). In the models of the human menstrual cycle presented by Reinecke/ Deuflhard (2006) and the GynCycle model from Röblitz/ Stötzel/ Deuflhard/ Jones/ Azulay/ van der Graaf/ Martin (2013) various other relevant hormones are included. For the current application these models seem to be either too complex or too general. The GynCycle model, consisting of 33 ODEs with 114 unknown parameters, includes the release of gonadotropin releasing hormone (GnRH). Its release controls by size and frequency FSH and LH concentration in the blood as well as the maturation process of the follicles. Reviewing the GynCycle model, difficulties arise when the model is to be matched to individualised data of one woman. Intra-woman variation in cycle length and hormone concentration levels could not be incorporated without loss a in the model's quality.
In view of the nature of the final application and the hereby available data, the GynCycle model has to be revised and reduced. BBT has to be included into the model, while the endocrinological dynamics have to be reduced to their core activity.

Since individual measurements are solely assumed to be available for E_2, gathered through a saliva assay, and basal body temperature, recorded through a clinical thermometer, these data are to be considered crucial to determine impending or passed ovulation. While the general interaction between those hormones is outlined in chapter 1, the focus now in chapter 2 is directed towards the key mechanisms of hormonal regulation the reduced model is expected to describe.

2.1. Endocrinological and Temporal Dynamics

Following WHO (1980), Royston (1991) and Collins (1985), the main ovarian and pituitary hormones of importance to determine the fertile period of the human menstrual cycle include (plasma) luteinizing hormone, estradiol and progesterone (Royston (1991), p. 222). If we now assume that LH and FSH are the relevant pituitary hormones, E_2 and P_4 are responsible for reproductive regulations and that BBT gives feedback of happening ovulation, the main endocrinological dynamics happen either in the ovaries or the pituitary.
Ovarian dynamics are driven by E_2 and P_4, which are released from the follicles into the blood. Experiencing a constant clearance rate, E_2 is mainly secreted by the preovulatory follicle while P_4 levels rise through release of the corpus luteum after ovulation (Collins (1985)).
In the pituitary, synthesis-release relationships happen at first place (Schlosser/ Selgrade

(2000) and Harris (2001)). Enzyme reactions can be considered as feedback effects. Distinguishing positive and negative feedback mechanisms, E_2 promotes rapid LH synthesis. In the same way, P_4 stimulates the release of LH if E_2 is in normal range, i.e. during follicular phase. Similarly, P_4 also has a positive feedback effect on the release of FSH as long as E_2 is in normal range (Selgrade/ Schlosser (2000), p. 874).
Due to the cyclic nature of hormonal regulation happening during the reproductive age of a woman, the positive feedback effects reverse under specific circumstances. Hence, P_4 inhibits synthesis of LH during the luteal phase. In the same way, E_2 has a negative feedback effect on the release of LH and FSH if E_2 concentration is beyond the normal range. Though, the response of LH to E_2 is reversed to positive feedback close to maturation of the egg.

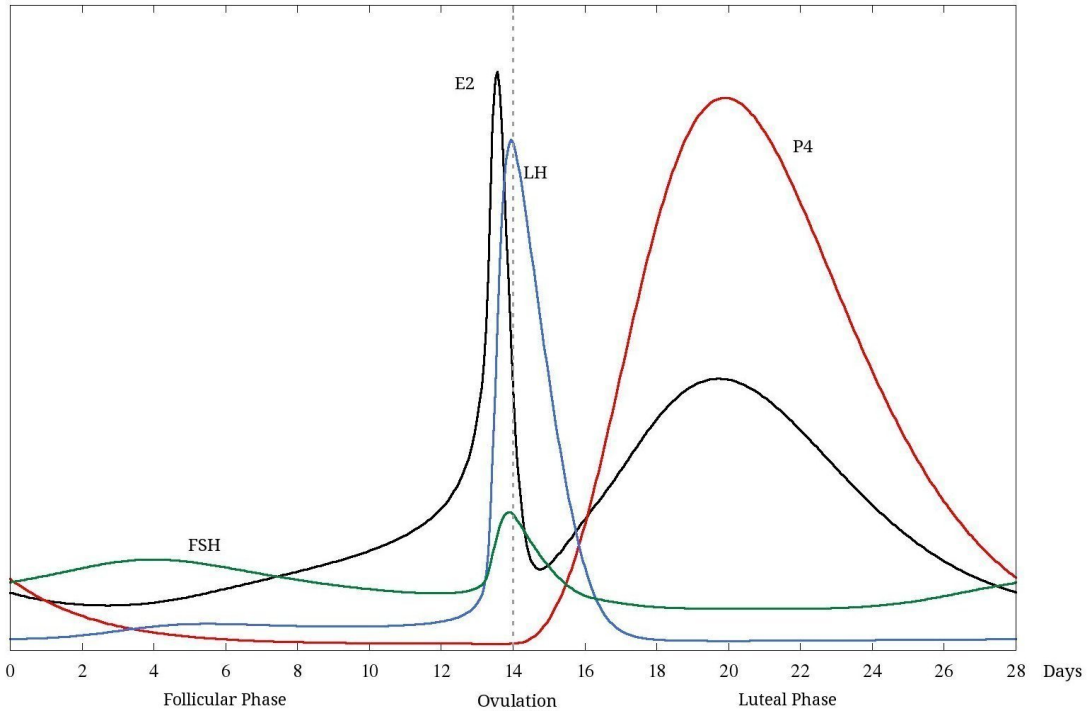

Figure 2.1.: The figure above displays the endocrine dynamics of E_2, P_4, LH and FSH for a 28 day cycle. Ovulation can be assumed to happen at day 14, the luteal phase starting then also. The important causality that should be picked up and reproduced in any model for the human menstrual cycle is basically the location and the delay within the components' peaks. Height and location may vary from woman to woman but also within cycles. Nevertheless, the basic dynamics and temporal relationships should form the fundamental of such a model. The underlying assumptions are stated and evidenced in the following, chapter 2.2 on p. 5 ff.

Shortly, the (scaled) temporal relationship of the endocrinological dynamics can be summarized as follows: E_2 reaches its preovulatory peak around 12 hours before the peak in LH. LH itself surges once E_2 is at its preovulatory peak. The LH peak can be considered the best indicator

for impending ovulation (see section 2.2, p. 5), occurring around 12-24 hours prior to ovulation. Consequently, E_2 reaches the peak 24-36 hours prior to the release of the egg. Once the ovum is released, postovulatory formation of the corpus luteum causes 16-20 hours after the peak in LH a significant increase in P_4 concentrations. Rapidly surging levels of P_4 induce a $0.2 - 0.5°C$ thermal shift in BBT. Usually, this thermal shift occurs around 24 hours after ovulation.
Hence, in mean, the peak in estrogen levels measured by E_2 is followed by ovulation after 24-26 hours which itself is followed by the BBT rise around 24 hours later.

2.2. Definition of the Potentially Fertile Period

Predicting human ovulation and detecting potentially fertile phases of the human menstrual cycle has been a central task within sciences after the 1980ies. Basically, the World Health Organization (1980) defines the probable fertile window of the menstrual cycle as days -3 to $+2$ with respect to the LH peak (day 0). The LH peak roughly occurs 24-28 hours prior to ovulation. In the following, the kind of data collection as well as assumptions crucial to predict the time of ovulation are tried to be clarified and justified. By the nature of the application, the model is expected to adequately describe not only the menstrual cycle with its characteristics but specifically potentially fertile periods. In the following, the basic temporal and hormonal dynamics are completed by a couple of assumptions that are expected to be represented in the proposed model.

First of all, a time window for the potentially fertile period of a woman's cycle needs to be defined. With estradiol, progesterone, LH and FSH being the main identified drivers for hormonal regulation of the human menstrual cycle, let us pick upon the interaction observable. If a tool either for managing fertile periods or for contraception embedded in a natural family planning (NFP) environment is to be developed, the main task is to provide an early warning of ovulation. The following assumptions are examined and supported by literature, and will guide to establish a best possible prediction-detection strategy for the precise time of ovulation.

Common fertility computers on the market use temperature as an indicator for ovulation.

Assumption 1: BBT is not an indicator for ovulation, but rather an indicator for the beginning of decreasing fertility.

Basically, after the rise in BBT the woman is still fertile for up to three days. Nevertheless, BBT is considered rather an indicator to afterwards detect than to beforehand predict the time of ovulation. Fertility is highest on the day of ovulation. Kerin (1982) states, that "knowledge of basal body temperature is not a prospective guide to ovulation, but once the thermal shift is established [...], the fertile period can be considered to have passed." (p. 27)
Clarifying the biochemical background around ovulation, Carter/ Blight (1981) describe that preovulatory estrogen concentration in blood remains on a constantly low level while in average, 3 days prior to ovulation, a gradual rise to a peak occurs. The increase in estrogens induces a surge of luteinizing hormone (LH) concentration to a peak which is followed by ovulation with a 12-24 hours delay. Ovulation happening, (plasma) progesterone (P_4) concentration surges while this jump induces an increase in BBT by averagely $0.2 - 0.5°$C. The statistical approach taken by Carter/ Blight (1981) is based on the Bayesian rule which enables to detect changes from constant mean values. Since both basal body temperature and estrogen levels undergo such a change at some point around ovulation, this method seems applicable to detect and predict potentially fertile periods in women. This is a sequential problem where mean levels, rate and magnitude of changes as well as change points might vary from woman to woman (p. 744). In

the end, an adequate idea is simply to use estradiol change point for prediction and the BBT change point for an *a posterior* detection of ovulation. In case, both estrogen and BBT change points could be detected (subject to sufficiently available pre- and post-ovulatory temperature values), these two events "bracket" ovulation and might be considered the mid-cycle fertile period according to Carter/ Blight (1981) (p. 750).

Assumption 2: Estradiol can be considered the most valuable predictor of ovulation of all estrogens in the human.

Adlercreutz/ Lehtinen/ Kairento (1980) found estrogens, and specifically estradiol (E_2) to be a valuable predictor of ovulation. In their studies performed, cycle lengths varied between 23 and 37 days (p. 395), while for each individual, the day with the highest LH excretion was followed by a significant increase in plasma progesterone (P_4). Data analysis of estrone (E_1), estrone-3-glucuronide ($E_1 - 3G$) and estradiol (E_2) revealed a slightly more pronounced increase of estradiol and also the smallest within-individual variation of mean basal values compared to E_1, $E_1 - 3G$ (p. 397).
Adlercreutz/ Lehtinen/ Kairento (1980) conclude in line with research of Baker/ Jennison/ Kellie (1979) that E_2 assays probably give best prediction of human ovulation by the highest mean ratio of peak-to-baseline values such that an earlier warning can be obtained if prediction is based on E_2 values.
Using time series, a statistical approach to detect increases in urinary estrogen levels by a *cum sum* procedure is presented by Blackwell/ Brown (1992). Analysing that in mean, ovulation occurs around 24 hours after serum LH peak and ca. 36 hours after the total estrogen peak, Brown/ Harrison/ Smith/ Burger (1981) measure a 12 hours shift between the estrogen and the LH peak. Though ovarian activity measurable through a rise in estrogen levels, i.e. among other E_2, does not necessarily need to be the beginning of potentially fertile periods, at the present time the first increase in urinary estrogens gives the best available hormonal indicator of "impending potential fertility" (p. 581 and World Health Organization (1983)). Schlosser/ Selgrade (2000) archived the LH peak during the normal mid-cycle as around $12 - 24$ hours subsequent to the peak in E_2 levels.

The core problem in using E_2 as a predictor for ovulation has been the clinical availability of the same. E_2 only being measurable through plasma, research on extracting hormonal values using saliva has been developing since the 1990ies. Recent outcomes of the *Fraunhofer Institute Potsdam-Golm* now make it possible to accurately collect E_2 values through saliva, which effectively established *Clue*'s business vision. E_2 plasma and saliva concentrations are assumed to be highly correlated.
Finally, estradiol values are assumed to give the best in-time-warning for ovulation. While E_2 data is assumed to be available within the *Clue* project, the precise time of ovulation is not identifiable neither by the peak in E_2 concentration nor by the peak in BBT alone. The potentially fertile window can hence only be considered as bracketed by those two peaks.

Assumption 3: The peak in LH concentration (in blood or urine) can be considered the best indirect indicator of impending ovulation.

The peak in LH is commonly considered the most reliable indicator for ovulation. Following Albrecht/ Fernando/ Regas/ Betz (1985), ovulation does not need to happen simultaneously to the peak in LH, but in the majority of cycles of normally menstruating women it is assumed to occur within at most 24 hours of the LH peak (p. 202).
Kerin (1982) states that the LH peak is the most clearly defined with a two to four fold increase

above baseline levels, happening in a relatively short 24 hours preovulatory phase. The temporary relationship can be summarised as follows: The first rise in LH concentration happens $28 - 36$ hours prior to ovulation. Once LH reached its peak concentration, it takes another 8-20 hours until ovulation. Royston (1991) and WHO (1980) give a more conservative estimation concerning the relationship of LH and the time point of ovulation. Surging $24 - 56$ hours prior to ovulation, they assume the LH peak to occur $8 - 40$ hours before ovulation. Still, by these authors *Assumption 3* is endorsed: "A common and convenient reference point for ovulation is the day of peak concentration of LH in blood or urine." (Royston (1991), p. 223)
Kerin (1982) notes furthermore that LH induces a "marked reduction" in estrogen production some 12 hours prior to ovulation while it induces at the same time a two to three fold increase in progesterone production about the baseline levels. Royston (1991) adds that E_2 is assumed to peak around 24 hours prior to ovulation (p. 223) while progesterone levels start to rise around the time of ovulation itself.

Assumption 4: If identifiable, the BBT nadir coincides with the surge in LH.

There exists evidence that the first surge in LH concentration coincides with a nadir in BBT. Morais/ Underwood/ Easterling (1976) analysed basal body temperature and serum luteinizing hormone for 27 normal human menstrual cycles and found rising LH levels to occur on the same day or within one day of the BBT nadir (81%). Similar results were obtained by Templeton (1982) who could show that for 39% of 51 observed cycles the preovulatory dip in BBT coincided with the surge in LH while it preceded or followed the surge in LH by more than 24 hours of 35% and 10% of the cycles reviewed. Also Nitschke-Dabelstein/ Hackelör/ Sturm (1980) could timely match the LH peak and the BBT nadir, while the first increase in BBT occurred the day when progesterone concentration reached $3.2ng/mL$. A more conservative result was formulated by Albrecht/ Fernando/ Regas/ Betz (1985), who linked BBT measurements to serum LH data for 18 cycles. The three days prior to LH peak BBT exhibited lower values than the baseline before it experienced a sharp increase on the first day after LH peak, rising for two more days (p. 203). They found the preovulatory dip in BBT rather to coincide with rising estrogen levels than with the LH peak itself. Nonetheless, BBT values were still at their nadir on the assumed day of LH peak (p. 203).

Assumption 5: Ovulation is followed by a rise in BBT of $0.2 - 0.5°C$ *with delay of at least 24 hours.*

Royston (1991) identifies the rise in BBT to be linked to the surge in progesterone levels, happening itself at the time of ovulation (p. 223). It is believed that a $0.2 - 0.5°$C elevated BBT above the preovulatory baseline is reached $24 - 92$ hours after ovulation (p. 223). The thermal shift of $0.2 - 0.5°$C from base level takes roughly three days, before temperature decreases again until after the onset of menstrual bleeding.

Consequently, we need to define the fertile window of a normally menstruating woman:

Assumption 6: The potentially fertile period of the human menstrual cycle ranges from -3 to +2 days around the LH peak.

By the definition of the World Health Organization (1980) the fertile period ranges from -3 to +2 days around the LH peak, where the dominant follicle reaches its maximum diameter (Freundl/ Godehardt/ Kern/ Frank-Herrmann/ Koubenec/ Gnoth (2003)). Collins (1989) supports these limits for the commencement of the fertile period on the ba-

sis that over 90% of the pregnancies happen during this time window.
Deposited sperm is usually considered to survive 3-5 days (Adlercreutz/ Lehtinen/ Kairento (1980), p. 400 and Brown/ Gronow (1985)) though the World Health Organization (1980) calculates with a maximum of 6 days and Blackwell/ Brown (1992) even assume a survival of 6-7 days for "very fertile couples" (p. 561).
As Adlercreutz/ Lehtinen/ Kairento (1980) point out, any contraception methods should predict the commencement of the fertile period at least 3 days prior to the LH peak. This would equivalently mean that ovulation, occurring 24-28 hours after the LH peak, needs to be predicted at least 5 days earlier – when estrogens and specifically E_2 have not yet started to increase significantly" (p. 400). Finally, they note that no practical methods predicting ovulation can ever be 100% safe since it cannot be known ad hoc if the assessed cycles are really fertile.
Contrary to the literature referred to above, *Clue* precisely aims at enabling women to be in charge of their fertility with the ultimate goal of supporting pregnancy opportunities – contraception purposes might be attacked at a later stage of their initiated project.
Blackwell/ Brown (1992) recommend to use a 95% instead of a 99% confidence interval if statistically approaching Natural Family Planning in the sense of contraception in order to reduce the probability of false indication of a fertile day as non-fertile. In our case, rather a non-conservative approach would be favourable that highlights the 3-4 days period around maximal fertility, i.e. ovulation (Royston (1991), p. 203/ 237 and Blackwell/ Brown (1992), p. 560).

The core drawback of the last insight is that LH is not user-friendly measurable. Building on the availability of BBT and E_2 data, we already ascertained that E_2 is a valuable predictor for ovulation. Nonetheless, identifying solely the E_2 peak might give a very short notice about impending ovulation. Due to the steep increase in E_2 concentration, the first remarkable rise in E_2 could give an earlier warning.

Assumption 7: The time span between the first increase in E_2 and its peak in mean amounts to 72 hours.

While Adlercreutz/ Lehtinen/ Kairento (1980) could identify a first rise in estradiol at day -6 and -5 relative to the peak day of LH for the majority of their subjects (p. 400), Blackwell/ Brown (1992) find by calculation of the Trigg's tracking signal the first rise in E_2 to statistically happen between day -6 and -4 (p. 589). Royston (1991) endorses the use of E_2 change points as indicator for the beginning fertile period, finding the E_2 concentration to first increase $2-7$ days prior to ovulation (p. 223). This range is also given by Collins (1985). In median, Collins determines a 83 hours interval between the first rise in E_2 and ovulation, which yields an averaged time span of around 60 hours between the first rise and the peak in E_2 if assuming ovulation to happen 24 hours subsequent to E_2 peak (p. 285).
Consequently, for the majority of the female population the detection of the first rise in estradiol would give a sufficiently early warning for impending ovulation, except for those, where Collins (1985) only identified a 48 hours delay of ovulation relative to the first rise of E_2. For all others, the time point of the first identifiable surge of E_2, i.e. its change point, is located around day -3 or earlier relative to the LH peak day.
By *Assumption 4, 5* and *7*, the *Assumption 6* can be modified towards:

Assumption 8: The potentially (most) fertile period of the human menstrual cycle starts with the first rise in E_2 concentrations and ends with the thermal shift in BBT.

Due to the availability of E_2 and BBT data within the *Clue* project, this modification seems reasonable to establish a fertility monitor. In the end, the idea is simply to use estradiol change-

point for prediction and the BBT change point for an *a posterior* detection of ovulation. As mentioned above, ovulation can be considered to be "bracket" by the change points of E_2 and BBT change points referring to CARTER/ BLIGHT (1981) (p. 750).
Existence of inter-woman and inter-cycle within-woman variation definitely represents a difficulty to individually and efficiently predict potentially fertile periods. Since so-called baseline levels constitute the reference points to detect changes, ROYSTON (1991) emphasizes the need to calculate new, individual baselines for each menstrual cycle. The following two assumptions regarding individual baseline levels of E_2 and BBT are based on his analysis (p. 225).

Assumption 9: E_2 levels are roughly stable during the first six days of a cycle.

Assumption 10: BBT is normally stable between day 3 and day 8 of the cycle, since it tends to decline from higher levels of the previous cycle until about the third day of the new cycle.

Another critical but crucial point in prediction of ovulation is the yet unknown length of the cycle. Throughout the following prediction process it is assumed that E_2 as well as BBT values have been collected for already three to four cycles. Due to inter-cycle variations, LIU/ GOLD/LASELY/ JOHNSON (2004) found that in most women a short cycle is followed by a longer cycle and vice versa (p. 139). The variations are mainly given through factors affecting the length of the follicular phase, like stress, sickness, etc. Though, it is known that the length of the luteal phase, starting with the day of ovulation until the onset menstrual bleeding, remains fixed with approximately 14 days for every woman in every cycle: "Increased cycle length is associated with delayed ovulation and increased follicular phase length, since luteal phases are self-limited to 14 days." (LIU/ GOLD/LASELY/ JOHNSON (2004), p. 139)
LIU/ GOLD/LASELY/ JOHNSON (2004) examined the effect of the length of the prior luteal phase on subsequent cycle lengths (p. 135). While cycle length could be negatively associated with age (> 35 years) because of shortening of the follicular phase (p. 137), greater variability in menstrual cycle lengths between women than within women could be demonstrated (p. 137). Patterns suggesting that short cycles are followed by longer cycles and vice versa (p. 139) gave an intra-woman correlation for cycle length of 0.51 between any adjacent pair of observation. Mean cycle length could be "significantly inversely associated" with the prior luteal phase (p. 137) with a correlation of -0.18 days. Thus, one can summarize:

Assumption 11: Luteal phase length remains constant at 14 *days even for inter-woman and inter-cycle within-woman variation of the (mean) menstrual cycle length.*

For absolute cycle length, it seems most reasonable to take the mean cycle length obtainable through the arithmetic average of the three previously collected cycles. In case this first estimate for the cycle length of the fourth cycle to be predicted is significantly higher than the minimum cycle length recorded, one should consider to further reduce the first estimate or even take the minimum cycle length. This approach seems very conservative, but matching historical data with the day to day measurements of the running cycle should induce a prolongation relative to the first estimate. Since viability of the proposed model cannot be judged ad hoc, it rather seems adequate to extend potentially fertile periods by some days than to completely miss the day of ovulation. Obviously, this consideration is again extremely dependent on the purpose of the model. To maintain a more general starting point, the arithmetic average will be adapted throughout considerations in subsection 2.4 and section 5 (p. 78 ff.).

2.3. A Model for the Human Menstrual Cycle

The whole modelling process is based on the assumption that reactions within the human body are driven by mass action kinetics. Dealing with a large kinetic network, under the general principle of mass action kinetics, a system of differential equations can be set up leading to an initial value problem. Changes over time, y', are assumed to be dependent on some parameter vector $x \in \mathbb{R}^n$. Aiming at developing a suitable model

$$y(t, x)$$

the task at hand reduces to quantify the unknown parameters $x \in \mathbb{R}^n$ by comparison of model values and measured data according to Dierkes/ Wade/ Nowak/ Röblitz (2011) (p. 5) for a proposed model.
In the Gaussian sense, this kind of parameter estimation also sometimes referred to as inverse problem leads to solving a nonlinear least square problem for the given initial value problem.

Former modelling of the human menstrual cycle incorporated either integro-differential or delay equations (Reinecke/ Deuflhard (2011)), but this was not found advantageous compared to modelling without delays. Feedback mechanisms play a major role within the modelling of the endocrine system of women and their menstrual cycle. Application of enzyme reaction kinetics renders modelling of positive feedback mechanisms possible through *Michaelis Menten* kinetics while negative feedbacks are represented by standard inhibitory enzymes mechanics (Segel (1975)). A common way to incorporate enzyme reaction kinetics in a model of ordinary differential equations is to use Hill functions (see for example Murray (2007)).

Definition 2.3.1. *The Hill function for stimulatory effects, i.e. positive feedback, is defined by*

$$H^+(X, Y, n_{Hill}) := \frac{\left(\frac{X}{Y}\right)^n_{Hill}}{1 + \left(\frac{X}{Y}\right)^n_{Hill}} \tag{2.3.1}$$

while inhibitory effects, i.e. negative feedback mechanisms, are modelled through

$$H^-(X, Y, n_{Hill}) := \frac{1}{1 + \left(\frac{X}{Y}\right)^n_{Hill}} \tag{2.3.2}$$

where $X \in \mathbb{R}^+ \cup \{0\}$ denotes the hormone concentration with the threshold value $Y \in \mathbb{R}^+$ with a positive or respectively, a negative feedback. n is the Hill coefficient and by definition of stimulating and inhibiting effects, it holds

$$H^+(X, Y, n_{Hill}) = 1 - H^-(X, Y, n_{Hill}). \tag{2.3.3}$$

Antecedently, four endocrinological components were identified as key drivers of the human menstrual cycle which are completed by basal body temperature. Disposing of E_2 and BBT data, it is straightforward to introduce a time dependency for these two components. P_4 closely interacting with E_2, also the steroid P_4 is modelled on a time continuous basis. The remaining two components, LH and FSH, directly and indirectly control the response of E_2 and its antagonist P_4. Since no individual data is collected in regard, it was decided upon modelling LH and FSH through standard curves which still adequately reflect the possibly happening dynamics in the woman's body.

The human menstrual cycle happens on a regular basis from puberty until menopause, meaning

that if pregnancy does not occur, menstrual bleeding initiates the next cycle. The gonadotropins LH and FSH are hence represented through periodic functions. These algebraic functions complete the system of differential equations to be constructed.

Denoting the constant base level of LH for the individual patient by p_1^{LH}, the peak in LH throughout the human menstrual cycle is reconstructed via an exponential function since LH displays exponential growth around midcycle.

$$LH(t) = p_1^{LH} + p_2^{LH} * \exp\left(-\left(p_3^{LH} \sin\left(\frac{\pi t}{p^{cyclelength}} + p_4^{LH}\right)\right)^2\right) \tag{2.3.4}$$

While the prefactor p_2^{LH} controls the height of the LH peak, the argument of the exponential term accounts for the periodicity of the LH peak on the one hand and its shape on the other hand. The square sinusoidal argument constitutes a periodic peak with period length p_4^{LH} days. The width of the LH peak is controlled by the prefactor p_3^{LH} while p_4^{LH} shifts the peak along the time axis to allow the LH peak to be happening during midycle.

FSH is also secreted by the anterior pituitary. Following the lines of LH, FSH is modelled through periodic peaks of a sinus curve as well. Contrary to LH solely exhibiting one single, steep peak prior to ovulation, the FSH peak is less pronounced. Happening around the same time as the LH peak, FSH concentration usually displays a wavelike development. The base level is followed by a small increase during menstrual bleeding and early follicular phase. With ceasing menstrual bleeding, also FSH decreases before experiencing a more pronounced peak simultaneously to the LH peak. While LH drops to its base level, FSH declines further before reaching the base level plateau during mid luteal phase. By its nature, the dominant FSH peak is modelled just as LH since they happen simultaneously during the human menstrual cycle.

$$\begin{aligned} FSH(t) = p_1^{FSH} + p_2^{FSH} * \exp\left(-\left(p_3^{FSH} \sin\left(\frac{\pi t}{p^{cyclelength}} + p_4^{FSH}\right)\right)^2\right) \\ + p_5^{FSH} * \sin\left(\frac{\pi t}{p^{cyclelength}} + p_6^{FSH}\right)^4 \end{aligned} \tag{2.3.5}$$

In the second part of the FSH function, a fourth power of the sinus function introduces the wavelike pattern described above. $p^{cyclelength}$ accounts again for the length of the cycle in days, while the sinusoidal movement is shaped through p_5^{FSH} in its oscillations' width and translation on the time axis through p_6^{FSH}.

During luteal phase, just after ovulation, the gonadotropins LH and FSH lead to transformation of the dominant follicle's remainings to corpus luteum. The corpus luteum produces P_4 which induces an increase in P_4 concentrations $12 - 16$ hours after the LH peak. While LH and FSH fall quickly over time by rising P_4 levels, the corpus luteum atrophies. Unless the egg is fertilised, withdrawal of progesterone happens and triggers the beginning of the next cycle. Usually extending over 14 days, this process gives a wide peak in P_4 over the base levels.
Since LH stimulates P_4, P_4 is represented through a double delayed reaction to the LH peak. A transformed delay differential equation involving a delay represented by a modified Lotka-Volterra equation was chosen. Continuous delay differential equations can be sometimes rewritten as a system of ordinary differential equations without an explicit delay τ. Substituting the chosen delay of the delay differential equation, partial integration gives the corresponding system of

ordinary differential equations. This system then consists of one differential equation that models the dynamics of the delay and one differential equation, describing the desired behaviour of P_4. The modification of a Lotka-Volterra equation seems adequate to model the delay in this system, since over time predator prey models depicture a sinusoidal oscillation with a delay between the prey and the predator. If LH is considered as prey with a peak before ovulation, P_4 will react with a slightly less pronounced peak at some time point later.
The delay for the peak in P_4 relative to the LH peak can be obtained through

$$P4d'(t) = p_1^{P4} * H^-(P4d(t), p_3^{P_4}, p_4^{P4}) * LH(t) * P4d(t) - p_2^{P4} * H^+(P4d(t), p_5^{P4}, p_4^{P4})$$

where the stimulating Hill function

$$H^+(P4d(t), p_3^{P4}, p_4^{P4}) = \frac{\left(\frac{P4d(t)}{p_3^{P4}}\right)^{p_4^{P4}}}{1 + \left(\frac{P4d(t)}{p_3^{P4}}\right)^{p_4^{P4}}}$$

stands instead of $P4d(t)$ itself, modifying the Lotka-Volterra equation. The incorporation of this stimulating effect could be found advantageous for the model's purpose. In order to enable variations within the cycle length, the inhibitory effect in the first part of the progesterone delay

$$H^-(P4d(t), p_3^{P_4}, p_4^{P4}) = \frac{1}{1 + \left(\frac{P4d(t)}{p_3^{P4}}\right)^{p_4^{P4}}}$$

needed to be incorporated. Hence, the delay for the progesterone profile writes

$$P4d'(t) = p_1^{P4} * \frac{1}{1 + \left(\frac{P4d(t)}{p_3^{P4}}\right)^{p_4^{P4}}} * LH(t) * P4d(t) - p_2^{P4} * \frac{\left(\frac{P4d(t)}{p_5^{P4}}\right)^{p_4^{P4}}}{1 + \left(\frac{P4d(t)}{p_5^{P4}}\right)^{p_4^{P4}}}.$$

The P_4 profile can be simply obtained through

$$P4'(t) = p_6^{P4} * P4d(t) - p_7^{P4} * P4(t)$$

where $P4d(t)$ is the delay of Lotka-Volterra type. Consequently, by this system of ordinary differential equations

$$P4d'(t) = p_1^{P4} * \frac{1}{1 + \left(\frac{P4d(t)}{p_3^{P4}}\right)^{p_4^{P4}}} * LH(t) * P4d(t) - p_2^{P4} * \frac{\left(\frac{P4d(t)}{p_5^{P4}}\right)^{p_4^{P4}}}{1 + \left(\frac{P4d(t)}{p_5^{P4}}\right)^{p_4^{P4}}} \tag{2.3.6}$$

$$P4'(t) = p_6^{P4} * P4d(t) - p_7^{P4} * P4(t) \tag{2.3.7}$$

the full dynamics of P_4 are taken into account.

During luteal phase, increasing levels of the warmth steroid P_4 induce a thermal shift of about $0.2 - 0.5°C$. Coming from the modelling of P_4, a modification of a predator prey equation seems applicable for BBT also, since there is a certain time gap between the peak in P_4 and the thermal

shift in BBT. A positive Hill function

$$H^+((BBT(t)-35.00), p_3^{BBT}, p_4^{BBT}) = \frac{\left(\frac{(BBT(t)-35.00)}{p_3^{BBT}}\right)^{p_4^{BBT}}}{1+\left(\frac{(BBT(t)-35.00)}{p_3^{BBT}}\right)^{p_4^{BBT}}}$$

is used to describe the BBT's sharp rise and and slow decrease to base levels. BBT commonly takes until the next menstrual bleeding to be back at its base level. Using this Hill function required scaling of BBT, where a minimum BBT of $35.00°C$ was assumed.

$$\begin{aligned} BBT'(t) &= p_1^{BBT} * P4(t) * (BBT(t)-35.00) \\ &\quad - p_2^{BBT} * (BBT(t)-35.00) * \frac{\left(\frac{(BBT(t)-35.00)}{p_3^{BBT}}\right)^{p_4^{BBT}}}{1+\left(\frac{(BBT(t)-35.00)}{p_3^{BBT}}\right)^{p_4^{BBT}}} \end{aligned} \tag{2.3.8}$$

E_2 displays two peaks, the first one being really steep and pronounced, the second showing less altitude but slower increase and decrease. P_4, FSH and E_2 itself stimulate E_2 and E_2 is inhibited by LH.

$$\begin{aligned} E2'(t) &= p_1^{E2} * H^-(FSH(t), p_5^{E2}, p_6^{E2}) - p_3^{E2} * E2(t) * H^+(LH(t), p_7^{E2}, p_8^{E2}) \\ &\quad + p_2^{E2} * H^+(E_2(t), p_9^{E2}, p_{10}^{E2}) - p_4^{E2} * E2(t) * H^+(P4(t), p_{11}^{E2}, p_{12}^{E2}). \end{aligned} \tag{2.3.9}$$

By this differential equation, FSH stimulates E_2 until E_2 reaches a certain threshold in the middle of the base and the peak level. E_2 is self-stimulating, while high levels of LH lead to clearance of E_2. Though P_4 induces a withdrawal of E_2 in this differential equation, this does not affect the model in a negative way: The threshold value p_{11}^{E2} for the Hill function is very small in comparison to the P_4 level. Hence, rather a clearance rate independent from E_2 and P_4 than an inhibitory effect can be observed, while the Hill function prevents $E2(t)$ to get smaller than zero. $P4d(t)$ can theoretically get negative, as it models the delay in P_4.

Hence, by these differential equations, a system of four ordinary differential equations

$$\begin{aligned} E2'(t) &= p_1^{E2} * H^-(FSH(t), p_5^{E2}, p_6^{E2}) - p_3^{E2} * E2(t) * H^+(LH(t), p_7^{E2}, p_8^{E2}) \\ &\quad + p_2^{E2} * H^+(E_2(t), p_9^{E2}, p_{10}^{E2}) - p_4^{E2} * E2(t) * H^+(P4(t), p_{11}^{E2}, p_{12}^{E2}) \\ P4'(t) &= p_6^{P4} * P4d(t) - p_7^{P4} * P4(t) \\ BBT'(t) &= p_1^{BBT} * P4(t) * (BBT(t)-35.00) \\ &\quad - p_2^{BBT} * (BBT(t)-35.00) * H^+((BBT(t)-35.00), p_3^{BBT}, p_4^{BBT}) \\ P4d'(t) &= p_1^{P4} * H^-(P4d(t), p_3^{P4}, p_4^{P4}) * LH(t) * P4d(t) - p_2^{P4} * H^+(P4d(t), p_5^{P4}, p_4^{P4}) \end{aligned}$$

and two algebraic functions

$$LH(t) = p_1^{LH} + p_2^{LH} * \exp\left(-\left(p_3^{LH}\sin\left(\frac{\pi t}{p^{cyclelength}} + p_4^{LH}\right)\right)^2\right)$$

$$FSH(t) = p_1^{FSH} + p_2^{FSH} * \exp\left(-\left(p_3^{FSH}\sin\left(\frac{\pi t}{p^{cyclelength}} + p_4^{FSH}\right)\right)^2\right) + p_5^{FSH} * \sin\left(\frac{\pi t}{p^{cyclelength}} + p_6^{FSH}\right)^4.$$

is constructed.

This model will be estimated, validated and evaluated in section 4.

2.4. Ovulation Prediction for the Individual

Now, provided that basal body temperature data is available and saliva estradiol values give the best in-time-warning for ovulation, the model constructed previously is hoped to accurately describe the dynamics happening during the whole menstrual cycle in human women.

The parameter identification problem to validate the proposed model is approached in section 4 and 5, after laying a theoretical background to solving inverse problems by nonlinear least squares calculus.
Nevertheless, by the model's application purpose there is need to define not only the potentially fertile window (see 2.2) but also to determine an appropriate strategy to early predict ovulation. It suggests by itself not to try a purely statistical approach to predict ovulation, but to make use of the model's specific properties. While Carter/ Blight (1981) stick to a Bayesian procedure and Blackwell/ Brown (1992) analyse collected time series, the idea now is to adopt Carter/ Blight's (1981) Ansatz to obtain an *a priori* estimator for ovulation through a change point in E_2 concentration which is to be completed by an *a posteriori* detection of the rise in basal body temperature (BBT).
As Royston (1991) points out, "by its nature, a peak can only be found retrospectively" (p. 227). An simple and intuitively appealing procedure is to define a peak as a value that is proceeded by increasing or just lower values and followed by a sequence of decreasing or just lower values (Royston (1991), p. 227).

Dealing with a system of ordinary differential equations completed with two algebraic equations, the approach to be taken aims at early identifying climbing E_2 and BBT values through an adaptive step length control of the integrator.
As it will be outlined in the two subsequent chapters, an adaptive trust region Gauss-Newton algorithm combined with a linearly-implicit Euler extrapolation routine is applied to the proposed model. Through the linearly-implicit Euler discretisation implemented in the Limex code of *Konrad-Zuse Zentrum für Informationstechnik Berlin*, adaptive step size and error control information can be extracted. Monitoring the latter can give hints on slope development and changes in the to given E_2 and BBT data fitted curves. Once the change points within measured and collected E_2 and BBT values have been identified through the steepest uphill slope (gradient) for any individual data set, the objective is to individualise the general model describing the dynamics of the human menstrual cycle. Since not only cycle length, but also mean levels, rate and magnitude of changes as well as change points in E_2 concentrations and basal body

temperature differ significantly from woman to woman, it would be desirable to include former collected E_2 and BBT measurements for further predictions. This would require (time) dynamic or step by step parametrisation.

For a test data set of four cycles, the model will be tested in chapter 5. If the model gives a satisfactory fit to the real data, the change points are tried to be identified for a standard cycle of 28 days.. The fertile window is then defined as in *Assumption 7* of section 2.2. Since cycle lengths are known for the test data, another estimate for the time point of ovulation could be given by subtracting the length of the luteal phase of 14 days from the total cycle length (*Assumption 11*). A critical review of those results should be carried out in order to obtain a first idea about the viability of the model for the purpose of ovulation prediction.
Simulation results, the parameter estimation and the model are further discussed in section 5 with respect to the task to individually predict ovulation. Mathematical background and algorithmic tools essential to evaluate the proposed model are presented in section 3 and 4.

3. Nonlinear Least Squares Problems

3.1. Motivation and Overview

One of the most common problems in computational sciences and mathematical modelling is to fit a system of measurement points to a conjectured model containing unidentified parameters such that a best possible match is obtained. Let us denote the data points measured for up to d species by

$$(t_i, z_i), \quad \text{for } t_i \in \mathbb{R}, z_i \in \mathbb{R}^d, i = 1, \ldots, M,$$

which are to be fitted to a d-dimensional model

$$y(t, x)$$

nonlinear with respect to the vector of parameter values

$$x \in \mathbb{R}^n.$$

Note, that in real applications, one usually has to deal with overdetermined systems where a perfect match of model and data is compromised by deficiencies of the model or in data measurement. Since model and given data are required to agree, let us define the residuals

$$F_i(x) = y(t_i, x) - z_i$$

for all $i = 1, \ldots, M$, $F_i(x) \in \mathbb{R}^d$ and hence the residual function $F : D \subseteq \mathbb{R}^n \to \mathbb{R}^m$ by

$$F(x) = (F_1(x), \ldots, F_M(x))^T$$

which is element of $\mathbb{R}^m$ if it is defined $m := Md$. In the following, F is assumed to be twice continuously differentiable or once continuously differentiable while satisfying some Lipschitz continuity in the first derivative. Restricting to the overdetermined case, let $m > n$ and let

$$D \subseteq \mathbb{R}^n$$

be an open and convex subset, while F is nonlinear with respect to $x \in D$.
The parameter identification problem presented above is commonly defined as a minimisation task in the Gaussian nonlinear least squares sense. Sufficient minimum conditions in paragraph 3.2 give that the local zeros of the residual function have to be determined. Since the standard approach to this task is by the Newton method, the latter will be examined with respect to local convergence behaviour and affine invariance theory (see 3.3) in the first part of the current section (see 3.4).

Nevertheless, the Newton method seems not to be adequate for the given application as pointed out in paragraphs 3.2 and 3.5. Under naturally arising further assumptions, the Gauss-Newton method is derived. Local convergence features as well as affine invariance are illustrated in paragraph 3.5.

This chapter presents the theoretical background for the application at hand, where parameter identification forms the core part. The algorithmic approach to estimate parameters by a nonlinear least squares problem is treated in the subsequent, chapter 4.

3.2. The Nonlinear Least Squares Problem

In a logical consequence, the above motivation about finding the closest fit as possible to some data can be considered as a special case to a general minimisation problem in respect to the sum of the residual squares.

Definition 3.2.1. *Given a function $F : D \subseteq \mathbb{R}^n \to \mathbb{R}^m$ nonlinear with respect to $x \in D$, we aim at finding a minimiser $x_* \in D$ such that*

$$\min_{x \in D} \|F(x)\|_2^2 = \|F(x_*)\|_2^2. \tag{3.2.1}$$

As often arising in natural problems, it is assumed to hold $Md > m > n$. So to speak, we aim at finding a interior, local minimizer $x_* \in D$ for the overdetermined problem such that

$$\min_{x \in D} \|F(x)\|_2^2 = \|F(x_*)\|_2^2.$$

This minimisation problem can be attacked by minimising the sum of n nonlinear equations

$$\min_{x \in D} \frac{1}{2} F(x)^T F(x) = \frac{1}{2} \sum_{i=1}^{M} F_i(x)^2.$$

due to the relation $\|F(x)\|_2^2 = F(x)^T F(x)$, while the factor $\frac{1}{2}$ is added for algebraic convenience when considering derivatives. Denoting the first derivative matrix of $F : D \subseteq \mathbb{R}^n \to \mathbb{R}^m$ by the Jacobian matrix $F'(x) \in \mathbb{R}^{m,n}$ where

$$F'(x) = \left(\frac{\partial}{\partial x_j} F(x) \right)_{j=1,\dots,n} = \begin{pmatrix} \nabla F_1^T(x) \\ \vdots \\ \nabla F_M^T(x) \end{pmatrix} = \begin{pmatrix} \frac{\partial F_1(x)}{\partial x_1} & \dots & \frac{\partial F_1(x)}{\partial x_n} \\ \vdots & \ddots & \vdots \\ \frac{\partial F_M(x)}{\partial x_1} & \dots & \frac{\partial F_M(x)}{\partial x_n} \end{pmatrix}$$

with the standard notation of the gradient,

$$\nabla F_i(x) = \left(\frac{\partial}{\partial x_1} F_i(x), \dots, \frac{\partial}{\partial x_n} F_i(x) \right)^T,$$

for $x \in \mathbb{R}^n$, $F_i : D \subseteq \mathbb{R}^n \to \mathbb{R}^d$, $F_i \in C^1(D)$ for $D \subseteq \mathbb{R}^n$ open and convex. Then the first derivative of

$$\frac{1}{2} F(x)^T F(x)$$

can be obtained by column wise differentiation for $F_i \in \mathbb{R}^d$

$$\begin{aligned}\frac{\partial}{\partial x_j}\left(\frac{1}{2}F_i(x)^T F_i(x)\right) &= \frac{\partial}{\partial x_j}\left(\frac{1}{2}\sum_{k=1}^{d} F_i^k(x)^2\right)\\ &= \frac{1}{2}\sum_{k=1}^{d}\frac{\partial}{\partial x_j}F_i^k(x)^2\\ &= \frac{1}{2}\sum_{k=1}^{d} 2(F_i'(x))_{kj}F_i^k(x)\\ &= (F_i'(x)^T F_i(x))_j\end{aligned}$$

such that it holds

$$\left(\frac{1}{2}F(x)^T F(x)\right)' = \left(\frac{\partial}{\partial x_j}\left(\frac{1}{2}F(x)^T F(x)\right)\right)_{j=1,\dots,n} = F'(x)^T F(x). \tag{3.2.2}$$

Component wise differentiation

(3.2.3)

$$\begin{aligned}&\left(\frac{1}{2}F_i(x)^T F_i(x)\right)''\\ &= \left(\frac{1}{2}\frac{\partial^2}{\partial x_j \partial x_l}F_i(x)^T F_i(x)\right)_{j,l=1,\dots,n}\\ &= \left(\left(\frac{\partial}{\partial x_j}F_i'(x)^T F_i(x)\right)_l\right)_{j,l=1,\dots,n}\\ &= \left(\frac{\partial}{\partial x_j}\sum_{k=1}^{d} F_i^k(x)\frac{\partial}{\partial x_l}F_i^k(x)\right)_{j,l=1,\dots,n}\\ &= \sum_{k=1}^{d}\left(\left(\frac{\partial}{\partial x_j}F_i^k(x)\right)_{j=1,\dots,n}\left(\frac{\partial}{\partial x_l}F_i^k(x)\right)^T_{l=1,\dots,n} + F_i^k(x)\left(\frac{\partial^2}{\partial x_j \partial x_l}(F_i^k(x))\right)_{j,l=1,\dots,n}\right)\\ &= \sum_{k=1}^{d}\left(\frac{\partial}{\partial x_j}F_i^k(x)\right)_{j=1,\dots,n}\left(\frac{\partial}{\partial x_l}F_i^k(x)\right)^T_{l=1,\dots,n} + \sum_{k=1}^{d} F_i^k(x)\left(\frac{\partial^2}{\partial x_j \partial x_l}(F_i^k(x))\right)_{l,j=1,\dots,n}\end{aligned}$$

yields the second derivative

$$\left(\frac{1}{2}F(x)^T F(x)\right)'' = F'(x)^T F'(x) + F''(x)^T F(x). \tag{3.2.4}$$

Now, let us define a local minimum as in Dennis/ Schnabel (1983) (p. 81) for single variable calculus:

Definition 3.2.2. *For $f : D \subseteq \mathbb{R}^n \to \mathbb{R}$ we call x_* a local minimum of f if there exists an open and convex neighbourhood $B(x_*, \rho) \subseteq \mathbb{R}^n$ such that*

$$f(x_*) \leq f(x) \tag{3.2.5}$$

for all $x \in B(x_*, \rho)$. *If* $B(x_*, \rho) = \mathbb{R}^n$, x_* *is called a global minimum.*

Definition 3.2.3. *If* $f \in \mathcal{C}^1(D)$ *and* $\nabla f(x_*) = 0$, $x_* \in D$ *is called a stationary point.*

Summarising, first and second order necessary conditions are listed in the following, whose proofs can be found in FORSTER (2006) and GEIGER/ KANZOW (2002).

Proposition 3.2.4. ***First order necessary optimality condition***
Let $f : D \subseteq \mathbb{R}^n \to \mathbb{R}$ *be continuously differentiable on the open subset* $D \subseteq \mathbb{R}^n$. *If* x_* *is a local minimum of* f *on* D, *it holds for the gradient*

$$f'(x_*) = 0.$$

Second order necessary optimality condition
If x_* *is a local minimum of the twice continuous differentiable mapping* $f : D \subseteq \mathbb{R}^n \to \mathbb{R}$ *on the open subset* $D \subseteq \mathbb{R}^n$, *then it holds for the Hessian*

$$f''(x_*) \leq 0.$$

The first order necessary optimality condition gives that every local minimum is a critical point, specifically a stationary point.

Proposition 3.2.5. *Let* $f : D \subseteq \mathbb{R}^n \to \mathbb{R}$ *be continuously differentiable. Then, if* x_* *is a local minimum, it is also a stationary point.*

Proof of 3.2.5. Let us assume, the descent direction does not vanish at x_*, i.e.

$$-\nabla f(x_*) \neq 0.$$

Then, Taylor expansion gives for arbitrarily small $\epsilon \to 0$ that

$$f(x_* - \epsilon \nabla f(x_*)) = f(x_*) - \epsilon \nabla f(x_*)^T \nabla f(x_*) + o(\epsilon^2).$$

Hence, for sufficiently small $\epsilon > 0$ it holds

$$f(x_* - \epsilon \nabla f(x_*)) < f(x_*)$$

and this contradicts with the assumption, that x_* is a local minimum. □

In order to guarantee that every stationary point is in effect a local minimum, further requirements concerning the Hessian need to be fulfilled. This gives the second order sufficient minimum condition.

Proposition 3.2.6. *Let* $f : D \subseteq \mathbb{R}^n \to \mathbb{R}$ *be twice continuously differentiable.* x_* *is a local minimum of* f *on* D *if*

$$f'(x_*) = 0 \text{ and } f''(x_*) > 0.$$

Since numerical algorithms mostly aim at identification of critical points, the sufficient optimality condition will form the fundamental for everything to follow. Known as FERMAT's Theorem about stationary points and local extremal points, the second order sufficient minimum condition writes in the setting of multivariable calculus (BJÖRCK (1996), p. 340) for nonlinear least squares problems:

Proposition 3.2.7. *For any multivariable function $F : D \subseteq \mathbb{R}^n \to \mathbb{R}^n$ the second order sufficient condition for $x_* \in D$ to be a local minimum is that*

$$F'(x_*) = 0,$$

and furthermore the Hessian is positive definite

$$z^T F''(x_*) z > 0,$$

for some $z \in \mathbb{R}^n$.

Consequently, approaching the minimisation task, we are actually looking for stationary points of

$$\frac{1}{2} F(x)^T F(x),$$

i.e. the zeros of its derivative.

Then, according to Deuflhard (2006), let us define the Newton method which solves the minimisation task by solving the gradient system of nonlinear equations

$$F'(x)^T F(x) = 0$$

through linearisation. Note that the Newton method applies as well for overdetermined systems $F : D \subseteq \mathbb{R}^n \to \mathbb{R}^m$ (Ortega/ Rheinboldt (1970), p. 181 ff., Stoer/ Burlisch (2007), pp. 298-305 and pp. 315 - 321 or Dedieu/ Shub (1999)). The overdetermined theory of course implies the case $m = n$. In line with Dennis/ Schnabel (1983) and Deuflhard (2006), the Newton method and its local convergence behaviour are reviewed for $F : D \subseteq \mathbb{R}^n \to \mathbb{R}^n$ only.

Definition 3.2.8. *For a nonlinear function $F : D \subseteq \mathbb{R}^n \to \mathbb{R}^n$ and the given system of nonlinear equations*

$$F(x) = 0$$

the Newton iteration is defined for $k = 0, 1, \ldots$ in its k^{th} iteration through

$$F'(x_k)\Delta x_k = -F(x_k) \tag{3.2.6}$$

$$x_{k+1} = x_k + \Delta x_k \tag{3.2.7}$$

for a given starting point $x_0 \in \mathbb{R}^n$ and the Jacobian $F'(x_k)$ invertible for all $x_k \in \mathbb{R}^n$.

The direct consequence of the second order sufficient minimum condition, solving the nonlinear least squares problem

$$\min_{x \in D} \|F(x)\|_2^2$$

reduces to detecting the interior local minimum $x_* \in D$ by identifying the residual function's Jacobian's zeros

$$\left(\frac{1}{2} F(x)^T F(x)\right)' = F'(x)^T F(x) = 0 \tag{3.2.8}$$

in $D \subseteq \mathbb{R}^n$ open and convex.

Obviously, the Newton approach applied to this system would write

$$\begin{aligned}\left(F'(x_k)^T F(x_k)\right)' \Delta x_k &= -F'(x_k)^T F(x_k)\\ x_{k+1} &= x_k + \Delta x_k\end{aligned}$$

which equivalently is

$$\begin{aligned}(F'(x_k)^T F'(x_k) + F''(x_k)^T F(x_k))\Delta x_k &= -F'(x_k)^T F(x_k)\\ x_{k+1} &= x_k + \Delta x_k\end{aligned}$$

using (3.2.3) for $k = 0, 1, \ldots$.

Due to computational effort, one would like to simply omit the Hessian tensor product on the left hand side. Though, this can only be justified, if this holds at least for the solution

$$F(x_*) = 0$$

such that the omitted term

$$F''(x_k)^T F(x_k)$$

becomes zero setting $x_k = x_*$. Second derivative information is either unavailable or just too expensive to be approximated by finite differences following Dennis/Schnabel (1983).

Definition 3.2.9. *For a solution $x_* \in D$ with $D \subseteq \mathbb{R}^n$ open and convex, the problem*

$$F(x_*) = 0$$

is called a zero-residual problem following Dennis/ Schnabel *(1983) or equivalently, introduced by* Deuflhard *(2003), a compatible nonlinear least squares problem.*

Now, if a problem is assumed to be compatible

$$F(x_*) = 0,$$

the term containing second order information vanishes at the solution point $x_* \in D$, which legitimates dropping the tensor term F''. The Newton iteration for this linearised substitute problem reads then

$$F'(x_k)^T F'(x_k)\Delta x_k = -F'(x_k)^T F(x_k),$$

which is exactly the Gauss-Newton iteration as in Definition 3.2.10.

Alternatively, the Gauss-Newton method can be motivated by (direct) linearisation of the residual function through application of Taylor's series.Newton's method for nonlinear problems seems inadequate to solve the given minimisation task, why Deuflhard/ Hohmann(2003) (p. 99) or Deuflhard (2006) (p. 174) propose to simply replace the nonlinear mapping by a linear one. This can immediately be obtained through a Taylor's expansion around some point x_k

$$F(x_*) = F(x_k) + F'(x_k)(x_* - x_k) + o(\|x_* - x_k\|_2)$$

for $x_* \to x_k$. The linear substitute map defines for the k^{th} iterative as

$$\overline{F}(x_*) := F(x_k) + F'(x_k)(x_* - x_k)$$

and equivalently for two neighbour iteratives

$$\overline{F}(x_{k+1}) = F(x_k) + F'(x_k)(x_{k+1} - x_k).$$

Since a local minimum $x_* \in D$ has to be found, the second order sufficient minimum condition implies that the system

$$\begin{aligned} &\overline{F}(x_{k+1})' = 0 \\ \Leftrightarrow\ &(F'(x_k)\Delta x_k + F(x_k))' = 0 \end{aligned}$$

has to be solved. This again requires second order derivative information, just as it is

$$(F'(x_k)^T F'(x_k) + F''(x_k)^T F(x_k))\Delta x_k + F'(x_k)^T F(x_k) = 0.$$

The same reasoning about omitting the Hessian tensor product as above gives that under compatibility of the problem, the zero can be found through solving the sequences of linear systems

$$F'(x_k)^T F'(x_k)\Delta x_k = -F'(x_k)^T F(x_k)$$

for $k = 0, 1, \ldots$. This is again, slightly different deduced, is the Gauss-Newton method.

By reviewing mathematical reasoning about the nonlinear least square problem, the following algorithm to detect a solution to the minimisation task is proposed:

Definition 3.2.10. *The Gauss-Newton iteration for $F : D \subseteq \mathbb{R}^n \to \mathbb{R}^m$ twice continuously differentiable follows for $k = 0, 1, \ldots$*

$$F'(x_k)^T F'(x_k)\Delta x_k = -F'(x_k)^T F(x_k) \tag{3.2.9}$$

$$x_{k+1} = x_k + \Delta x_k. \tag{3.2.10}$$

Note, that by determining the Newton correction Δx_k as solution to the above stated linear system without explicit calculation of the inverse, the problem of solving a nonlinear system is reduced to solving a sequence of linear systems. The advantage of such Newton methods for optimisation tasks is obvious. The Hessian does not need to be formed (Boyd/ Vandenberghe (2004), p. 496).
in Newton method's related convergence theory either nonsingularity of the Jacobian matrix is claimed or under the Moore Penrose definition of the generalised inverse certain rank conditions. The local convergence theory will be reviewed in the following, while necessary assumptions will be individually stated for any convergence result.

3.3. Affine Transformations and Invariance

Most problems arising in Biology or Health Sciences, make scaling of variables necessary. In general, two different cases have to be distinguished: Either the residual function F is scaled through application of a diagonal matrix

$$\tilde{F}(x) := D_L F(x)$$

or the argument vector $x \in \mathbb{R}^n$ is scaled

$$x = D_R y.$$

Applying those nonsingular diagonal scaling matrices, they are referred to as left or right scaling (Deuflhard (2006), p. 13). Different scaling within the nonlinear least squares problem leads to a different solution, the question to be asked then for arising problems in sciences is under which circumstances affine transformations of the problem yield the same solutions. This leads us naturally to the concept of affine invariance.

At a later stage in chapter 4 (p. 52 ff.), the focus on affine covariant theory is justified by right scaling invariance of the problem under the Gauss-Newton method, while scaling invariance does not happen for application of left scaling.

Definition 3.3.1. *Let now $A, B \in \mathbb{R}^{n,n}$ be arbitrarily nonsingular matrices. For the given nonlinear system*

$$F(x) = 0$$

we define the affine transformation without translation component as

$$\begin{aligned} G(y) = AF(By) &= 0 \\ x &= By. \end{aligned}$$

Obviously, this is equivalent to solving the initial problem $F(x) = 0$ since on the one hand it holds

$$\begin{aligned} F(x) &= 0 \\ \Leftrightarrow AF(x) &= 0 \end{aligned}$$

and on the other hand we have

$$\begin{aligned} F(x) &= 0 \\ \Leftrightarrow F(By) &= 0 \end{aligned}$$

for $x = By$ and any nonsingular $A, B \in \mathbb{R}^{n,n}$.

Annotation 3.3.2. *The linear least squares problem such as it is defined*

$$\|F(x_*)\|_2^2 = \min_{x \in D} \|F(x)\|_2^2$$

is not affine invariant. Since

$$\|F(x)\|_2^2 = \frac{1}{2} F(x)^T F(x),$$

its affine transformations

$$\|AF(By)\|_2^2 = \frac{1}{2}(AF(By))^T AF(By) = \frac{1}{2} F(By)^T A^T AF(By)$$

gives back the initial problem only if A is orthogonal and non-singular and if B satisfies further conditions.

Annotation 3.3.3. Deuflhard *(2006) (pp. 14–19) distinguishes mainly four different types of affine invariance. Affine covariance is the interesting concept throughout this work (see paragraph 3.3.3, 26). For the purpose of completeness, note that invariance properties under transformations of the image space by $A \in \mathbb{R}^{n,n}$ are summarised under the name affine covariance whereas any transformations in the whole original space by $B \in \mathbb{R}^{n,n}$ are called affine contravariance.*

The other two invariance classes, affine conjugacy and affine similarity, account for either a convex minimization problem or transformations taking place in the original and the image space.

3.3.1. Affine Covariance

Let $A \in \mathbb{R}^{n,n}$ be arbitrarily nonsingular. Approaching the problem

$$F(x) = 0$$

with $F : D \subset \mathbb{R}^n \to \mathbb{R}^n$ with the common Newton method, it is

$$\begin{aligned} F'(x_k)\Delta x_k &= -F(x_k) \\ x_{k+1} &= x_k + \Delta x_k. \end{aligned}$$

Affine covariant transformation of the nonlinear system performs

$$G(x) := AF(x) = 0 \tag{3.3.1}$$

for $A \in \mathbb{R}^{n,n}$ arbitrarily nonsingular. Obviously, this only affects the image space of the problem.

Solving the initial nonlinear system

$$F(x) = 0$$

is equivalent to solving the transformed system in (3.3.1).

Proposition 3.3.4. *For a given starting point x_0, the sequence $\{x_k\}$ obtained by Newton's method for the affine transformed nonlinear system*

$$G(x) = 0$$

is independent under transformations by the matrix $A \in \mathbb{R}^{n,n}$ arbitrarily nonsingular.

Proof of 3.3.4. Assuming $A \in \mathbb{R}^{n,n}$ is invertible, the Newton iteration for the affine transformed system

$$G(x) = 0$$

where $G(x) := AF(x)$ is defined through

$$\begin{aligned} G'(x_k)\Delta x_k &= -G(x_k) \\ x_{k+1} &= x_k + \Delta x_k \end{aligned}$$

for $k = 0, 1, \ldots$. By use of the affine transformation's definition, one obtains for the Newton correction that

$$\begin{aligned} \Delta x_k &= (G'(x_k))^{-1} G(x_k) \\ &= (AF'(x_k))^{-1} AF(x_k) \\ &= (F'(x_k))^{-1} A^{-1} AF(x_k) \\ &= (F'(x_k))^{-1} F(x_k) \end{aligned}$$

is independent of $A \in \mathbb{R}^{n,n}$. □

3.3.2. Affine Contravariance

As mentioned above, the property that the sequence of iteration points obtained after transformations of the definition space can be expressed as transformed iteration points of the definition space, is called affine contravariance.

Let $B \in \mathbb{R}^{n,n}$ be arbitrarily nonsingular. Again, considering the problem

$$F(x) = 0,$$

affine contravariance now means exactly the iterate's invariance to transformations in the whole original space

$$\begin{aligned} G(y) = F(By) &= 0 \\ x &= By. \end{aligned}$$

Consequently, for the affine contravariant system, it holds

$$G'(y) = F'(By)B$$

for the Jacobian by use of the chain rule.

Proposition 3.3.5. *Newton's method for the system $F(x) = 0$ remains unchanged after application of affine contravariant transformation and performs*

$$\begin{aligned} F'(x_k)\Delta x_k &= -F(x_k) \\ x_{k+1} &= x_k + \Delta x_k \end{aligned}$$

with starting guess $y_0 = B^{-1}x_0$.

Proof of 3.3.5. Due to the equivalence

$$\begin{aligned} & G'(y_k)\Delta y_k && = -G(y_k) \\ \Leftrightarrow \quad & F'(By_k)B\Delta y_k && = -F'(By_k)B \\ \Leftrightarrow \quad & B\Delta y_k && = -(F'(By_k))^{-1}F(By_k). \end{aligned}$$

and as $x_k = By_k$, we immediately obtain the Newton iteration

$$\Delta x_k = -(F(x_k))^{-1}F(x_k)$$

for $k = 0, 1, \ldots$ in the affine contravariant setting. Hence, any affine contravariant transformation on the definition space leads to the same transformation of the iteration and their Newton corrections $\{\Delta x_k\}$ as long as

$$y_0 := B^{-1}x_0$$

for the starting guess. □

Specifically, one can show that the Newton Method is even invariant under any general affine transformation

$$\begin{aligned} G(y) = AF(By) &= 0 \\ x = By & \end{aligned}$$

with $A, B \in \mathbb{R}^{n,n}$ arbitrarily nonsingular (Boyd/ Vandenberghe (2004), p. 476 and Deuflhard (2006), p. 13). This holds by the equivalence

$$\begin{aligned} & G'(y_k)\Delta y_k && = -G(y_k) \\ \Leftrightarrow \quad & (AF(By_k))'\Delta y_k && = -AF(By_k) \\ \Leftrightarrow \quad & AF'(By_k)B\Delta y_k && = -AF(By_k). \end{aligned}$$

As then, $x_k = By_k$, the proof proceeds

$$\begin{aligned} \Leftrightarrow \quad & AF'(x_k)\Delta x_k && = -AF(x_k) \\ \Leftrightarrow \quad & \Delta x_k && = -(AF'(x_k))^{-1}(AF(x_k)) \\ \Leftrightarrow \quad & \Delta x_k && = -F'(x_k)^{-1}A^{-1}AF(x_k) \\ \Leftrightarrow \quad & \Delta x_k && = -F'(x_k)^{-1}F(x_k), \end{aligned}$$

while $x_k = By_k$ for $k = 0, 1, \ldots$ if the starting point is chosen according to $y_0 = B^{-1}x_0$. Hence, we call the problem $F(x) = 0$ and the Newton method affine invariant.

Annotation 3.3.6. *Contrary to the Newton method, the Gauss-Newton as it is defined for some $F : D \subseteq \mathbb{R}^n \to \mathbb{R}^m$ is not invariant under affine transformations in general.*

Summarizing, any affine covariant convergence theorem will lead to results concerning the iterates $\{x_k\}$ and error norms $\|x_k - x_*\|_2$ whereas affine contravariant Newton-Mysovskikh theorems build convergence estimates in terms of residual norms $\|F(x_k)\|_2$. This motivates the distinction between error-oriented and residual-based algorithms.

3.3.3. Lipschitz Continuity

Regarding the numerical application, the modelling and the prediction of human ovulation, the further sections restrict to the concept of affine covariance and the hereby induced error-oriented methods. Usually requiring Lipschitz continuity, it remains to show that this continuity condition is affine invariant.

Standard convergence theorems typically claim not only the function $F : D \subseteq X \to Y$ in the overdetermined, nonlinear operator equation

$$F(x) = 0$$

to be invertible for all $x \in X$ but also require boundedness within the Banach spaces X, Y. These *a priori* assumptions hence also need to be satisfied within the affine covariant setting. Referring to Deuflhard (2006) and the herein mentioned Newton-Kantrovich theorem, for the affine transformed system,

$$G(x) := AF(x) = 0$$

the boundedness of the inverse for the starting value $x_0 \in D$ and all $x \in D$ writes

$$\begin{aligned} \|G'(x)^{-1}\|_{Y\to X} = \|(AF'(x))^{-1}\|_{Y\to X} \quad & \|G'(x_0)^{-1}\|_{Y\to X} = \|(AF'(x_0))^{-1}\|_{Y\to X} \\ \leq \|A^{-1}\|_{Y\to X}\|F'(x)^{-1}\|_{Y\to X} \quad & \leq \|A^{-1}\|_{Y\to X}\|F'(x)^{-1}\|_{Y\to X} \\ \leq \beta(A) \quad & \leq \beta_0(A) \end{aligned}$$

since the inverse of the Jacobian was assumed to exist and to be bounded obeying

$$\begin{aligned}\|F'(x_0)^{-1}\|_{Y\to X} &\leq \beta_0 < \infty \text{ for } x_0 \in D \text{ respectively}\\ \|F'(x)^{-1}\|_{Y\to X} &\leq \beta < \infty \text{ for } x \in D\end{aligned}$$

in the operator norm $\|\cdot\|_{Y\to X}$. Furthermore, second derivative information that needs to be examined during convergence studies is commonly included via a Lipschitz condition like

$$\|F'(y) - F'(x)\|_{X\to Y} \leq \gamma\|y - x\|_X$$

for all $x, y \in D$. Then, affine transformation does only affect the Lipschitz constant $\gamma > 0$ in the sense that it depends on the affine transformation matrix $A \in \mathbb{R}^{n,n}$. First, it is

$$\begin{aligned}\|G'(y) - G'(x)\|_{X\to Y} &= \|A(F'(y) - F'(x))\|_{X\to Y}\\ &\leq \|A\|_{X\to Y}\|F'(y) - F'(x))\|_{X\to Y}\\ &\leq \gamma\|A\|_{X\to Y}\|y - x\|_X\\ &:= \gamma(A)\|y - x\|_X\end{aligned}$$

for all $x, y \in D$.

Deuflhard (2006) (p. 14) merges the boundedness of the Jacobian's inverse and the Lipschitz continuity of the Jacobian to one requirement

$$\|F'(x_0)^{-1}(F'(y) - F'(x))\|_{Y\to X} \leq \omega_0\|y - x\|_X$$

for $x_0, x, y \in D$ exploiting the Newton-Kantrovich theorem. The hereby defined Lipschitz constant $\omega_0 > 0$ is affine covariant since

$$\begin{aligned}G'(x_0)^{-1}(G'(y) - G'(x)) &= (AF'(x_0))^{-1}(AF'(y) - AF'(x))\\ &= F'(x_0)^{-1}A^{-1}A(F'(y) - F'(x))\\ &= F'(x_0)^{-1}(F'(y) - F'(x)),\end{aligned}$$

where $A \in \mathbb{R}^{n,n}$ is nonsingular. Though, this definition of the Lipschitz constant ω_0 still involves the operator norm $\|\cdot\|_{Y\to X}$ on the left hand side by using the Banach perturbation lemma. Motivated by the difficulties to estimate the Lipschitz constant ω_0 under the operator norm, Deuflhard (2006) (p. 14) proposes the affine covariant Lipschitz condition

$$\|F'(x)^{-1}(F'(y) - F'(x))(y - x)\|_X \leq \omega\|y - x\|_X \tag{3.3.2}$$

that solely contains vector norms for $x, y \in D$. In the subsequent, we consider the overdetermined function $F : D \subseteq \mathbb{R}^n \to \mathbb{R}^m$ under the l_2 norm, which is the Euclidean standard norm in this case. Most importantly, under the l_2 norm it is possible to differentiate the Jacobian and to easily perform QR decompositions, as the l_2 norm is invariant under orthogonal transformations. Finally, using the Euclidean standard norm, we remain all over in the Hilbert space setting.

This Lipschitz type condition (3.3.2) allows an affine covariant convergence theory of the Newton and later the Gauss-Newton method including the uniqueness of the solution $x_* \in D$. Due to the scaling necessary to be applied to the minimisation problem at hand, the subsequent will

restrict to the concept of affine covariance for further theoretical preparation. Since furthermore the Gauss-Newton correction remains invariant under right scaling (see chapter 4, p. 52 ff.), only error-oriented algorithms will be considered.

3.4. Local Convergence of the Newton Method

$F : D \subseteq \mathbb{R}^n \to \mathbb{R}^n$ be once continuously differentiable and $x_0 \in D$, $D \subseteq \mathbb{R}^n$ open and convex. Recalling the Newton method at each iteration k is

$$F(x_k)'\Delta x_k = -F(x_k)$$
$$x_{k+1} = x_k + \Delta x_k$$

for $k = 0, 1, \ldots$ in the Euclidean space associated with the Euclidean standard norm $\|\cdot\|_2$, the open neighbourhood around $x \in D$ of radius $\rho > 0$ writes

$$B(x, \rho) = \{y \in \mathbb{R}^n : \|y - x\|_2 < \rho\}$$

and similarly for its closure

$$\overline{B}(x, \rho) = \{y \in \mathbb{R}^n : \|y - x\|_2 \leq \rho\}.$$

3.4.1. Classical Local Convergence Theory

Local convergence of the Newton method referring to Dennis/ Schnabel (1983) (p. 90) is examined first.

Theorem 3.4.1. *Let $F : D \subseteq \mathbb{R}^n \to \mathbb{R}^n$ continuously differentiable. Assuming that there exists $x_* \in D$ and $\beta, \rho > 0$ such that $B(x_*, \rho) \subseteq D, F(x_*) = 0$, that $F'(x_*)$ exists with $\|F'(x_*)^{-1}\|_2 \leq \beta$ and that $\|F'(x) - F'(x_*)\|_2 \leq \gamma\|x - x_*\|_2$ Lipschitz continuity holds for all $x \in B(x_*, \rho)$. Then, there exists $\epsilon > 0$ such that for all $x_0 \in B(x_*, \rho)$ the sequence $\{x_k\}$ generated by the Newton method is well defined and converges quadratically to x_* obeying*

$$\|x_{k+1} - x_*\|_2 \leq \beta\gamma\|x_k - x_*\|_2^2 \tag{3.4.1}$$

for $k = 0, 1, \ldots$.

Lemma 3.4.2. *Let now $F : D \subseteq \mathbb{R}^n \to \mathbb{R}^m$, $m \geq n$ be at least once continuously differentiable in an open and convex set D. For any $x, x + p \in D$*

$$F(x + p) - F(x) = \int_0^1 F'(x + tp)p \, dt = p \int_0^1 F'(x + tp) \, dt \tag{3.4.2}$$

if we denote the Jacobian matrix at $x \in D$ by $F'(x)$. Though an analogous mean value theorem for vector valued functions like the classical mean value theorem does not exist, this can be considered a mean value theorem for vector valued functions in the sense that the integral of the matrix valued function is interpreted componentwise. It is widely referred to as the Lagrangian mean value theorem.

Proof of 3.4.2. For $F : D \subseteq \mathbb{R}^n \to \mathbb{R}^m$ a vector valued function on D open and convex, we write componentwise

$$F = (F_1, \ldots, F_M)^T$$

where all F_i are vector valued of dimension d for $i = 1, \ldots, m$. Defining a mapping $G_i^k : [0,1] \to \mathbb{R}$ by

$$G_i^k(t) := F_i^k(x + pt)$$

we obtain the vector valued function $G = (G_1, \ldots, G_M)^T \in \mathbb{R}^m$. Then, by the fundamental theorem of calculus, componentwise for $k = 1, \ldots, d$ one obtains

$$F_i^k(x+p) - F_i^k(x) = G_i^k(1) - G_i^k(0) = \int_0^1 \left(G_i^k(t)\right)' \, dt.$$

Since

$$F'(x) = \left(\frac{\partial}{\partial x_j} F(x)\right)_{j=1,\ldots,n} = \begin{pmatrix} \nabla F_1(x)^T \\ \vdots \\ \nabla F_M(x)^T \end{pmatrix} = \begin{pmatrix} \frac{\partial F_1(x)}{\partial x_1} & \cdots & \frac{\partial F_1(x)}{\partial x_n} \\ \vdots & \ddots & \vdots \\ \frac{\partial F_M(x)}{\partial x_1} & \cdots & \frac{\partial F_M(x)}{\partial x_n} \end{pmatrix}$$

for each component G_i columnwise differentiation gives

$$(G_i^k(t))' = \nabla F_i^k(x + tp)^T p = \sum_{j=1}^{M} \frac{\partial}{\partial x_j} F_i^k(x + pt) p_j$$

such that

$$F_i^k(x+p) - F_i^k(x) = G_i^k(1) - G_i^k(0) = \int_0^1 (G_i^k(t))' \, dt = \int_0^1 \sum_{j=1}^{M} \left(\frac{\partial}{\partial x_j} F_i^k(x + pt)\right) p_j \, dt.$$

The definition of the Jacobian F' gives the lemma assuming continuous differentiability of $F : D \subseteq \mathbb{R}^n \to \mathbb{R}^m$. The same result is obtained of course if $m = n$. □

Proof of 3.4.1. Choose $\epsilon > 0$ such that for any $x \in B(x_*, \epsilon)$ the Jacobian $F'(x)$ is nonsingular. Let

$$\epsilon = \min\left\{\rho, \frac{1}{2\beta\gamma}\right\}. \tag{3.4.3}$$

In the subsequent, we show by induction over k that for each iteration step the convergence is q-quadratic and that

$$x_{k+1} \in B(x_*, \epsilon)$$

for $k = 0, 1, \ldots$.

$k = 0$:
For a given start value x_0, the Jacobian $F'(x_0)$ is nonsingular since by $\|x_0 - x_*\|_2 \leq \epsilon$ and by the Lipschitz continuity of the Jacobian at the solution point x_* it is

$$\begin{aligned} \left\|F'(x_*)^{-1}(F'(x_0) - F'(x_*))\right\|_2 &\leq \|F'(x_*)^{-1}\|_2 \|F'(x_0) - F'(x_*)\|_2 \\ &\leq \beta\gamma\|x_0 - x_*\| \\ &\leq \beta\gamma\epsilon \\ &\leq \frac{1}{2} \end{aligned}$$

using the consistency of the Euclidean norm and $\epsilon > 0$ as in (3.4.3). It is well known that for

the Euclidean norm, if $A, B \in \mathbb{R}^{n,n}$ and A is nonsingular with $\|A^{-1}(B-A)\|_2 < 1$, then B is also nonsingular and it holds

$$\|B^{-1}\|_2 \leq \frac{\|A^{-1}\|_2}{1 - \|A^{-1}(B-A)\|_2}. \tag{3.4.4}$$

Consequently, as it is

$$\|F'(x_*)^{-1}(F'(x_0) - F'(x_*))\|_2 \leq \frac{1}{2} < 1,$$

and $F'(x_*)$ nonsingular by assumption, $F'(x_0)$ is invertible and can be estimated likewise

$$\begin{aligned}
\|F'(x_0)^{-1}\|_2 &\leq \frac{\|F'(x_*)^{-1}\|_2}{1 - \|F'(x_*)^{-1}(F'(x_0) - F'(x_*))\|_2} \\
&\leq \frac{\|F'(x_*)^{-1}\|_2}{1 - \frac{1}{2}} \\
&= 2\|F'(x_*)\|_2 \\
&\leq 2\beta.
\end{aligned}$$

Therefore, the first iterative x_1 is well defined and by the Newton method, one can write

$$\begin{aligned}
x_1 - x_0 &= x_0 - F'(x_0)^{-1}F(x_0) - x_* \\
&= x_0 - x_1 - F'(x_0)^{-1}F(x_0).
\end{aligned}$$

Provided the problem considered is compatible in the sense that $F(x_*) = 0$ for a solution $x_* \in D$, also the matrix product $F(x_0)^{-1}F(x_*) = 0$ and it can be proceeded

$$\begin{aligned}
x_1 - x_* &= x_0 - x_1 - F'(x_0)^{-1}F(x_0) + F(x_0)^{-1}F(x_*) \\
&= x_0 - x_* - F'(x_0)^{-1}(F(x_0) - F(x_*)) \\
&= F'(x_0)^{-1}(F(x_*) - F(x_0) - F'(x_0)(x_* - x_0)).
\end{aligned}$$

Beyond, the Lagrange mean value theorem amounts to

$$\begin{aligned}
F(x+p) - F(x) - F'(x)p &= \int_0^1 F'(x+tp)p\, dt - F'(x)p \\
&= \int_0^1 (F'(x+tp) - F'(x))p\, dt.
\end{aligned}$$

Now, bounding the integral in terms of the integrand, writing the integral as a vector Riemann sum and application of the triangle inequality give for the l_2 norm and its induced matrix norm the estimate

$$\begin{aligned}
\|F(x+p) - F(x) - F'(x)p\|_2 &= \left\| \int_0^1 (F'(x+tp) - F'(x))p\, dt \right\|_2 \\
&\leq \int_0^1 \|F'(x+tp) - F'(x)\|_2 \, \|p\|_2\, dt \\
&= \|p\|_2 \int_0^1 \|F'(x+tp) - F'(x)\|_2 \, dt
\end{aligned}$$

while basically the Cauchy-Schwarz inequality is exploited. This result is given as a Lemma in Ortega/ Rheinboldt (1970), p. 73. The Jacobian $F' : D \subseteq \mathbb{R}^n \to \mathbb{R}^{n,n}$ being Lipschitz continuous, one can proceed likewise

$$\begin{aligned}\|F(x+p) - F(x) - F'(x)p\|_2 &\leq \|p\|_2 \int_0^1 \|F'(x+tp) - F'(x)\|_2 \, dt \\ &\leq \gamma \|(x+p) - x\|_2 \|p\|_2 \int_0^1 t^2 \, dt \\ &= \frac{\gamma}{2}\|p\|_2^2\end{aligned}$$

for the integral's bound. Hence, precisely by application of the Lagrange mean value theorem and using the consistency of the norm, we obtain

$$\begin{aligned}\|x_1 - x_*\|_2 &= \|F'(x_0)^{-1}(F(x_*) - F(x_0) - F'(x_0)(x_* - x_0))\|_2 \\ &\leq \|F'(x_0)^{-1}\|_2 \|F(x_*) - F(x_0) - F'(x_0)(x_* - x_0)\|_2 \\ &\leq \|F'(x_0)^{-1}\|_2 \frac{\gamma}{2}\|x_0 - x_*\|_2^2 \\ &\leq 2\beta\frac{\gamma}{2}\|x_0 - x_*\|_2^2 \\ &= \beta\gamma\|x_0 - x_*\|_2^2.\end{aligned}$$

Since furthermore it is

$$\|x_0 - x_*\|_2 \leq \frac{1}{2}\beta\gamma$$

by the Lipschitz continuity and the choice of $\epsilon > 0$, we obtain that

$$\begin{aligned}\|x_1 - x_*\|_2 &\leq \beta\gamma\|x_0 - x_*\|_2^2 \\ &\leq \frac{1}{2}\|x_0 - x_*\|_2\end{aligned}$$

in the end, such that $x_1 \in B(x_*, \epsilon)$ which completes the proof for $k = 0$.

$k \to k+1$:
Assume, that $\|x_k - x_*\|_2 \leq \epsilon$ holds. Then, by the Lipschitz continuity of the Jacobian at x_* it follows immediately that

$$\begin{aligned}\left\|F'(x_*)^{-1}(F'(x_k) - F'(x_*))\right\|_2 &\leq \|F'(x_*)^{-1}\|_2 \|F'(x_0) - F'(x_*)\|_2 \\ &\leq \beta\gamma\|x_k - x_*\| \\ &\leq \beta\gamma\epsilon.\end{aligned}$$

$F'(x_*)^{-1}$ is still nonsingular and it is

$$\|F'(x_*)^{-1}(F'(x_k) - F'(x_*))\|_2 \leq \beta\gamma\epsilon \leq \frac{1}{2} < 1$$

such that nonsingularity also holds true for $F'(x_k)$. Consequently, it follows that

$$\|F'(x_k)^{-1}\|_2 \leq \frac{\|F'(x_k)^{-1}\|_2}{1 - \|F'(x_*)(F'(x_k) - F'(x_*))\|_2} \leq 2\beta.$$

x_{k+1} is well defined. Thus

$$\begin{aligned}\|x_{k+1} - x_*\|_2 &= \|x_k - F'(x_k)^{-1}F(x_k) - x_*\|_2 \\ &= \|x_k - x_* - F'(x_k)^{-1}(F(x_k) + F(x_*))\|_2 \\ &= \|F'(x_k)^{-1}(F(x_*) - F(x_k) - F'(x_k)(x_* - x_k))\|_2 \\ &\leq \|F'(x_k)^{-1}\|_2\|(F(x_*) - F(x_k) - F'(x_k)(x_* - x_k))\|_2 \\ &\leq \beta\gamma\|x_k - x_*\|_2^2,\end{aligned}$$

which proves q-quadratic convergence for the $k+1^{\text{th}}$ Newton iterate. Furthermore, for all $k = 0, 1, \ldots$ the iterates remain in the neighbourhood of the solution x_* since

$$\|x_{k+1} - x_*\|_2 \leq \beta\gamma\|x_k - x_*\|_2^2 \leq \frac{1}{2}\|x_k - x_*\|_2$$

such that $x_{k+1} \in B(x_*, \epsilon)$.

Dennis/Schnabel (1983) finally remark that combining the constants $\beta, \gamma > 0$ to one constant

$$\gamma_{rel} = \beta\gamma$$

yields a Lipschitz constant γ_{rel}, measuring the relative nonlinearity of F at x_* for all $x \in B(x_*, \epsilon)$ by

$$\|F'(x_*)^{-1}(F(x) - F(x_*))\|_2 \leq \gamma_{rel}\|x - x_*\|_2.$$

□

This can also be interpreted as the convergence radius of the Newton method being inversely proportional to the relative nonlinearity of F at the solution x_*. In view of the problems' nonlinearity, we want to take the step forward to the affine invariance theory of the Newton method. Note, that by the claimed conditions and the idea followed during the proof, the local convergence behaviour can be modified towards an affine invariant setting. As mentioned before, taking any matrix $A \in \mathbb{R}^{n,n}$ arbitrarily invertible, the affine (covariant) transformation does not affect the Newton sequence $\{x_k\}$. Due to this invariance, the Newton method can be called *affine invariant* under the affine transformation $F \to G$ according to Deuflhard/ Hohmann (2003) (p. 100).

Taking Dennis/ Schnabel (1983)'s theorem for the Newton method's local convergence behaviour as a basis, it can be showed that the same holds true if an affine transformation is applied.

Theorem 3.4.3. *Let $F : D \subseteq \mathbb{R}^n \to \mathbb{R}^n$ continuously differentiable. For $A \in \mathbb{R}^{n,n}$ nonsingular we define the affine transformation without translation component*

$$G(x) := AF(x).$$

Then, assume there exists $x_* \in D$ and $\beta, \rho > 0$ such that $B(x_*, \rho) \subseteq D, F(x_*) = 0$ and $F'(x_*)$ exists with $\|F'(x_*)^{-1}\|_2 \leq \tilde{\beta}$, $\tilde{\beta} := \frac{\beta}{\|A^{-1}\|_2}$ and $\|F'(x) - F'(x_*)\|_2 \leq \gamma\|x - x_*\|_2$ for all $x \in B(x_*, \rho)$ Lipschitz continuous.
Then, there exists $\epsilon > 0$ such that for all $x_0 \in B(x_*, \rho)$ the sequence $\{x_k\}$ generated by the Newton method

$$G'(x_k)\Delta x_k = -G(x_k)$$

is well defined, converges quadratically to x_* obeying

$$\|x_{k+1} - x_*\|_2 \leq \beta\gamma\|x_k - x_*\|_2^2 \tag{3.4.5}$$

for $k = 0, 1, \ldots$.

Proof of 3.4.3. Following closely the proof present by Dennis/ Schnabel (1983) (p. 90/91), we start the induction over k for $k = 0, 1, \ldots$ with the case $k = 0$:

First, $G'(x_0)$ is nonsingular for a given start value x_0 as long as it is provided that $F'(x_*)$ is arbitrarily nonsingular since by

$$\|x_0 - x_*\|_2 \leq \epsilon$$

and the Lipschitz continuity of the initial function's Jacobian $F'(\cdot)$ at the solution $x_* \in D$, it follows that

$$\begin{aligned}
\|G'(x_*)^{-1}(G'(x_0) - G'(x_*))\|_2 &= \|(AF'(x_*))^{-1}(AF'(x_0) - AF(x_*))\|_2 \\
&= \|F'(x_*)^{-1}A^{-1}A(F'(x_0) - F'(x_*))\|_2 \\
&= \|F'(x_*)^{-1}(F'(x_0) - F'(x_*))\|_2 \\
&\leq \|F'(x_*)^{-1}\|_2\|F'(x_0) - F'(x_*)\|_2 \\
&\leq \frac{\beta}{\|A^{-1}\|_2}\gamma\|x_0 - x_*\|_2 \\
&\leq \beta\gamma\|x_0 - x_*\|_2 \\
&\leq \frac{1}{2}.
\end{aligned}$$

Since for $F : \mathbb{R}^n \to \mathbb{R}^n$ and for its affine transformation $G : \mathbb{R}^n \to \mathbb{R}^n$ the image space remains the same for any $A \in \mathbb{R}^{n,n}$ nonsingular and $\mathbb{R}^n$ is a Banach space under the l_2 norm, the operator norm is just the norm itself. Hence, the required continuity is sufficient for the further conduction of the proof. The perturbation relation, (3.4.4), mentioned above in proof 3.4.1 for the *classical* convergence result by Dennis/ Schnabel (1983) gives that consequently also $G'(x_0)$ is nonsingular.

$$\begin{aligned}
\|G'(x_0)^{-1}\|_2 &\leq \frac{\|G'(x_*)^{-1}\|_2}{1 - \|G'(x_*)^{-1}(G'(x_0) - G'(x_*))\|_2} \\
&\leq \frac{\|F'(x_*)^{-1}A^{-1}\|_2}{1 - \|F'(x_*)^{-1}\|_2\|F'(x_0) - F'(x_*)\|_2} \\
&\leq \|A^{-1}\|_2\frac{\|F'(x_*)^{-1}\|_2}{1 - \|F'(x_*)^{-1}\|_2\|F'(x_0) - F'(x_*)\|_2} \\
&\leq 2\|A^{-1}\|_2\|F'(x_*)^{-1}\|_2.
\end{aligned}$$

The Jacobian $F'(x_*)$ is upper bounded by the constant $\beta > 0$ within the Euclidean standard norm

$$\|F^{-1}(x_*)\|_2 \leq \frac{\beta}{\|A^{-1}\|_2},$$

such that we can proceed with the estimate

$$\begin{aligned}\|G'(x_0)^{-1}\|_2 &\leq 2\|A^{-1}\|_2\|F'(x_*)\|_2\\ &\leq 2\|A^{-1}\|_2\|F'(x_*)^{-1}\|_2\\ &\leq 2\beta.\end{aligned}$$

x_1 is well defined and

$$x_1 - x_* = x_0 - G'(x_0)^{-1}G(x_0) - x_* = x_1 - x_* - G'(x_0)^{-1}G(x_0).$$

Claiming the initial problem to be compatible, meaning $F(x_*) = 0$ for the solution $x_* \in D$, under the transformation of the image space by $A \in \mathbb{R}^{n,n}$ the equivalence

$$\begin{aligned}&(F'(x_0))^{-1}F(x_*) &&= 0\\ \Leftrightarrow\quad &(F'(x_0))^{-1}A^{-1}AF(x_*) &&= 0\\ \Leftrightarrow\quad &(AF'(x_0))^{-1}AF(x_*) &&= 0\\ \Leftrightarrow\quad &(G'(x_0))^{-1}G(x_*) &&= 0\end{aligned}$$

holds. Hence,

$$\begin{aligned}x_1 - x_* &= x_1 - x_* - G'(x_0)^{-1}G(x_0)\\ &= x_1 - x_* + G'(x_0)^{-1}(G(x_*) - G(x_0))\\ &= G'(x_0)^{-1}(G(x_*) + G(x_0) - G'(x_0)(x_* - x_0)).\end{aligned}$$

Likewise in the *classical* proof presented by Dennis/ Schnabel (1983), q-quadratic convergence can be proven. First, consistency of the norm yields

$$\begin{aligned}\|x_1 - x_*\|_2 &= \|(G'(x_0))^{-1}(G(x_*) - G(x_0) - G'(x_0)(x_* - x_0))\|_2\\ &\leq \|(G'(x_0))^{-1}\|_2\|G(x_*) - G(x_0) - G'(x_0)(x_* - x_0)\|_2.\end{aligned}$$

Application of the affine covariant version of the Lipschitz condition gives that

$$\begin{aligned}\|x_1 - x_*\|_2 &\leq \|(G'(x_0))^{-1}(G(x_*) - G(x_0) - G'(x_0)(x_* - x_0))\|_2\\ &= \|(F'(x_0))^{-1}A^{-1}A(F(x_*) - F(x_0) - F'(x_0)(x_* - x_0))\|_2\\ &\leq \|F'(x_0)^{-1}\|_2\|F(x_*) - F(x_0) - F'(x_0)(x_* - x_0)\|_2\\ &\leq \frac{2\beta}{\|A^{-1}\|_2}\frac{\gamma}{2}\|x_0 - x_*\|_2^2\\ &= \beta\gamma\|x_0 - x_*\|_2^2\end{aligned}$$

since naturally, $\frac{1}{\|A^{-1}\|_2} > 0$. Furthermore, the first iterate x_1 lies within the predefined neighbourhood of x_* since by

$$\|x_0 - x_*\|_2 \leq \frac{1}{2}\beta\gamma$$

for the first iterate it holds

$$\|x_1 - x_*\|_2 \leq \beta\gamma\|x_0 - x_*\|_2\|x_0 - x_*\|_2 \leq \frac{1}{2}\|x_0 - x_*\|_2$$

such that $x_1 \in B(x_*, \epsilon)$ with $\epsilon > 0$ appropriately chosen. The induction step $k \to k+1$ for $k > 0$ follows obviously the same lines, why it is omitted. □

3.4.2. Affine Invariant Local Convergence Theory

The main step towards the affine invariant Newton convergence theory has been taken, but for matters of completeness, in outlook to the convergence theory of the Gauss-Newton method and the computations to be performed, let us state and prove quadratic convergence for the Newton method under a more general affine invariant context as proposed in DEUFLHARD/ HOHMANN (2003) (p. 100/101).

Theorem 3.4.4. *Let $F : D \subseteq \mathbb{R}^n \to \mathbb{R}^n$ continuously differentiable with invertible Jacobian $F'(x)$ for all $x \in D$. For an $\omega > 0$ we claim the following affine invariant Lipschitz condition*

$$\|F'(x)^{-1}(F'(x+sv) - F'(x))v\|_2 \leq sw\|v\|_2^2 \tag{3.4.6}$$

for all $s \in [0,1]$, $x \in D$ and $v \in \mathbb{R}$ such that $x + v \in D$. Furthermore we assume there exists a solution $x_* \in D$ and a start value $x_0 \in D$ such that

$$\rho := \|x_* - x_0\|_2 < \frac{2}{\omega} \text{ and } B(x_*, \rho) \subseteq D.$$

Then, the sequence $\{x_k\}$ defined by the Newton method stays in the open ball $B(x_*, \rho) \subseteq D$ for $k > 0$ and converges towards x_*, i.e.

$$\|x_k - x_*\|_2 < \rho \text{ for } k < 0 \text{ and } \lim_{k\to\infty} x_k = x_*.$$

The speed of convergence can be estimated by

$$\|x_k - x_*\|_2 \leq \frac{\omega}{2}\|x_k - x_*\|_2^2 \tag{3.4.7}$$

for $k = 0, 1, \ldots$. Furthermore, the solution $x_* \in D$ is unique in $B(x_*, \frac{\omega}{2})$.

Proof of 3.4.4. The Lagrangian mean value theorem for vector valued functions in Lemma 3.4.2 yields for any $p \in [0,1]$, setting $\tilde{x} := x + p$ that

$$\begin{aligned} F(\tilde{x}) - F(x) - F'(x)(\tilde{x} - x) &= F(x+p) - F(x) - pF'(x) \\ &= \int_0^1 (F'(x+tp) - F'(x))\, p\, dt \\ &= \int_0^1 (F'(x + t(\tilde{x} - x)) - F'(x))\, (\tilde{x} - x)\, dt. \end{aligned}$$

Consequently, we can estimate

$$\begin{aligned} \|F'(x)^{-1}\left(F'(\tilde{x}) - F(x) - F'(x)(\tilde{x} - x)\right)\|_2 &= \left\| \int_0^1 F'(x)^{-1}\left(F'(x + t(\tilde{x} - x)) - F'(x)\right)(\tilde{x} - x)\, dt \right\|_2 \\ &\leq \int_0^1 \left\| F'(x)^{-1}\left(F'(x + t(\tilde{x} - x)) - F'(x)\right)(\tilde{x} - x) \right\|_2 dt \\ &\leq \int_0^1 \omega t \|\tilde{x} - x\|_2^2\, dt \end{aligned}$$

$$= \frac{\omega}{2}\|\tilde{x} - x\|_2^2$$

provided the Jacobian $F'(x)$ is nonsingular for all $x \in D$. The second inequality follows from condition (3.4.6). Under the assumption that the problem is compatible with

$$F(x_*) = 0$$

one Newton iteration writes

$$\begin{aligned} x_{k+1} - x_* &= x_k - F'(x_k)^{-1}F(x_k) - x_* \\ &= x_k - x_* - F'(x_k)^{-1}(F(x_k) - F(x_*) \\ &= F'(x_k)^{-1}(F(x_*) - F(x_k) - F'(x_k)(x_* - x_k)). \end{aligned}$$

Making use of the above shown yields in the standard Euclidean norm that

$$\begin{aligned} \|x_{k+1} - x_*\|_2 &= \|F'(x_k)^{-1}\left(F(x_*) - F(x_k) - F'(x_k)(x_* - x_k)\right)\|_2 \\ &\leq \frac{\omega}{2}\|x_* - x_k\|_2^2. \end{aligned}$$

If furthermore $0 < \|x_k - x_*\|_2 \leq \rho$ holds true, then

$$\begin{aligned} \|x_{k+1} - x_*\|_2 &\leq \frac{\omega}{2}\|x_k - x_*\|_2^2 \\ &\leq \frac{\omega\rho}{2}\|x_k - x_*\|_2 \\ &< \|x_k - x_*\|_2 \end{aligned}$$

since it was defined

$$\rho := \|x_* - x_0\|_2 < \frac{2}{\omega}$$

and such that it is for $\omega > 0$ by assumption

$$\frac{\omega}{2}\rho < \frac{\omega}{2}\frac{2}{\omega} = 1.$$

Thus, for all $k = 0, 1, \ldots$ the Newton sequence $\{x_k\}$ stays in the open ball around the solution $x_* \in D$ with radius $\rho < 0$ in the sense that $\|x_k - x_*\|_2 < \rho$.

The proof is completed by showing the uniqueness of the solution x_* within the open neighbourhood $B(x_*, \frac{2}{\omega})$. Considering the open ball $B(x_*, \frac{2}{\omega})$, we assume the contrary to show contradiction. Let hence x_{**} be another solution minimising the given nonlinear least squares problem with $x_{**} \neq x_*$. Under the compatibility of the problem, $F(x_{**}) = 0$ and $F(x_*) = 0$, one obtains the Lipschitz similar result

$$\begin{aligned} \|x_{**} - x_*\|_2 &= \|F'(x_*)^{-1}F'(x_*)(x_{**} - x_*)\|_2 \\ &= \|F'(x_*)^{-1}(\underbrace{F(x_{**})}_{=0} - \underbrace{F(x_*)}_{=0} - F'(x_*)(x_{**} - x_*))\|_2 \\ &= \|F'(x_*)^{-1}(F(x_{**}) - F(x_*) - F'(x_*)(x_{**} - x_*))\|_2 \\ &\leq \frac{\omega}{2}\|x_{**} - x_*\|_2^2. \end{aligned}$$

Assuming that $x_{**} \in B(x_*, \frac{2}{\omega})$, the above equivalently writes as

$$\|x_{**} - x_*\|_2 < \frac{2}{\omega}$$

such that finally the estimate

$$\frac{\omega}{2}\|x_{**} - x_*\|_2 < 1$$

holds. Consequently, it is

$$\|x_{**} - x_*\|_2 \leq \frac{\omega}{2}\|x_{**} - x_*\|_2^2 < \|x_{**} - x_*\|_2$$

which holds if and only if $x_{**} = x_*$, which contradicts the assumption taken at the beginning of the uniqueness proof. □

Note that by the affine covariant Lipschitz condition, ω in the latest proof accounts for the product $\beta\gamma$ of the classical convergence proof by Dennis/ Schnabel (1983) (p. 90) in an affine invariant setting. Dennis/ Schnabel (1983) (p. 91) propose to measure the convergence radius of the Newton method with respect to the nonlinearity of the problem by combining

$$\gamma_{rel} := \beta\gamma$$

which in Deuflhard's (2006) notation is referred to as

$$\omega,$$

being the affine invariant Lipschitz quantity.

3.5. Local Convergence of Gauss-Newton Method

Getting back to the motivating part at the beginning of this chapter, solving the overdetermined nonlinear least squares problem

$$\min_{x \in D} \|F(x)\|_2^2$$

for $F : D \subseteq \mathbb{R}^n \to \mathbb{R}^m$ with the second order sufficient condition on x_* to be a local minimum solution on the open and convex set D without consideration of the boundary ∂D is precisely $(\|F(x_*)\|_2^2)' = 0$ with $z^T(\|F(x_*)\|_2^2)''z > 0$ positive definite for any $z \in D$. Taking the matrix

$$\frac{1}{2}F(x)^T F(x)$$

to be minimised, the problem incorporating writes then

$$\left(\frac{1}{2}F(x_*)^T F(x_*)\right)' = F'(x_*)^T F(x_*) = 0 \tag{3.5.1}$$

where $F''(x_*)$ is required to be positive definite (see also Proposition 3.2.7 (p. 19)). Newton's method to solve the system of m nonlinear equations where $F : D \subseteq \mathbb{R}^n \to \mathbb{R}^m$ is twice continuously differentiable is based on successive linearisation. When introducing the Gauss-Newton method at an earlier stage, it was already acknowledged that application of the classical Newton method to the nonlinear least squares problem given would require evaluation of the

Hessian $F''(x)$ in terms of iterating

$$(F'(x_k)^T F'(x_k) + F''(x_k)^T F(x_k))\Delta x_k = -F'(x_k)^T F(x_k)$$

for $k = 0, 1, \ldots$. Omitting the second derivative on the left hand side and the effort in computations can only be justified if treating the small or even zero residual case. Hence, this gets us back to requiring compatibility

$$F(x_*) = 0$$

to hold for a solution $x_* \in D$ of the minimisation problem within the further. The first derivative of the substitute (3.5.1) problem becomes at $x_* \in D$

$$\big(F'(x_*)^T F(x_*)\big)' = F'(x_*)^T F'(x_*) + F''(x_*)^T F(x_*) = F'(x_*)^T F'(x_*).$$

By this and the fact, that positive definiteness of the substitute problem's first derivative $\big(F'(x_*)^T F(x_*)\big)'$ is equivalent to claiming full rank for the Jacobian, namely $rank(F'(x_*)) = n$, the Gauss-Newton method is defined as

$$\begin{aligned} F'(x_k)^T F'(x_k)\Delta x_k &= -F'(x_k)^T F(x_k) \\ x_{k+1} &= x_k + \Delta x_k \end{aligned}$$

for all $k = 0, 1, \ldots$.

Annotation 3.5.1. *Application of the Gauss-Newton method, gives a linearisation of the nonlinear least squares problem. The problem ad hand reduces to a sequence of linear gradient systems, where evaluation of the Hessian tensor product is omitted by requiring compatibility.*

Annotation 3.5.2. *Note that the Gauss-Newton method corresponds to solving the normal equation for the linear least squares problem*

$$\min_{x_k \in D} \|F'(x_k)\Delta x_k + F(x_k)\|_2 \tag{3.5.2}$$

since we know that for $A \in \mathbb{R}^{m,n}$ and $m > n$ to

$$\min \|Ax - b\|_2$$

the normal equation is given by

$$A^T Ax = A^T b$$

whose solution $x \in D$ is unique if $rank(A) = n$.

Under the assumption of compatibility, the Gauss-Newton method displays locally q-quadratic convergence. Let us first refer to the classical result by Dennis/ Schnabel (1983) (p. 222/223):

Theorem 3.5.3. *Let $F : D \subseteq \mathbb{R}^n \to \mathbb{R}^m$, D again open and convex subset of $\mathbb{R}^n$ and $\frac{1}{2}F(x)^T F(x)$ be twice continuously differentiable. Provided that the Lipschitz condition for the Jacobian*

$$\|F'(y) - F'(x)\|_2 \leq \gamma \|y - x\|_2$$

holds and $x, y \in D$, $\beta > 0$

$$\|F'(x)\|_2 \leq \beta$$

holds, we have to assume that there exists $x_* \in D$ solution and $\sigma \leq 0$ constant such that

$$\|(F'(x) - F'(x_*))^T F(x_*)\|_2 \leq \sigma \|x - x_*\|_2$$

within D. Finally, let $\lambda > 0$, $\sigma \geq 0$ such that for $F'(x_*)^T F(x_*) = 0$, λ is the smallest eigenvalue of the matrix product of the Jacobian $F'(x_*)^T F'(x_*)$. If $0 \leq \sigma < \lambda$, then for any constant $c \in (1, \frac{\lambda}{\sigma})$ there exists $\rho > 0$ so that the Gauss-Newton sequence $\{x_k\}$ is well defined and converges towards $x_* \in D$ for all starting values $x_0 \in B(x_*, \rho)$ in the ρ-neighbourhood of the solution obeying

$$\|x_{k+1} - x_*\|_2 \leq \frac{c\sigma}{\lambda}\|x_k - x_*\|_2 + \frac{1}{2}\frac{c\beta\gamma}{\lambda}\|x_k - x_*\|_2^2 \tag{3.5.3}$$

and

$$\|x_{k+1} - x_*\|_2 \leq \frac{c\sigma + \lambda}{2\lambda}\|x_k - x_*\|_2 < \|x_k - x_*\|_2. \tag{3.5.4}$$

Proof of 3.5.3. Assume that $\lambda > \sigma \geq 0$ and let hence $c \in (1, \frac{\lambda}{\sigma})$ be a fixed constant. The proof is performed by induction on $k = 0, 1, \ldots$.

$k = 0$:
$\|\cdot\|_2$ denoting the standard Euclidean vector or induced matrix norm, respectively, we can find $\tilde{\rho} > 0$ such that $F'(x_0)^T F'(x_0)$ is nonsingular for any starting value $x_0 \in B(x_*, \tilde{\rho})$ with

$$\|F'(x_0)^T F'(x_0)\|_2 \leq \frac{c}{\lambda}.$$

Furthermore, let

$$\rho = \min\left\{\tilde{\rho}, \frac{\lambda - c\sigma}{c\beta\gamma}\right\}.$$

The Gauss-Newton iteration performs

$$\begin{aligned} x_{k+1} &= x_k + \Delta x_k \\ &= x_k - (F'(x_k)^T F'(x_k))^{-1} F'(x_k)^T F(x_k). \end{aligned}$$

and the first iterative x_1 is well defined by

$$\begin{aligned} x_1 - x_* &= x_0 - (F'(x_0)^T F'(x_0))^{-1} F'(x_0)^T F(x_0) - x_* \\ &= (F'(x_0)^T F'(x_0))^{-1} \left(-F'(x_0)^T F(x_0) - F'(x_0)^T F'(x_0)(x_* - x_0)\right) \\ &= (F'(x_0)^T F'(x_0))^{-1} \left(-F'(x_0)^T F(x_0) - F'(x_0)^T F'(x_0)(x_* - x_0)\right) \\ &= (F'(x_0)^T F'(x_0))^{-1} \left(F'(x_0)^T F(x_*) - F'(x_0)^T F(x_*) - F'(x_0)^T F(x_0)\right. \\ &\quad \left. -F'(x_0)^T F'(x_0)(x_* - x_0)\right) \\ &= (F'(x_0)^T F'(x_0))^{-1} \left(F'(x_0)^T F(x_*) + F'(x_0)^T \left(F(x_*) - F(x_0)\right.\right. \\ &\quad \left.\left. -F'(x_0)(x_* - x_0)\right)\right) \\ &= F'(x_0)^{-1}(F'(x_0))^T)^{-1} F'(x_0)^T \left(F(x_*) - F(x_0) - F'(x_0)(x_* - x_0)\right) \\ &\quad - F'(x_0)^{-1}(F'(x_0))^T)^{-1} F'(x_0)^T F(x_*) \\ &= F'(x_0)^{-1} \left(F(x_*) - F(x_0) - F'(x_0)(x_* - x_0)\right) - F'(x_0)^{-1} F(x_*). \end{aligned}$$

$F : D \subseteq \mathbb{R}^n \to \mathbb{R}^m$ is continuously differentiable and $x_0 \in B(x_*, \rho)$, it is

$$\begin{aligned} F(x_*) - F(x_0) - F'(x_0)(x_* - x_0) &\overset{x_* := x+p}{=} F(x_0 + p) - F(x_0) - F'(x_0)P \\ &= \int_0^1 F'(x_0 + tp)p \, dt - F'(x_0)p \\ &= \int_0^1 F'(x_0 + tp)p - F'(x_0)p \, dt \\ &= \int_0^1 (F'(x_0 + tp) - F'(x_0))p \, dt. \end{aligned}$$

The triangle inequality for the appropriate Riemann integral yields

$$\left\| \int_0^1 F'(x_0 + tp)p \, dt \right\|_2 \leq \int_0^1 \|F'(x_0 + tp)p\| \, dt$$

such that by the homogeneity of the norms

$$\begin{aligned} \|F(x_*) - F(x_0) - F'(x_0)(x_* - x_0)\|_2 &= \left\| \int_0^1 (F'(x_0 + tp) - F'(x_0))p \, dt \right\|_2 \\ &\leq \int_0^1 \|(F'(x_0 + tp) - F'(x_0))p\|_2 \, dt \\ &\leq \int_0^1 \|(F'(x_0 + tp) - F'(x_0))\|_2 \, \|p\|_2 \, dt. \end{aligned}$$

Claiming Lipschitz continuity of the Jacobian matrix F' at x_* in the open and convex neighbourhood D, yields

$$\begin{aligned} \|F(x_*) - F(x_0) - F'(x_0)(x_* - x_0)\|_2 &\leq \int_0^1 \gamma \|(x_0 + tp) - x_0\|_2 \|p\|_2 \, dt \\ &= \int_0^1 \gamma \|t\|_2 \|p\|_2^2 \, dt \\ &= \gamma \|p\|_2^2 \int_0^1 \|t\|_2 \, dt \\ &= \frac{\gamma}{2} \|x_* - x_0\|^2 \end{aligned}$$

since $p := x_* - x_0$. The problem is furthermore assumed to satisfy

$$F'(x_*)^T F(x_*) = 0.$$

The second condition in Theorem 3.5.3 consequently gives

$$\begin{aligned} \|F'(x_0)^T F(x_*)\|_2 &= \|F'(x_0)^T F(x_*) - F'(x_*)^T F(x_*)\|_2 \\ &= \|(F'(x_0)^T - F'(x_*)^T)F(x_*)\|_2 \\ &\leq \sigma \|x_0 - x_*\|_2. \end{aligned}$$

The previously shown combined with the knowledge of the Jacobian's upper boundedness by

$$\|F'(x_0)\|_2 \leq \beta$$

for the initial value x_0, q-quadratic local convergence is obtained by application of the triangle inequality.

$$\begin{aligned}
\|x_1 - x_*\|_2 &= \|(F'(x_0)^T F'(x_0))^{-1}\big(F'(x_0)^T F(x_*) + F'(x_0)^T(F(x_*) - F(x_0) \\
&\quad - F'(x_0)(x_* - x_0))\big)\|_2 \\
&\leq \|(F'(x_0)^T F'(x_0))^{-1}\|_2 \|F'(x_0)^T F(x_*) + F'(x_0)^T\big(F(x_*) - F(x_0) \\
&\quad - F'(x_0)(x_* - x_0)\big)\|_2 \\
&\leq \|(F'(x_0)^T F'(x_0))^{-1}\|_2 \left(\|F'(x_0)^T F(x_*)\|_2 + \|F'(x_0)^T(F(x_*) - F(x_0)\right. \\
&\quad \left. -F'(x_0)(x_* - x_0))\|_2\right) \\
&\leq \frac{c}{\lambda}\left(\sigma\|x_0 - x_*\|_2 + \frac{\beta\gamma}{2}\|x_0 - x_*\|^2\right) \\
&= \frac{c\sigma}{\lambda}\|x_0 - x_*\|_2 + \frac{\beta c\gamma}{2\lambda}\|x_0 - x_*\|_2^2
\end{aligned}$$

Local convergence behaviour of the Gauss-Newton method is driven by a linear and a quadratic factor. Completing the proof for the case $k = 0$, it remains to show that the first iterate x_1 remains in the neighbourhood of the solution x_*. This can be acknowledged viewing

$$\begin{aligned}
\|x_1 - x_*\|_2 &\leq \left(\frac{1}{2}\frac{\beta c\gamma}{\lambda}\|x_0 - x_*\|_2 + \frac{c\sigma}{\lambda}\right)\|x_0 - x_*\|_2 \\
&\leq \left(\frac{1}{2}\frac{\lambda - c\sigma}{\lambda} + \frac{c\sigma}{\lambda}\right)\|x_0 - x_*\|_2 \\
&= \frac{1}{2}\frac{c\sigma + \lambda}{\lambda}\|x_0 - x_*\|_2 \\
&< \|x_0 - x_*\|_2,
\end{aligned}$$

since on the one hand it is

$$\|x_0 - x_*\|_2 \leq \frac{\lambda - c\sigma}{c\beta\gamma}$$

by the choice of $\rho > 0$ and by the choice of $c \in (1, \frac{\lambda}{c})$

$$\frac{1}{2}\frac{c\sigma + \lambda}{\lambda} = \frac{1}{2}\left(\frac{c\sigma}{\lambda} + 1\right) < 1$$

for $0 \leq \sigma < \lambda$ and $x_0 \in B(x_*, \rho)$ already by the induction assumption. The induction step $k \to k + 1$ performs analogously and will be omitted here. □

Dennis/ Schnabel (1983) (p. 222) remark that the Gauss-Newton method may not locally converge at all if the evaluation of the Hessian $F''(x)$ is omitted even if one is not dealing with a zero- or small residual problem.

Comparing the convergence statements for the Gauss-Newton method by Dennis/Schnabel (1983) and by Deuflhard (2006), Dennis/ Schnabel do not claim explicitly compatibility

$$F(x_*) = 0.$$

Nonetheless the condition given in Theorem 3.5.3, it was

$$F'(x_*)^T F(x_*) = 0,$$

implicitly claims a zero residual problem as simultaneously

$$F'(x_*)^T F'(x_*)$$

is required to have strictly positive eigenvalues. This equivalently means that the Jacobian is assumed to have full rank and $F'(x_*)^T F'(x_*)$ should not be rank deficient. Then, of course, the uniqueness of the solution $x_* \in D$ is guaranteed.

Obviously, one can also prove local q-quadratic convergence for a rank deficient Jacobian, whereas the uniqueness of the solution x_* cannot be maintained. For this reason, getting back to affine invariance theory, convergence of the Gauss-Newton method is examined referring to Deuflhard/ Hohmann (2003) and Deuflhard (2006) (p. 175 ff). The more general convergence statement also applicable for rank deficient Jacobians is reviewed. In order to obtain the corresponding convergence result as Dennis/ Schnabel (1983), Deuflhard (2006) still needs to claim full rank of the Jacobian. This result will follow in the second part of this paragraph together with a useful error estimate. A direct application of affine covariant transformations to the classical statement of Dennis/ Schnabel (1983) would require further assumptions, since the Lipschitz continuity

$$\|F'(y) - F'(x)\| \leq \gamma \|y - x\|_2$$

and the nonlinearity measure

$$\|F'(x)\|_2 \leq \beta$$

of Theorem 3.5.3 are not affine invariant. Deuflhard (2006), p. 175ff., introduces a more general Lipschitz condition specifically designed for the affine invariant framework and some useful tools within solving the nonlinear least square problems.

Lemma 3.5.4. *The overdetermined linear least squares problem*

$$\min \|Ax - b\|_2$$

where $A \in \mathbb{R}^{m,n}$, $x \in \mathbb{R}^n$, $b \in \mathbb{R}^m$ and $m > n$ has a unique solution x_* if and only if

$$rank(A) = n.$$

In the rank deficient case, namely $rank(A) = p \leq n$, the solutions form an affine subspace X_*. If we denote by x_* the shortest distance solution in the sense of

$$\|x_*\|_2 \leq \|x\|_2$$

for all possible solutions $x \in X_*$, the general solution can be written as

$$x = x_* + z$$

where $z \in \mathcal{N}(A)$ the null space of A. Consequently, all solutions can be obtained by translation of $\mathcal{N}(A)$ by x_* and the shortest distance solution x_* is precisely the unique vector orthogonal to the null space.

Definition 3.5.5. *For $0 \leq rank(A) \leq n$ the solution x_* is unique in both the full rank and the*

rank deficient case and is formally written as

$$x_* = A^+ b.$$

A^+ is called Moore Penrose pseudo inverse and is a special generalised inverse that is uniquely defined by the following four Penrose axioms

$$\begin{aligned}(A^+A)^T &= A^+A\\ (AA^+)^T &= AA^+\\ A^+AA^+ &= A^+\\ AA^+A &= A.\end{aligned}$$

If $rank(A) = n$, then the minimisation problem

$$\min \|Ax - b\|_2^2$$

can be equivalently rewritten as the normal equation

$$A^T Ax = A^T b$$

which is uniquely solvable with

$$x = A^+ b$$

for $A^+ = (A^T A)^{-1} A^T b$ a since $A^T A$ is nonsingular if $rank(A) = n$.

Annotation 3.5.6. *Note that for $x \in D$, solving*

$$F'(x)^{-1} F(x) = 0$$

is equivalent to considering the equation

$$F'(x)^+ F(x) = 0$$

as by the definition of the pseudo inverse it holds

$$F'(x)^+ = (F'(x)^T F'(x))^{-1} F'(x)^T = F'(x)^{-1} (F'(x)^T)^{-1} F'(x)^T = F'(x)^{-1}$$

if $rank(F'(x)) = n$.

Annotation 3.5.7. *Remark, that* Deuflhard *(2006) (p. 176) introduces two more generalised inverses, the outer and inner inverse which satisfy each only two of the Penrose axioms. In case of full rank, i.e. $rank(A) = n$, the outer or respectively the inner inverse and the Moore Penrose pseudo inverse are identical.*
Hence, the Moore Penrose pseudo inverse is both an inner and outer inverse and has to be considered a special case since contrary to inner and outer inverses, it is uniquely defined by the Penrose axioms even in the rank deficient case.

Full rank problems are rather uncommon in applications. A local convergence proof in an affine invariant setting holding true also for the rank deficient case is presented. Deuflhard (2006) (p. 176) does herein introduce the outer inverse and herewith conducts the local convergence proof for the Gauss-Newton method. Note that this generalised convergence result only gives an estimate for two neighbour iterates. The result corresponding to the *classical* theory of Dennis/

SCHNABEL (1983), considering $\|x_k - x_*\|_2$ requires a full rank Jacobian matrix again.

Before continuing with the local Gauss-Newton convergence result in the error-oriented setting, presented in DEUFLHARD (2006), note that especially in the rank deficient case, the outer inverse is not uniquely defined. At a later stage, when a globalisation of the Gauss-Newton method is considered, one needs a uniquely defined generalised inverse to estimate the Lipschitz constants for the damping strategy. For this reason, the proof presented by DEUFLHARD (2006) (p. 194) is restricted here in the sense that only the special case involving the Moore Penrose pseudo inverse is considered.

Theorem 3.5.8. *Let $F : D \subseteq \mathbb{R}^n \to \mathbb{R}^m$, D open and convex, denote a continuously differentiable mapping. The Jacobian being possibly rank deficient, let $F'(x)^+$ be its Moore Penrose inverse for any $x \in D$. Assume that one can find a starting point $x_0 \in D$, a mapping $\kappa : D \to \mathbb{R}^+$ and constants $\alpha, \omega, \overline{\kappa} \geq 0$ such that*

(i) $\|\Delta x_0\|_2 \leq \alpha$,

(ii) $\|F'(z)^+(F'(y) - F'(x))(y - x)\|_2 \leq \omega\|y - x\|_2^2$ *Lipschitz type continuous for all $x, y, z \in D$ collinear and $(y - x) \in \mathcal{R}(F'(x)^+)$,*

(iii) $\|F'(y) - \overline{P}^{\perp}(x)F(x)\|_2 \leq \kappa(x)\|y - x\|_2$ *for all $x, y \in D$, $\kappa(x) \leq \overline{\kappa} < 1$ for all $x \in D$ and*

(iv) $\overline{B}(x_o, \rho) \subseteq D$ *with* $\rho := \dfrac{\alpha}{1 - \overline{\kappa} - \frac{1}{2}\alpha\omega}$ *while $\alpha\omega < 2(1 - \overline{\kappa})$.*

Then, the sequence $\{x_k\}$ of the Gauss-Newton iterates is well defined and remains in the closed ball $\overline{B}(x_o, \rho)$, i.e.

$$\|x_k - x_0\|_2 \leq \rho.$$

Furthermore, $\{x_k\}$ converges to some $x_* \in \overline{B}(x_o, \rho)$ with

$$F'(x_*)^+F(x_*) = 0$$

and a convergence rate that can be estimated through

$$\|x_{k+1} - x_k\|_2 \leq \frac{1}{2}\omega\|x_k - x_{k-1}\|_2^2 + \kappa(x_{k-1})\|x_k - x_{k-1}\|_2. \tag{3.5.5}$$

Proof of 3.5.8. Let $x_{k-1}, x_k \in D$ for $k \geq 1$. A^+ denotes the Moore Penrose inverse. The following projectors naturally emerge by its definition

$$\overline{P} := AA^+$$
$$\overline{P}^{\perp} := I_m - \overline{P} = I_m - AA^+$$

whilst the orthogonality properties directly follow as $\overline{P}^2 = \overline{P}$ and $\overline{P}^T = \overline{P}$. In the Gauss-Newton iteration

$$F'(x_k)^T F'(x_k)\Delta x_k = -F'(x_k)^T F(x_k)$$
$$x_{k+1} = x_k + \Delta x_k$$

one formally needs to solve

$$\Delta x_k = -F'(x_k)^+ F(x_k).$$

This immediately yields

$$\begin{aligned}
\|x_{k+1} - x_k\|_2 &= \|x_k - \Delta x_k - x_k\|_2 = \| - F'(x_k)^+ F(x_k)\|_2 \\
&= \|F'(x_k)^+ (F(x_k) - F(x_{k-1}) + F(x_{k-1}) - F'(x_{k-1})(x_k - x_{k-1}) \\
&\quad + F'(x_{k-1})(x_k - x_{k-1}))\|_2 \\
&= \|F'(x_k)^+ (F(x_k) - F(x_{k-1}) - F'(x_{k-1})(x_k - x_{k-1})) + F'(x_k)^+ F(x_{k-1}) \\
&\quad + F'(x_k)^+ F'(x_{k-1})(-F'(x_{k-1})^+ F(x_{k-1})\|_2 \\
&= \|F'(x_k)^+ (F(x_k) - F(x_{k-1}) - F'(x_{k-1})(x_k - x_{k-1})) + F'(x_k)^+ F(x_{k-1}) \\
&\quad - F'(x_k)^+ F'(x_{k-1} F'(x_{k-1})^+ F(x_{k-1})\|_2 \\
&= \|F'(x_k)^+ (F(x_k) - F(x_{k-1}) - F'(x_{k-1})(x_k - x_{k-1})) \\
&\quad + F'(x_k)^+ (I - F'(x_{k-1}) F'(x_{k-1})^+) F(x_{k-1})\|_2 \\
&\leq \|F'(x_k)^+ (F(x_k) - F(x_{k-1}) - F'(x_{k-1})(x_k - x_{k-1}))\|_2 \\
&\quad + \|F'(x_k)^+ (I - F'(x_{k-1}) F'(x_{k-1})^+) F(x_{k-1})\|_2.
\end{aligned}$$

The Lipschitz type condition and the defined orthogonal projectors then directly give

$$\begin{aligned}
&\|F'(x_k)^+ F(x_{k-1}) - F'(x_k)^+ F'(x_{k-1}) F'(x_{k-1})^+ F(x_{k-1})\|_2 \\
&\qquad = \|F'(x_k)^+ (I - F'(x_{k-1}) F'(x_{k-1})^+) F(x_{k-1})\|_2 \\
&\qquad = \|F'(x_k)^+ (I - \overline{P}(x_{k-1}) F(x_{k-1})\|_2 \\
&\qquad = \|F'(x_k)^+ \overline{P}^{\perp}(x_{k-1}) F(x_{k-1})\|_2 \\
&\qquad \leq \kappa(x_{k-1}) \|x_k - x_{k-1}\|_2
\end{aligned}$$

using condition (iii) from above. Claiming condition (ii) to hold, application of the Lagrangian mean value theorem consequently yields

$$\begin{aligned}
\|x_{k+1} - x_k\|_2 &\leq \|F'(x_k)^+ (F(x_k) - F(x_{k-1}) - F'(x_{k-1})(x_k - x_{k-1}))\|_2 \\
&\quad + \|F'(x_k)^+ (I - F'(x_{k-1}) F'(x_{k-1})^+) F(x_{k-1})\|_2 \\
&\leq \frac{\omega}{2} \|x_k - x_{k-1}\|_2^2 + \kappa(x_{k-1}) \|x_k - x_{k-1}\|_2.
\end{aligned}$$

This already proves the local estimate for two neighbour Gauss-Newton iterates and it remains to show that for all iterates $x_k, x_{k-1} \in D$, $k \geq 1$ it holds true

$$\|x_k - x_{k-1}\|_2 \leq \rho.$$

Let therefore the starting point $x_0 \in D$ satisfy condition (i), i.e.

$$\|\Delta x_0\|_2 \leq \alpha$$

where $\overline{B}(x_0, \rho) \subseteq D$ by condition (iv). Defining the radius $\rho := \dfrac{\alpha}{1 - \overline{\kappa} - \dfrac{\alpha\omega}{2}}$ with $\alpha\omega < 2(1 - \overline{\kappa})$, it is precisely

$$\overline{B}(x_0, \rho) := \{x \in \mathbb{R}^n : \|x - x_0\|_2 \leq \rho\}.$$

First, for $k = 1$ it is

$$\begin{aligned}\|x_2 - x_1\|_2 &\leq \kappa(x_0)\|x_1 - x_0\|_2 + \frac{\omega}{2}\|x_1 - x_0\|_2^2 \\ &\leq \left(\kappa(x_0) + \frac{\alpha\omega}{2}\right)\|x_1 - x_0\|_2 \\ &\leq \left(\overline{\kappa} + \frac{\alpha\omega}{2}\right)\|\Delta x_0\|_2.\end{aligned}$$

Choosing $\alpha\omega < 2(1 - \overline{\kappa})$, it hence holds by definition that $\frac{\omega\alpha}{2} + \overline{\kappa} < (1 - \overline{\kappa}) - \overline{\kappa} = 1$, such that

$$\|x_1 - x_0\|_2 < \|\Delta x_0\|_2 \leq \alpha.$$

The induction step $(k-1) \to k$ for $k \geq 1$ builds on the same arguments, i.e. for all $k \geq 1$

$$\begin{aligned}\|x_{k+1} - x_k\|_2 &\leq \kappa(x_{k-1})\|x_k - x_{k-1}\|_2 + \frac{\omega}{2}\|x_k - x_{k-1}\|_2^2 \\ &\leq \left(\kappa(x_{k-1}) + \frac{\alpha\omega}{2}\right)\|x_k - x_{k-1}\|_2 \\ &\leq \left(\overline{\kappa} + \frac{\alpha\omega}{2}\right)\|x_k - x_{k-1}\|_2.\end{aligned}$$

For any $l \geq k \geq 0$, applying the Gauss-Newton iteration gives with the triangle inequality

$$\begin{aligned}\|x_{l+1} - x_k\|_2 &= \|x_l + \Delta x_l - x_k\|_2 \\ &= \|x_{l-1} + \Delta x_{l-1} + \Delta x_l - x_k\|_2 \\ &\leq \|\Delta x_l\|_2 + \cdots + \|\Delta x_k\|_2.\end{aligned}$$

Since

$$\begin{aligned}\|x_{l+1} - x_l\|_2 &\leq \left(\overline{\kappa} + \frac{\alpha\omega}{2}\right)\|x_l - x_{l-1}\|_2^2 \\ &\leq \left(\overline{\kappa} + \frac{\alpha\omega}{2}\right)^{l-k}\|x_k - x_{k-1}\|\end{aligned}$$

by the induction argumentation, one straightforward obtains for all $l \geq k$

$$\begin{aligned}\|x_{l+1} - x_k\|_2 &\leq \|x_{l+1} - x_l\|_2 + \|x_l - x_{l-1}\|_2 + \cdots + \|x_{k+1} - x_k\|_2 \\ &\leq \sum_{j=0}^{\infty}\left(\overline{\kappa} + \frac{\alpha\omega}{2}\right)^j\|x_k - x_{k-1}\|_2 \\ &= \frac{1}{1 - \left(\overline{\kappa} + \frac{\alpha\omega}{2}\right)}\|x_k - x_{k-1}\|_2 \\ &= \frac{1}{1 - \overline{\kappa} - \frac{\alpha\omega}{2}}\|x_k - x_{k-1}\|_2\end{aligned}$$

Consequently, for the case $k = 0$ this estimate gives for all $l \geq 0$ that

$$\begin{aligned}\|x_{l+1} - x_0\|_2 &\leq \frac{1}{1 - \overline{\kappa} - \frac{\alpha\omega}{2}}\|x_1 - x_0\|_2 \\ &\leq \frac{\alpha}{1 - \overline{\kappa} - \frac{\alpha\omega}{2}},\end{aligned}$$

which defines the radius of the ball $\overline{B}(x_0, \rho)$ for $\|\Delta x_0\|_2 \leq \alpha$. Summarising, all Gauss-Newton iterates $\{x_k\}$ remain in the closure of the ball $\overline{B}(x_0, \rho)$ around the starting value $x_0 \in D$ with radius

$$\rho := \frac{\alpha}{1 - \overline{\kappa} - \frac{\alpha\omega}{2}} > 0.$$

For $k \to \infty$, the distance between two neighbour iterates gets arbitrarily small such that for the sequence of the Gauss-Newton correction it holds

$$\Delta x_k = -F'(x_k)^+ F(x_k) \overset{k\to\infty}{\longrightarrow} 0 = F'(x_*)^+ F(x_*),$$

resulting in

$$\lim_{k\to\infty} x_k = x_*.$$

□

The above results apply for the full rank as well as for the rank deficient case regarding the Jacobian. One can show that there exists a solution x_* in terms of shortest distance. But if now a full rank Jacobian matrix is claimed – which means sharper assumptions than in the previous Theorem – then the solution x_* is unique. Under this additional assumption, Deuflhard (2006), p. 195, proves q-quadratic convergence rate for the Gauss-Newton method with respect to the solution point x_*. This is the (directly) comparable result to the *classical* convergence theorem of Dennis/ Schnabel (1983).

Theorem 3.5.9. *Under the same assumptions as in Theorem 3.5.8, let the Jacobian satisfy*

$$rank(F'(x)) = n$$

for all $x \in D$. Then, the orthogonal projector defines $P(x) = F'(x)^+ F'(x) = I \in \mathbb{R}^{n,n}$. Assuming that a solution $x_* \in D$ exists with $F'(x_*)^+ F(x_*) = 0$, let it be

$$\|x_0 - x_*\|_2 < \frac{2}{\omega}(1 - \kappa(x_*)) := \alpha_*.$$

Then, the solution $x_* \in D$ is unique in the open neighbourhood $B(x_*, \alpha_*)$ and the Gauss-Newton method converges in the closure of the ball $\overline{B}(x_*, \|x_0 - x_*\|_2)$ for any $x_0 \in B(x_*, \alpha_*)$ with an estimated rate of

$$\|x_{k+1} - x_*\|_2 \leq \left(\kappa(x_*) + \frac{\omega}{2}\|x_k - x_*\|_2\right) \|x_k - x_*\|_2.$$

Proof of 3.5.9. Previously, under the condition that $\|\Delta x_0\|_2 \leq \alpha$ it was

$$\alpha\omega < 2(1 - \overline{\kappa}).$$

Assuming a full rank Jacobian, let $\kappa(x_*)$ be such that on the one hand

$$\kappa(x_*) \leq \overline{\kappa} < 1$$

and on the other hand

$$\alpha\omega < 2(1 - \overline{\kappa}) \leq 2(1 - \kappa(x_*)).$$

This simultaneously implies

$$\alpha < \frac{2}{\omega}(1 - \overline{\kappa}) \leq \frac{2}{\omega}(1 - \kappa(x_*)) := \alpha_*.$$

The requirement

$$\|x_0 - x_*\|_2 < \frac{2}{\omega}(1 - \kappa(x_*)) := \alpha_*$$

is sharper than the corresponding result of Theorem 3.5.8, referring to Deuflhard (2006), p. 195, where all Gauss-Newton iterates remain in the closed neighbourhood $\overline{B}(x_0, \rho)$ for $\rho = \frac{\alpha}{1-\overline{\kappa}-\frac{\alpha\omega}{2}}$ since

$$\|x_0 - x_*\|_2 \leq \frac{\alpha}{1 - \overline{\kappa} - \frac{\alpha\omega}{2}} < \frac{\alpha_*}{1 - \overline{\kappa} - \frac{\alpha\omega}{2}}.$$

Then, the estimate for the convergence rate proceeds

$$\begin{aligned}
\|x_{k+1} - x_*\|_2 &= \|F'(x_k)^+ F(x_*) - F'(x_k)^+ F(x_*) - F'(x_k)^+ F(x_k) - (x_* - x_k)\|_2 \\
&= \|F'(x_k)^+ (F(x_*) - F(x_k) - F'(x_k)(x_* - x_k)) - F'(x_k)^+ F(x_*)\|_2 \\
&\leq \|F'(x_k)^+ (F(x_*) - F(x_k) - F'(x_k)(x_* - x_k))\|_2 + \|F'(x_k)^+ F(x_*)\|_2 \\
&\leq \frac{\omega}{2}\|x_* - x_k\|_2^2 + \|F'(x_k)^+ (I - F'(x_*)F'(x_*)^+) F(x_*)\|_2 \\
&= \frac{\omega}{2}\|x_* - x_k\|_2^2 + \|F'(x_k)^+ \overline{P}^{\perp} F(x_*)\|_2 \\
&\leq \left(\kappa(x_*) + \frac{\omega}{2}\|x_k - x_*\|_2\right) \|x_k - x_*\|_2
\end{aligned}$$

which clearly incorporates a term of locally linear convergence for adequate and a term of quadratic convergence for compatible problems. For all Gauss-Newton iterates holds true

$$x_{k+1} \in \overline{B}(x_*, \|x_0 - x_*\|_2)$$

for any $x_0 \in B(x_*, \alpha_*)$ chosen close enough to the solution x_* with $\|x_0 - x_*\|_2 < \alpha_*$, as due to the estimated speed of convergence in the full rank case

$$\|x_{k+1} - x_*\|_2 \leq \left(\kappa(x_*) + \frac{\omega}{2}\|x_k - x_*\|_2\right) \|x_k - x_*\|_2$$

the multiplier becomes

$$\begin{aligned}
\left(\kappa(x_*) + \frac{\omega}{2}\|x_k - x_*\|_2\right) &\leq \left(\kappa(x_*) + \frac{\omega}{2}\|x_0 - x_*\|_2\right) \\
&< \frac{\alpha_*\omega}{2} + \kappa(x_*).
\end{aligned}$$

Consequently,

$$\|x_0 - x_*\| \leq \frac{\alpha}{1 - \overline{\kappa} - \frac{\alpha\omega}{2}} < \frac{\alpha_*}{1 - \overline{\kappa} - \frac{\alpha\omega}{2}}$$

and as by

$$\frac{\alpha_*\omega}{2} + \kappa(x_*) = \left(\frac{2(1 - \kappa(x_*))}{\omega}\frac{\omega}{2} + \kappa(x_*)\right) < 1,$$

the multiplier satisfies

$$\kappa(x_*) + \frac{\omega}{2}\|x_k - x_*\|_2 < \frac{\alpha_*\omega}{2} + \kappa(x_*) < 1.$$

Inductively the proof contracts for all $k \geq 0$ with

$$\|x_{k+1} - x_*\|_2 < \alpha_* = \frac{2}{\omega}(1 - \kappa(x_*)).$$

A unique solution solely exists in case the Jacobian displays full rank, which can be shown by contradiction. Let $x_{**} \neq x_*$ denote a different solution and $x_{**} \in B(x_*, \alpha_*)$. Starting with $x_0 := x_{**}$, the above shown indeed implies on the one hand

$$\|x_{**} - x_*\|_2 < \alpha_*$$

and on the other hand by application of the Lipschitz continuity and the Lagrange mean value theorem that

$$\begin{aligned}\|x_{**} - x_*\|_2 &\leq \left(\kappa(x_*) \ + \frac{\omega}{2}\|x_{**} - x_*\|_2\right)\|x_{**} - x_*\|_2 \\ &\leq \left(\kappa(x_*) + \frac{\alpha_*\omega}{2}\right)\|x_{**} - x_*\|_2\end{aligned}$$

with

$$\kappa(x_*) + \frac{\alpha_*\omega}{2} < 1.$$

This immediately gives the contradiction, why it must hold $x_{**} = x_*$. □

In the case of a full rank Jacobian, an error estimate relating the Euclidian distance between an iterate and the solution to the one between two neighbour iterates can be obtained by a similar deduction referring to Deuflhard (2006), p. 196.

Lemma 3.5.10. *Under the assumptions of Theorem 3.5.9, the distance between the k^{th} iterate of the Gauss-Newton sequence and the solution $x_* \in D$ can be bounded from above by the distance between two neighbour iterates x_k, x_{k-1} within the Euclidean standard norm, i.e.*

$$\|x_k - x_*\|_2 \leq \frac{1}{1 - \overline{\kappa} - \frac{\omega}{2}\|x_{k+1} - x_k\|_2}\|x_{k+1} - x_k\|_2. \tag{3.5.6}$$

Proof of 3.5.10. In the proof of Theorem 3.5.9, the convergence rate of the Gauss-Newton method could be estimated

$$\|x_{k+1} - x_*\|_2 \leq \left(\overline{\kappa} + \frac{\omega}{2}\|x_k - x_*\|_2\right)\|x_k - x_*\|_2.$$

Since Theorem 3.5.8 gave

$$\|x_{k+1} - x_k\|_2 \leq \left(\overline{\kappa} + \frac{\omega}{2}\|x_k - x_{k-1}\|_2\right)\|x_k - x_{k-1}\|_2.$$

For any $l \geq k \geq 0$ it holds true that

$$\begin{aligned}\|x_{l+1} - x_k\|_2 &\leq \|x_{l+1} - x_l\|_2 + \cdots + \|x_{k+1} - x_k\|_2 \\ &\leq \sum_{j=0}^{\infty}\left(\overline{\kappa} + \frac{\omega}{2}\|x_k - x_{k-1}\|_2\right)^j\|x_k - x_{k-1}\|_2\end{aligned}$$

since the induction argument gives

$$\|x_{l+1} - x_l\|_2 \leq \left(\overline{\kappa} + \frac{\omega}{2}\|x_k - x_{k-1}\|_2\right)^{l-k}\|x_k - x_{k-1}\|_2.$$

For the purpose of repeated induction, transforming the estimated convergence rate of Theorem

3.5.8 gives

$$\|x_{k+1} - x_k\|_2 \leq \left(\frac{\overline{\kappa}}{\|x_k - x_{k-1}\|_2} + \frac{\omega}{2} \right) \|x_k - x_{k-1}\|_2^2.$$

Abbreviating

$$\tilde{h}_k := \left(\frac{\overline{\kappa}}{\|x_k - x_{k-1}\|_2} + \frac{\omega}{2} \right) \|x_k - x_{k-1}\|_2,$$

multiplying the estimated convergence rate with

$$\frac{\overline{\kappa}}{\|x_k - x_{k-1}\|_2} + \frac{\omega}{2}$$

reveals the relation

$$\tilde{h}_k \leq (h_k)^2.$$

Contraction of these $\{\tilde{h}_k\}$ is obtained for

$$\tilde{h}_0 = \left(\frac{\overline{\kappa}}{\|\Delta x_0\|_2} + \frac{\omega}{2} \right) \|\Delta x_0\|_2 < 1.$$

Since the limit

$$\lim_{k \to \infty} \tilde{h}_k = 0$$

exists, and

$$\tilde{h}_k < \tilde{h}_{k-1} < \tilde{h}_0 < 1$$

application of the geometric series to the induction argument, given that

$$\kappa(x_*) + \frac{\omega}{2} \|x_k - x_*\|_2 < 1$$

from the proof of Theorem 3.5.9, yields

$$\|x_{l+1} - x_k\|_2 \leq \frac{1}{1 - \left(\overline{\kappa} + \frac{\omega}{2} \|x_k - x_{k-1}\|_2 \right)} \|x_k - x_{k-1}\|_2$$

which is

$$\|x_{l+1} - x_k\|_2 \leq \frac{1}{1 - \overline{\kappa} - \frac{\omega}{2} \|x_k - x_{k-1}\|_2} \|x_k - x_{k-1}\|_2.$$

For $l \to +\infty$, provided that the Gauss-Newton method terminates, after finitely many steps the solution $x_* \in D$ is reached.

$$\|x_* - x_k\|_2 \leq \frac{1}{1 - \overline{\kappa} - \frac{\omega}{2} \|x_k - x_{k-1}\|_2} \|x_{k+1} - x_k\|_2$$

□

Finally, before terminating this section, let us remark that Deuflhard (2006) (p. 198) introduces the so named incompatibility factor measuring the compatibility of the nonlinear least square problem. Defining

$$\kappa(x_*) := \sup_{x \in D} \frac{\|F'(x)^+ F(x_*)\|_2}{\|x - x_*\|_2} < 1$$

motivated by the previous local convergence proofs, a compatible problem obviously satisfies

$$F(x_*) = 0 \text{ with } \kappa(x_*) = 0.$$

A noncompatible problem, still satisfying

$$F(x_*) \neq 0 \text{ with } \kappa(x_*) < 1,$$

is called adequate nonlinear least square problem.

While Dennis/ Schnabel (1983) (p. 220) would refer to compatible and adequate nonlinear least square problems as zero or small residual problems, the Gauss-Newton method converges q-quadratically for the first (since the linear term vanishes) and locally linear for the second case (Deuflhard (2006), p. 199). Reviewing and comparing the proofs performed by Dennis/ Schnabel (1983) and Deuflhard (2006), classical convergence theory for the Newton method could easily be transferred to an affine invariant setting. The Newton method itself is affine invariant.
The Gauss-Newton method was deduced as a linearisation of the Newton method, where the evaluation of the Hessian tensor product is omitted, to adequately and efficiently solve compatible nonlinear least squares minimisation problems. The Gauss-Newton method was demonstrated not to be affine invariant in general. Applying affine contravariant transformations required a different approach to examine convergence behaviour. The Gauss-Newton method is only affine invariant with respect to so called right scaling (see chapter 4.2, 54 ff.). It converges "locally linearly for adequate and quadratically for compatible nonlinear least squares problems" (Deuflhard (2006), p. 199). Two corresponding convergence results, one emerging from *classical* theory and one from the affine contravariant setting were reviewed. In both cases, full rank of the Jacobian is required. The advantage of the affine invariant approach turned out to be Theorem 3.5.8, which gives a local convergence rate for rank deficient Jacobians also. Allowing rank deficiency as well as the use of inner and outer inverses makes Deuflhard's (2006) result slightly more general. Inner and outer inverses were not considered here though, only the Moore Penrose inverse as a special case.

After monitoring the convergence of the Gauss-Newton method which is to be applied to solve the parameter identification task in terms of a nonlinear least squares problem, highly nonlinear applications such as arising in medicine and biology require an enlarged convergence domain. Aiming at reducing the algorithm's dependence on starting values, an adaptive trust region approach is introduced to the Gauss-Newton method in chapter 4. This introduced step length strategy can be considered a globalisation of the standard Gauss-Newton approach. Once defined, a well performing algorithm to attack the nonlinear least squares problem is obtained. Evaluation of the sequences of linear systems involving the Jacobian matrix of the residual function is approached with a linearly-implicit Euler extrapolation, see section 4.4. The arising linear systems are solved via a customised QR decomposition or LU factorisation.
Summarising, the following chapter will adjust the parameter identification tools for the proposed model of section 2.3 from a computational point of view. These methods are applied to the proposed model using the Nlscon and Limex codes from *Konrad-Zuse Zentrum für Informationstechnologie Berlin* to obtain the simulation results presented in chapter 5.

4. Applied Parameter Identification

4.1. Motivation to Parameter Identification Problems

Following the idea of Gauss, parameter identification problems can be formulated as nonlinear least squares problems. In most applications, the parameters to be identified are given different weights to account for different magnitudes of the parameters. Hence, let us define the overdetermined, weighted nonlinear least squares problem

$$\min \frac{1}{M} \sum_{i=1}^{M} \left(\frac{y(t_i, x) - z_i}{\delta y_i} \right)^2 \tag{4.1.1}$$

where data points $z_i \in \mathbb{R}^d$ are measured for (up to) d components for $t_i \in \mathbb{R}$, $i = 1, \ldots, M$ time points. These pairs

$$(t_i, z_i)$$

are to be fitted to a model conjectured

$$y(t, x),$$

which is nonlinear with respect to the vector of parameters

$$x \in \mathbb{R}^n.$$

Equivalently, the weighting can be represented by a diagonal matrix

$$D_i := \begin{pmatrix} (\delta z_i)_1 & & 0 \\ & \ddots & \\ 0 & & (\delta z_i)_d \end{pmatrix} \in \mathbb{R}^{d,d} \tag{4.1.2}$$

while the δz_i denote the error tolerances. The problem then writes with the Euclidean norm

$$\min \frac{1}{M} \sum_{i=1}^{M} \| D_i^{-1} \left(y(t_i, x) - z_i \right) \|_2^2 \tag{4.1.3}$$

for $i = 1, \ldots, M$ measurement points, d species, a total number of n unknown parameters and $m := Md > n$. All theoretical background of chapter 3 applies also for the weighted nonlinear least squares problem if only it is defined

$$F(x) = \begin{pmatrix} F_1(x) \\ \vdots \\ F_M(x) \end{pmatrix} = \begin{pmatrix} D_1^{-1} \left(y(t_1, x) - z_1 \right) \\ \vdots \\ D_M^{-1} \left(y(t_M, x) - z_M \right) \end{pmatrix} \in \mathbb{R}^m \tag{4.1.4}$$

This notation yields the minimisation problem

$$\min_{x \in D} \| F(x) \|_2 \tag{4.1.5}$$

for $F : D \subseteq \mathbb{R}^n \to \mathbb{R}^m$, D open and convex. Minimising the relative deviation between measurement data and the proposed d dimensional model $y(t, x)$, the nonlinear least squares problem equivalently writes

$$\min_{x \in D} \frac{1}{2} F(x)^T F(x).$$

Sufficient conditions for a local minimum $x_* \in D$ are

$$\left(\frac{1}{2} F(x_*)^T F(x_*) \right)' = 0 \text{ with}$$

$$\left(\frac{1}{2} F(x_*)^T F(x_*) \right)''$$

positive definite. Hence, the problem can be reformulated as finding the solution to the nonlinear system

$$F'(x)^T F(x) = 0.$$

Let us claim that the model and data fully agree at the solution

$$F(x_*) = 0.$$

The initial problem is linearised by applying the Gauss-Newton method, which leads to a sequence of linear least squares problems for each iteration step k

$$\begin{aligned} \min_{x \in D} & \|F'(x_k)\Delta x_k + F(x_k)\|_2^2 \\ x_{k+1} &= x_k + \Delta x_k, \\ k &= 1, 2, \ldots. \end{aligned}$$

For computational reasons, an enlarged convergence domain is preferable for the Gauss-Newton method. A globalisation is reviewed in paragraph 4.3, treating an adaptive trust region step length strategy applicable for the Gauss-Newton method (Deuflhard (2006), p. 212 ff.). Basically, the damping strategy is based on a predictor corrector method testing the monotonicity of two neighbour iterate's descent. The gradient system arising by application of the Gauss-Newton algorithm requires evaluation of the residual function and computation of the latter's Jacobian matrix. Since

$$F_i(x_k) := D_i^{-1} \left(y(t_i, x) - z_i \right)$$

is componentwise defined for all $i = 1, \ldots, M$, for a fixed parameter set $x_k \in \mathbb{R}^n$, a solution to the initial DAE model

$$B(y, x_k) y'(t, x_k) = f(y, x_k)$$

has to be computed. In this case, an extrapolation method based on the linearly-implicit Euler discretisation seems applicable to solve the DAE system which is introduced in paragraph 4.4. An appropriate algorithmic implementation is realized in the Limex code available through Poem software (Hairer/ Nørsett/ Wanner (1987), Ehrig/ Nowak/ Deuflhard (1996), Deuflhard/ Hairer/ Zugck (1987), Schlegel/ Marquardt/ Ehrig/ Nowak (2002)). Once a solution to the DAE system is obtained for the k^{th} iteration, the initial problem has reduced to a system of linear equations which is solved by a customised QR or LU decomposition.

In the subsequent, first a short note on incorporation of constraints during the optimisation process is made.

Followed by the idea and definition of the globalised Gauss-Newton method applied, an adaptive trust region damping strategy is deduced referring to Deuflhard (2006).
Then, the mathematical background necessary to solve the DAE system for every Gauss-Newton update is shortly reviewed. After these preparations motivated from the computational point of view, the initial task can be approached.
The proposed model is evaluated using the tools of this chapter and parameters are identified. A simulation and model analysis for a test data set is given in the following chapter (chapter 5, p. 78).

4.2. Parametrisation and Constraints

Enforcing either positiveness, upper or lower boundedness of the parameters to be identified in the model, optimisation is subject to specific constraints. Any differentiable transformation can be applied to the parameter vector $x \in D \subseteq \mathbb{R}^n$ Following Dierkes/Wade/ Nowak/Röblitz (2011) (p. 6), the model's differential equation system is parametrised by a transformation

$$\Phi : \mathbb{R}^n \to \mathbb{R}^n$$

such that with $x = \Phi(u)$ and

$$F(x) = F(\Phi(u)) =: \tilde{F}(u)$$

the initial differential system writes

$$F(\Phi(u))' = F'(x)\Phi(u) \Leftrightarrow \tilde{F}'(u) = F'(x)\Phi(u)$$

where $u \in \mathbb{R}^n$ stands for changed parametrisation. Covering the above mentioned three fundamental constraints to be applied, it is proposed to use a componentwise exponential transformation

$$x_i = exp(u_i)$$

for $i = 1, \ldots, n$, if a global positivity constraint $x > 0$ is imposed. Requiring the parameters to be bounded by a lower bound A and an upper bound B such that

$$A \leq x \leq B$$

Dierkes/Wade/ Nowak/Röblitz (2011) propose a sinusoidal transformation

$$x_i = \Phi(u_i) = A + \frac{B - A}{2}(1 + \sin(u_i))$$

for $i = 1, \ldots, n$. For a single bound, C, accounting either for a lower or an upper bound

$$x \leq C \text{ or } x \geq C$$

a simple square root transformation would be eligible following componentwise

$$x_i = \Phi(u_i) = C \pm \left(1 - \sqrt{1 + (u_i)^2}\right).$$

Dierkes/Wade/ Nowak/Röblitz (2011) (p. 6) note that variation within parametrisation of the system lead to changes in the sensitivities of the parameters. in order to maintain the dynamical behaviour of the model as well as its physical meaning (e.g. positivity constraint for population dynamics), only necessary constraints should be applied.

The weighted nonlinear least squares problem obviously involves left scaling of the residual function through application of a diagonal matrix . In the case of row scaling, different scaling applied to the nonlinear least squares problem leads to different solutions, while right scaling leaves the problem affine invariant. The Gauss-Newton method itself is only affine invariant to parameter scaling generally defined by

$$x = D_R \tilde{x}$$

provided the Jacobian matrix has full rank, since this gives for the Gauss-Newton correction of the scaled vector $\tilde{x} \in \mathbb{R}^n$

$$\Delta \tilde{x}_k = -H'(D_R^{-1} x_k)^+ H(D_R^{-1} x_k) = -(F'(x_k) D_R)^+ F(x_k)$$

where $H(\tilde{x}) = H(D_R^{-1} x) := F(x)$ such that $H'(\tilde{x}) = H'(D_R^{-1} x) = F'(x) D_R$. If now $F'(x_k)$ has full rank for each iterate $x_k \in D$ this gives

$$\Delta \tilde{x}_k = D_R^{-1}(-F'(x_k)^+ F(x_k)) = D_R^{-1} \Delta x_k,$$

hence right scaling invariance under the Gauss-Newton method. This affine invariance idea justifies the use of affine covariant transformations and the hereby induced error oriented algorithms for the application given. For left scaling, unfortunately, invariance does not hold true. Assuming that left scaling is applied by

$$\tilde{F}_i(x) := D_L F_i(x)$$

where $D_L = diag(\delta z_1, \ldots, \delta z_d)$ might account for the error tolerance in the given data, the problem to be solved in the affine covariant Gauss-Newton sense writes

$$\min_{x \in D} \|\tilde{F}'(x_k) \Delta x_k + \tilde{F}(x_k)\|_2^2$$

for the k^{th} iteration. Obviously, this is equivalently

$$\min_{x \in D} \|D_L(F'(x_k) \Delta x_k + F(x_k))\|_2^2.$$

This immediately gives reason to note that for different weighting respectively left scaling, a different sequence of linear least squares problems is solved during the Gauss-Newton iterations such that different scaling leads to different solutions. This fact is crucial to interpretation of the solutions obtained and should be kept in mind while solving any nonlinear least squares problem.

4.3. Globalisation of the Gauss-Newton Method

The Gauss-Newton method is the standard method of choice for parameter identification problems. Dependence on the starting values and local convergence significantly diminishes its performance. By the difficulty to obtain *good* initial values for most applications, the need for robustness and an increased convergence radius emerges naturally. Adaptive step length strategies controlling the descent have widely been used. A short review on trust region methods is given underneath, before the damped Gauss-Newton method such as Deuflhard (2006) proposes it and such as it is implemented in the Nlscon code is introduced. The corresponding predictor corrector based damping strategy is also sketched for the purpose of understanding and completeness.

A common approach to increase robustness of the Gauss-Newton method was taken by Kenneth Levenberg and Donald Marquardt (Dennis/ Schnabel (1983) / Levenberg (1944) / Marquardt (1963)). Divergence eventually occurring in the Gauss-Newton framework is handled in the Levenberg-Marquardt algorithm by first identifying a *trust region* and then determining a step length towards the *steepest descent*.
Basically, the idea of the Levenberg Marquardt algorithm is that local linearisation performed during the Gauss-Newton iterations is solely to be trusted in a small neighbourhood, i.e. the trust region (see Björck (1996), p. 346/347) of the k^{th} iterate x_k. Hence, the nonlinear least squares problem as deduced in (3.5.2) when introducing the Gauss-Newton method then writes

$$\begin{aligned} &\min \|F'(x_k)\Delta x_k + F(x_k)\|_2^2 \\ &s.t. \quad \|\Delta x_k\|_2 \leq \delta. \end{aligned}$$

The Levenberg-Marquardt step is the solution of the hereby obtained normal equation of the kind

$$(F'(x_k)^T F'(x_k) + \mu I_n)\Delta x_k = -F'(x_k)^T F(x_k) \tag{4.3.1}$$

where $\delta \geq 0$ defines the radius of the trust region as an inequality constraint and $\mu > 0$ stands for the Lagrange multiplier. Summarising, this gives the regularised nonlinear least squares problem

$$\min \|F'(x_k)^+ \Delta x_k + F(x_k)\|_2^2 + \mu \|\Delta x_k\|_2^2 \tag{4.3.2}$$

where the increment vector Δx_k is rotated by the trust region's radius $\mu \geq 0$ in the steepest descent direction.

Obviously, for $I_n \in \mathbb{R}^{n,n}$ the identity matrix in (4.3.1), the Levenberg-Marquardt step approaches the steepest descent direction

$$-F'(x_k)^T F(x_k)$$

with magnitude

$$\|\Delta x_k\|_2 \to 0$$

for $\mu \to +\infty$ while it is parallel to the steepest descent direction for small μ (Björck (1996), p. 347). Note that, on the other hand, the Levenberg-Marquardt method for $\mu = 0$ gives the standard Gauss-Newton minimisation for the objective function. This ensures a downhill step in each iteration for any $\mu > 0$ sufficiently large, in the sense of

$$F(x_k + \Delta x_k) < F(x_k).$$

There exist numerous other optimisation algorithms related to or based on the Newton method. In large residual problems for example, that are not treated in detail in this context, a Broyden-Fletscher-Goldfarb-Shannon updating routine would be preferable according to Björck (1996) (p. 347).
Though, let us direct the attention to small or zero residual problems. Under the assumption of compatibility, the Levenberg-Marquardt algorithm's robustness occasionally pays for its improvement by detecting merely saddle points – whose gradient are also zero but which do not satisfy the sufficient conditions for local interior minima. This can be explained by the steepest descent approach which may result in termination once the gradient gets small (Deuflhard (2006), p. 119).

Summarising, there exist in general two different strategies towards globalising convergence of

the Gauss-Newton method – either by line search or by trust region approaches. Though names are misleading in literature, the subsequently presented methodology based on an adaptive trust region approach will be referred to as the *damped Gauss-Newton* method. Dennis/ Schnabel (1983) in contrary only call Gauss-Newton based algorithms improved by a line search routine *damped*.
Damping here in this context actually accounts for an adaptive variation within the step length to be taken during the Gauss-Newton descent.

Before continuing, it seems appropriate to emphasize that a globalisation of the Gauss-Newton method does not mean in any way global convergent algorithm in the common way. Newton and Newton like methods' convergence behaviour remains locally dependent on the initial guess, though globalised methods might deal better with bad initial guesses.
Furthermore, the damped Gauss-Newton method as presented by Deuflhard (2006) claims to give an improvement with respect to the appropriate detection of local minima in the sense that the algorithm would give additional information if terminating at a saddle point and would indicate if there exist manifold minimum solutions. Especially as it is well known that standard Newton methods terminate if they reach the nearest solution point x_*, if they come sufficiently close to a singularity of the Jacobian or at if they come close to some point on the boundary ∂D (Björck(1996), p. 346 and Deuflhard (2006), p. 124).

Damping the Gauss-Newton correction Δx_k by some damping factor $0 < \lambda_k \leq 1$ in every of the k iterations can also be embedded into the affine covariant context of solving nonlinear least squares problems which will stand in the focus of attention.
Compared to other damping strategies as the *Armijo* rule, Deuflhard (2006) develops a adaptive step length rule that carefully maintains the affine invariant framework and performs better also under ill conditioned Jacobians (p. 121).

The drawback about the globalisation of the Gauss-Newton method even in an affine covariant setting is that convergence can neither be guaranteed nor proved. Though, the modified Gauss-Newton method as it will be defined in the following locally behaves like the standard Gauss-Newton method and heuristically yields better results (Deuflhard (2006)).

Definition 4.3.1. *For $F : D \subseteq \mathbb{R}^n \to \mathbb{R}^m$ the damped Gauss-Newton method is defined by*

$$\begin{aligned} F'(x_k)\Delta x_k &= -F(x_k) \\ x_{k+1} &= x_k + \lambda_k \Delta x_k \end{aligned}$$

for $0 < \lambda_k \leq 1$ and $k = 0, 1, \ldots$.

Similar to the previous chapter, considering the nonlinear system, emerging from the initial minimisation task,

$$F'(x)^+ F(x) = 0$$

would introduce a second order derivative tensor term. As a modification of the Gauss-Newton method by global features is to be given, the task at hand is to solve

$$F'(x_*)^+ F(x) = 0$$

for $x_* \in D$ the yet unknown solution of the minimisation problem in the nonlinear least squares sense applied to parameter identification. According to Deuflhard (2006) (p. 206), the problem

specification gives immediately rise to the nontrivial affine covariance class

$$\mathcal{A}(x_*) := \{A = BF'(x_*)^+ : B \text{ nonsingular}\}$$

which obviously implies the equivalence

$$\begin{aligned} & AF(x) = 0 \\ \Leftrightarrow\ & F'(x_*)^+F(x) = 0 \end{aligned}$$

for any $A \in \mathcal{A}(x_*)$. Considering test functions

$$T(x|A) := \frac{1}{2}\|AF(x)\|_2^2$$

for $A \in \mathcal{A}(x_*)$, a proper theory about choosing the damping factor λ_k within global Gauss-Newton's k^{th} iteration requires that

$$rank(F'(x)) = n$$

i.e. the Jacobian is not rank deficient for $x \in D$.

Annotation 4.3.2. Deuflhard *(2006) annotates that the theoretical condition that*

$$F'(x_*)^+F(x)$$

should be nonsingular for $x \in D$ and the solution $x_* \in D$ would enable global convergence statements for the damped Gauss-Newton method. The necessity of this additional requirement builds upon the fact that $F'(x_*)^*F(x)$ is certainly singular if the Jacobian $F'(x)$ is rank deficient but vice versa, $F'(x_*)^+F(x)$ does not need to be regular if the Jacobian has full rank. Summarizing, the idea then builds up to that if the Jacobian is not rank deficient and $F'(x_*)^+F(x)$ is nonsingular for $x \in D$, there exists a path, the so called Gauss-Newton path such that all general level functions

$$T(x|A) := \frac{1}{2}\|AF(x)\|_2^2$$

decrease along this path for $A \in \mathcal{A}(x_*)$.

But the most crucial point Deuflhard *(2006) makes in this context is that due to the nonavailability of information about the solution $x_* \in D$ during computation, the damped Gauss-Newton path as mentioned above can never be realised for any Newton method (p. 207).*

Briefly, construction of a global Gauss-Newton method would require global information about the Jacobian at the solution point x_* in order to guarantee global convergence. The way out intuitively is to insert the best possible, hence most recent local Gauss-Newton estimate x_k instead of $x_* \in D$. This approach proposed by Deuflhard (2006) (p. 212) can be categorised as an adaptive trust region strategy.
A local Gauss-Newton path can be obtained hereby and leads to the loss of guarantee of global convergence. Similarly, for the local Gauss-Newton path the local natural level functions for the nonlinear least squares problem writes

$$T(x|F'(x_k)^+) := \frac{1}{2}\|F'(x_k)^+F(x)\|.$$

Consequently by applying the Moore Penrose axioms, the damped Gauss-Newton method decreases in the steepest descent direction with respect to $T(x|F'(x_k)^+)$ (Deuflhard (2006), p. 212).

For the purpose of completeness, let us define the affine invariant version of residual level functions (Deuflhard (2006), p. 114) accounting for monotonicity behaviour specifically for the Gauss-Newton method's descent as follows:

Definition 4.3.3. *For any $x \in D$, the global level function within the affine invariant setting of the Gauss-Newton method is defined as*

$$T(x|F'(x_*)^+) := \frac{1}{2}\|F'(x_*)^+F(x)\|_2^2 \tag{4.3.3}$$

while its local counterpart writes

$$T(x|F'(x_k)^+) := \frac{1}{2}\|F'(x_k)^+F(x)\|_2^2. \tag{4.3.4}$$

Annotation 4.3.4. *The definition of level functions is motivated by the objective that any algorithm should successively approach a solution point $x_* \in D$. If the affine invariant natural level functions – both local and global – are defined via*

$$T(x|A) := \frac{1}{2}\|AF(x)\|_2^2$$

exploiting the representation

$$\frac{1}{2}\|AF(x)\|_2^2 = \frac{1}{2}(AF(x))^T AF(x) = \frac{1}{2}F(x)^T A^T AF(x).$$

The following properties are satisfied:

$$T(x|A) = 0 \Leftrightarrow x = x_*$$
$$T(x|A) > 0 \Leftrightarrow x \neq x_*.$$

The task at hand now is to identify sequences of damping factors λ_k such that

$$\|F'(x_k)^+F(x_k)\|_2^2$$

decays monotonously along all iterates x_k. This requires successive iterates x_k, x_{k+1} of the globalised Gauss-Newton sequence x_k to satisfy

$$T(x_{k+1}|A) < T(x_k|A)$$

for any $A \in \mathcal{A}(x_*)$. This will be referred to as *monotonicity criterion* in terms of natural level functions.
The damped Gauss-Newton method

$$\begin{aligned} x_{k+1} &= x_k + \lambda_k \Delta x_k \\ &= x_k - \lambda_k F'(x_k)^+ F(x_k) \end{aligned}$$

for $k = 0, 1, \ldots$ requires successive recomputation of the step length $0 < \lambda_k \leq 1$ in each iteration. Furthermore, as we have already seen before, the standard Gauss-Newton method gives the

minimum norm solution to the linear substitute least squares problem

$$\min_{x \in D} \|F'(x_k)\Delta x_k + F(x_k)\|_2$$

where the Jacobian matrix can be approximated analytically, solved by its variational equality or by finite differences during simulation. Here, the linearly-implicit Euler extrapolation routine is used to evaluate the Jacobian system (see 4.4, p. 70).

In order to lay a theoretical fundamental, let us introduce the simplified Gauss-Newton method, going back to an approach by Ortega/ Rheinboldt (2000).

Definition 4.3.5. *The simplified Gauss-Newton method solves the minimisation problem*

$$\min \|F'(x_k)\overline{\Delta x_{k+1}} + F(x_{k+1})\|_2 \tag{4.3.5}$$

and is introduced for problems with incompatibility factor $\kappa(x) \leq \overline{\kappa} < 1$ as it requires only computational available information about the Jacobian at a fixed point. Then, the simplified Gauss-Newton routine performs

$$F'(x_k)\overline{\Delta x_{k+1}} = -F(x_{k+1}) \tag{4.3.6}$$

$$x_{k+1} = x_k + \overline{\Delta x_{k+1}} \tag{4.3.7}$$

such that the simplified Gauss-Newton correction is determined by

$$\overline{\Delta x_{k+1}} = -F'(x_k)^+ F(x_{k+1}). \tag{4.3.8}$$

4.3.1. Natural Monotonicity and Descent Directions

The *natural monotonicity test* ensures throughout simulations that for any step length λ_k the descent direction is followed, improving the convergence rate. During computation it is clearly not helpful to estimate convergence with respect to the solution $x_* \in D$ which is unknown at that time. In order to surround this obstacle and aiming at obtaining a convergence monitor after a few first iteration steps of the method already, Deuflhard (1972) and Deuflhard/ Hohmann (2003) (p. 102) propose an affine invariant version of the *standard monotonicity test*.

Lemma 4.3.6. *In an affine invariant setting, local monotonicity of the globalised Gauss-Newton method can be inspected by the* natural monotonicity test

$$\|F'(x_k)^+ F(x_{k+1})\|_2 \leq \overline{\theta}_k \|F'(x_k)^+ F(x_k)\|_2. \tag{4.3.9}$$

for some local constant $\overline{\theta}_k < 1$.

Note that the left hand side accounts for the simplified Gauss-Newton correction while the right hand side is exactly the standard damped Gauss-Newton method in this case. Evaluating the simplified Gauss-Newton method obviously does not require additional effort since at the next iteration point x_{k+1} a system of equations involving the same Jacobian $F'(x_k)$ as already computed during the Gauss-Newton routine has to be solved.

First, the theoretical approach involves $x_* \in D$ which will not be known during computation. Nonetheless, convergence of the damped Gauss-Newton approach requires that the following

monotonicity criterion

$$\overline{\theta}_k \leq \overline{\theta}_* \tag{4.3.10}$$

in terms of a global contraction factor $0 < \overline{\theta}_* < 1$ holds for any iteration k and where the global contraction factor is required to satisfy

$$\|F'(x_*)^+ F(x_{k+1})\|_2 \leq \overline{\theta}_* \|F'(x_*)^+ F(x_k)\|_2. \tag{4.3.11}$$

Deuflhard (2006) (p. 213) proposes to take the best estimate available for x_*, namely the latest iterate x_k instead. Using the best available local estimates, one arrives at the computational available local contraction factor $\overline{\theta}_k$ with

$$[\overline{\theta_k}] := \frac{\|F'(x_k)^+ F(x_{k+1})\|_2}{\|F'(x_k)^+ F(x_k)\|_2} = \frac{\|\overline{\Delta x_{k+1}}\|_2}{\|\Delta x_k\|_2} \tag{4.3.12}$$

which satisfies

$$[\overline{\theta}_k] \leq \overline{\theta}_k$$

and the required

$$[\overline{\theta}_k] \leq \overline{\theta}_k \leq \overline{\theta}_*$$

by definition, where $0 < \overline{\theta}_* < 1$ accounts for the theoretical, global contraction factor. Assuming that $D_0 \subseteq D$ convex and $x, y, x_k, x_{k+1} \in D_0$, Deuflhard (2006) (p. 209) claims some global continuity of the second derivatives with respect to the solution x_*in terms of the following Lipschitz condition

$$\|F'(x_*)^+ (F'(y) - F'(x))(y - x)\|_2 \leq \omega_* \|y - x\|_2^2. \tag{4.3.13}$$

Lemma 4.3.7. *Under assumption* (4.3.13) *for the simplified Gauss-Newton direction the following estimate holds*

$$\begin{aligned}\|F(x_*)^+ F(x_{k+1})\|_2 = \|F'(x_*)^+ &\int_{s=0}^{\lambda_k^*} (F'(x_k + s\Delta x_k) - F'(x_k))\, \Delta x_k \, ds \\ &+ (1 - \lambda_k^*) F'(x_*) + \lambda_k^* F'(x_*)^+ (I - F'(x_k) F'(x_k)^+) F(x_k)\|_2\end{aligned}$$

with respect to the solution $x_* \in D$ and a globally optimal damping factor $\lambda_k^* > 0$.

Proof of 4.3.7. In a first step, application of the Lagrangian mean value theorem yields under the definition of the damped Gauss-Newton method that

$$\begin{aligned}F(x_{k+1}) - F(x_k) - F'(x_k)(x_{k+1} - x_k) &= F(x_k + \lambda_k^* \Delta x_k) - F(x_k) - F'(x_k)(x_{k+1} - x_k) \\ &= F(x_k + \lambda_k^* \Delta x_k) - F(x_k) - F'(x_k)(x_k + \lambda_k^* \Delta x_k - x_k) \\ &= \int_0^1 (F'(x_k + t\lambda_k^* \Delta x_k) - F'(x_k)) \lambda_k^* \Delta x_k \, dt \\ &= \int_{s=0}^{\lambda_k^*} (F'(x_k + s\Delta x_k) - F'(x_k)) \Delta x_k \, ds\end{aligned}$$

if $s := t\lambda_k^*$. Then left multiplication with the Moore Penrose inverse of the Jacobian matrix at

the solution point x_* gives for $F(x_k) - F'(x_k)(x_{k+1} - x_k)$ that

$$\begin{aligned} F'(x_*)^+(F(x_k) - F'(x_k)(x_{k+1} - x_k)) &= F'(x_*)^+(F(x_k) - F'(x_k)(x_k + \lambda_k^* \Delta x_k - x_k)) \\ &= F'(x_*)^+ F(x_k) - F'(x_*)^+ F'(x_k)\lambda_k^* \Delta x_k. \end{aligned}$$

Since indeed, the damped Gauss-Newton correction was defined as

$$\lambda_k^* \Delta x_k = \lambda_k^*(-F'(x_k)^+ F(x_k))$$

we can proceed as follows:

$$\begin{aligned} F'(x_*)^+(F(x_k) + F'(x_k)(x_{k+1} - x_k)) &= F'(x_*)^+(F(x_k) + F'(x_k)(-\lambda_k^* F'(x_k)^+ F(x_k))) \\ &= F'(x_*)^+ F(x_k) - F'(x_*)^+ F'(x_k)\lambda_k^* F'(x_k)^+ F(x_k) \\ &= (1 - \lambda_k^* + \lambda_k^*)F'(x_*)^+ F(x_k) - \lambda_k^* F'(x_*)^+ F'(x_k)F'(x_k)^+ F(x_k) \\ &= (1 - \lambda_k^*)F'(x_*)^+ F(x_k) + \lambda_k^* F'(x_*)^+ F(x_k) - \lambda_k^* F'(x_*)^+ F'(x_k)F'(x_k)^+ F(x_k) \\ &= (1 - \lambda_k^*)F'(x_*)^+ F(x_k) + (\lambda_k^* F'(x_*)^+ - \lambda_k^* F'(x_*)^+ F'(x_k)F'(x_k)^+)F(x_k) \\ &= (1 - \lambda_k^*)F'(x_*)^+ F(x_k) + \lambda_k^* F'(x_*)^+(I - F'(x_k)F'(x_k)^+)F(x_k). \end{aligned}$$

By these two representations, taking norms of the left hand side expression of the natural monotonicity test with respect to the solution x_* finally yields

$$\begin{aligned} \|F'(x_*)^+ F(x_{k+1})\|_2 &= \|F'(x_*)(F(x_{k+1}) - F(x_k) - F'(x_k)(x_{k+1} - x_k)) \\ &\quad + F(x_*)^+ F(x_k) + F'(x_*)F'(x_k)(x_{k+1} - x_k)\|_2 \\ &= \|F'(x_*)^+(F(x_{k+1}) - F(x_k) - F'(x_k)(x_{k+1} - x_k)) \\ &\quad + F'(x_*)^+(F(x_k) + F'(x_k)(x_{k+1} - x_k))\|_2 \\ &= \|F'(x_*)^+ \int_{s=0}^{\lambda_k^*} (F'(x_k + s\Delta x_k) - F'(x_k))\, \Delta x_k \, ds \\ &\quad + (1 - \lambda_k^*)F'(x_*)^+ F(x_k) + \lambda_k^* F'(x_*)^+(I - F'(x_k)F'(x_k)^+)F(x_k)\|_2. \end{aligned}$$

where λ_k^* accounts for the globally optimal step size with respect to the solution point. □

Since the solution $x_* \in D$ is computationally not available at any stage during the performance of the damped Gauss-Newton algorithm , using the global level function

$$T(x|F'(x_*)^+) := \frac{1}{2}\|F'(x_*)^+ F(x)\|_2^2$$

one can obtain useful theoretical estimates if it is introduced

$$h_k^* := \omega_* \|(F'(x_*)^+ F'(x_k))^{-1}\|_2 \|\Delta x_k\|_2.$$

Lemma 4.3.8. *If $x_* \in D$ denotes the solution to the nonlinear least squares problem, under the damped Gauss-Newton method the following estimate holds true*

$$T(x_k + \lambda_k^* \Delta x_k|F'(x_*)^+) \leq \left(1 - \lambda_k^* + \frac{1}{2}\lambda_k^{*2} h_k^*\right)^2 T(x_k|F'(x_k)^+), \tag{4.3.14}$$

where $h_k^* := \omega_* \|(F'(x_*)^+ F(x_k))^{-1}\|_2 \|\Delta x_k\|_2$.

The proof for the above stated theorem will be omitted, as it follows just as for the case that x_k is involved as a local substitute for x_* (see Proposition 4.3.10, p. 64).

Determination of a locally optimal damping factor $0 < \lambda_k \leq 1$ is based on the assumption, that additionally local Lipschitz constants exist such that

$$\|F'(x_k)^+(F'(y) - F'(x))(y - x)\|_2 \leq \omega_k \|y - x\|_2^2, \quad x, x_k, y, \in D_0 \text{ open and convex} \tag{4.3.15}$$

and for $v \in D_0 \subseteq \mathbb{R}^n$, also

$$\|F'(x_k)^+(F'(y) - F'(x))v\|_2 \leq \overline{\omega}_k \|v\|_2 \|y - x\|_2 \tag{4.3.16}$$

with $\omega_k \leq \overline{\omega}_k < \infty$ it holds for the residual function's first derivative.

Lemma 4.3.9. *For some $\lambda_k > 0$, the above local Lipschitz conditions and a full rank Jacobian matrix $F'(x_k)$, it holds*

$$\|F'(x_k)^+ F(x_{k+1})\|_2 = \|F'(x_k)^+ \int_{s=0}^{\lambda_k} (F'(x_k + s\Delta x_k) - F'(x_k))\, \Delta x_k \, ds + (1-\lambda_k) F'(x_k)^+ F(x_k)\|_2.$$

Proof of 4.3.9. Under the knowledge that

$$F(x_{k+1}) - F(x_k) - F'(x_k)(x_{k+1} - x_k) = \int_{s=0}^{\lambda_k} (F'(x_k + s\Delta x_k) - F'(x_k))\Delta x_k \, ds$$

one immediately obtains the representation

$$\begin{aligned} F'(x_k)^+(F(x_k) + F'(x_k)(x_{k+1} - x_k)) &= F'(x_k)^+(F(x_k) + F'(x_k)\lambda_k \Delta x_k) \\ &= F'(x_k)^+(F(x_k) - \lambda_k F'(x_k) F'(x_k)^+ F(x_k)) \\ &= (I - \lambda_k F'(x_k)^+ F'(x_k)) F'(x_k)^+ F(x_k). \end{aligned}$$

Provided that the Jacobian matrix at x_k has maximal rank, then

$$F'(x_k)^+ F'(x_k) = I$$

by the definition of the Moore Penrose inverse. Combining these two results gives

$$\begin{aligned} F'(x_k)^+(F(x_k) + F'(x_k)(x_{k+1} - x_k)) &= (1 - \lambda_k) F'(x_k)^+ F(x_k) \\ &= (1 - \lambda_k)\Delta x_k. \end{aligned}$$

Taking norms, this consequently yields for the simplified Gauss-Newton correction that

$$\begin{aligned} &\|F'(x_k)^+ F(x_{k+1})\|_2 \\ &\quad = \|F'(x_k)^+ \left(F(x_{k+1}) - F(x_k) - F'(x_k)(x_{k+1} - x_k)\right) \\ &\qquad + F'(x_k)^+(F(x_k) + F'(x_k)(x_{k+1} - x_k))\|_2 \\ &\quad = \|F'(x_k)^+ \int_{s=0}^{\lambda_k} (F'(x_k + s\Delta x_k) - F'(x_k))\Delta x_k \, ds + (1 - \lambda_k)\Delta x_k\|_2. \end{aligned}$$

□

Similarly as for the global estimates above, it is introduced locally for any iteration $k = 0, 1, \ldots$

$$h_k := \omega_k \|(F'(x_k)^+ F(x_k))\|_2 = \omega_k \|\Delta x_k\|_2.$$

Proposition 4.3.10. *Under the assumptions that* (4.3.15) *and* (4.3.16) *with* $\omega_k \leq \overline{\omega}_k < \infty$ *local Lipschitz constants hold true for* $x, x_k, x_{k+1}, y \in D_0$, $D_0 \subseteq \mathbb{R}^n$ *open and convex, it is claimed for the simplified Gauss-Newton correction that*

$$\|F'(x_k)^+ F(x_{k+1})\|_2 \leq \left(1 - \lambda_k + \frac{1}{2}\lambda_k^2 h_k\right) \|F'(x_k)^+ F(x_k)\|_2.$$

Proof of 4.3.10. As previously shown, it is

$$\|F(x_k)^+ F(x_{k+1})\|_2 = \|F'(x_k)^+ \int_{s=0}^{\lambda_k} (F'(x_k + s\Delta x_k) - F'(x_k))\, \Delta x_k \, ds + (1-\lambda_k) F'(x_k)^+ F(x_k)\|_2.$$

Hence, application of the triangle inequality yields

$$\begin{aligned}
&\|F(x_k)^+ F(x_{k+1})\|_2 \\
&\qquad \leq \|F'(x_k)^+ \int_{s=0}^{\lambda_k} (F'(x_k + s\Delta x_k) - F'(x_k))\, \Delta x_k \, ds\|_2 + (1 - \lambda_k)\|F'(x_k)^+ F(x_k)\|_2 \\
&\qquad = \|F'(x_k)^+ \int_0^1 (F'(x_k + t\lambda_k \Delta x_k) - F'(x_k))\, \lambda_k \Delta x_k \, dt\|_2 + (1 - \lambda_k)\|F'(x_k)^+ F(x_k)\|_2.
\end{aligned}$$

Under assumption of the first stated local Lipschitz continuity (4.3.16), one obtains

$$\begin{aligned}
&\|F(x_k)^+ F(x_{k+1})\|_2 \\
&\qquad \leq \int_0^1 \|F'(x_k)^+ (F'(x_k + t\lambda_k \Delta x_k) - F'(x_k))\, \lambda_k \Delta x_k\|_2 \, dt + (1 - \lambda_k)\|F'(x_k)^+ F(x_k)\|_2 \\
&\qquad \leq \int_0^1 \omega_k \|(x_k + t\lambda_k \Delta x_k) - x_k\|_2 \|\lambda_k \Delta x_k\|_2 \, dt + (1 - \lambda_k)\|F'(x_k)^+ F(x_k)\|_2 \\
&\qquad = \int_0^1 \omega_k t \|\lambda_k \Delta x_k\|_2 \, dt + (1 - \lambda_k)\|F'(x_k)^+ F(x_k)\|_2 \\
&\qquad = \frac{1}{2}\omega_k \lambda_k^2 \|\Delta x_k\|_2^2 + (1 - \lambda_k)\|F'(x_k)^+ F(x_k)\|_2 \\
&\qquad = \frac{1}{2}\omega_k \lambda_k^2 \|\Delta x_k\|_2^2 + (1 - \lambda_k)\|\Delta x_k\|_2.
\end{aligned}$$

By the definition of the damped Gauss-Newton iteration, this immediately results in the estimate

$$\|F(x_k)^+ F(x_{k+1})\|_2 \leq \left(1 - \lambda_k + \frac{1}{2}\omega_k \lambda_k^2 \|F'(x_k)^+ F(x_k)\|_2\right) \|F'(x_k)^+ F(x_k)\|_2$$

which is equivalent to

$$\|F(x_k)^+ F(x_{k+1})\|_2 \leq \left(1 - \lambda_k + \frac{1}{2}\lambda_k^2 h_k\right) \|F'(x_k)^+ F(x_k)\|_2.$$

□

As a direct consequence of the previous Theorem 4.3.10 (p. 64), application to the local level

function

$$T(x|F'(x_k)^+) := \frac{1}{2}\|F'(x_k)^+F(x)\|_2^2.$$

gives equivalently that

$$T(x_k + \lambda_k + \Delta x_k|F'(x_k)^+) \leq \left(1 - \lambda_k + \frac{1}{2}\lambda_k^2 h_k\right)^2 T(x_k|F'(x_k)^+).$$

since it holds

$$\begin{aligned} T(x_{k+1}|F'(x_k)^+) &= \frac{1}{2}\|F'(x_k)^+F(x_{k+1})\|_2^2 \\ \Leftrightarrow T(x_k + \lambda_k + \Delta x_k|F'(x_k)^+) &= \frac{1}{2}\|F'(x_k)^+F(x_k + \lambda_k + \Delta x_k)\|_2^2 \end{aligned}$$

and just the same

$$T(x_k|F'(x_k)^+) = \frac{1}{2}\|F'(x_k)^+F(x_k)\|_2^2.$$

Applying the local natural level function to the simplified Gauss-Newton correction gives under the above shown results

$$\begin{aligned} T(x_{k+1}|F'(x_k)^+) &= \frac{1}{2}\|F'(x_k)^+F(x_{k+1})\|_2^2 \\ &\leq \left(1 - \lambda_k + \frac{1}{2}\lambda_k^2 h_k\right)^2 \frac{1}{2}\|F'(x_k)^+F(x_k)\|_2^2 \\ &= \left(1 - \lambda_k + \frac{1}{2}\lambda_k^2 h_k\right)^2 T(x_k|F'(x_k)^+). \end{aligned}$$

Clearly, the descent measured in terms of the global natural level function is maximized, if the expression

$$1 - \lambda_k^* + \frac{1}{2}(\lambda_k^*)^2 h_k^*$$

is minimized or equivalently, for the local counterpart, if

$$1 - \lambda_k + \frac{1}{2}\lambda_k^2 h_k$$

gets minimal. $h_k = \omega_k\|\Delta x_k\|_2$ herein denotes the associated Kantrovich quantity (Deuflhard (2006), p. 199).

4.3.2. Adaptive Step Length Predictor-Corrector Strategy

The adaptive trust region strategy, based on the idea of Armijo step length control, performs basically in two steps: Assuming that an initial step length $\lambda_0^{(0)}$ is given, recursively for each iteration k the adequate step size has to be identified. Then in the k^{th} iteration, the first step is to compute an *a priori estimate* for the next damping factor $\lambda_{k+1}^{(0)}$, which is called *prediction strategy*. Second, for the estimated damping factor, a natural monotonicity test in terms of natural level functions is to be performed. If the proposed damping factor $\lambda_{k+1}^{(0)}$ does not satisfy this descent condition, a correction strategy is applied. This leads to the *a posteriori estimate* $\lambda_{k+1}^{(\nu)}$ for $\nu = 1, 2, \ldots$ corrections applied.

For the prediction strategy, let us assume that a global Lipschitz constant

$$\omega_* < \infty$$

exists for the Jacobian with

$$\|F'(x_*)^+(F'(y) - F'(x))(y - x)\|_2 \leq \omega_* \|y - x\|_2 \tag{4.3.17}$$

the affine invariant Lipschitz condition, $x, y \in D$, $D \subseteq \mathbb{R}^n$ open and convex and $x_* \in D$ the yet unknown solution of the minimisation task. Let then furthermore exist local Lipschitz constants such that

$$\|F'(x_k)^+(F'(y) - F'(x))(y - x)\|_2 \leq \omega_k \|y - x\|_2^2$$

and for $v \in D_0 \subseteq \mathbb{R}^n$, also

$$\|F'(x_k)^+(F'(y) - F'(x))v\|_2 \leq \overline{\omega}_k \|v\|_2 \|y - x\|_2$$

with $\omega_k \leq \overline{\omega}_k < \infty$ just as defined earlier within this section hold. Introducing the quantity

$$\overline{\Delta}_k := -F'(x_k)^+ \left(F(x_k) + F'(x_{k-1})\overline{\Delta x_k}\right) \tag{4.3.18}$$

involving the simplified Gauss-Newton correction

$$\overline{\Delta x_k} = -F'(x_{k-1})^+ F(x_k)$$

gives

$$\overline{\Delta}_k := -F'(x_k)^+ \left(F(x_k) - F'(x_{k-1})F'(x_{k-1})^+ F(x_k)\right).$$

Then, one can estimate

$$\begin{aligned}
&\|\overline{\Delta x_k} - \Delta x_k + \overline{\Delta}_k\|_2 \\
&\quad = \| - F'(x_{k-1})^+ F(x_k) + F'(x_k)^+ F(x_k) - F'(x_k)^+ (F(x_k) + F'(x_{k-1})(-F'(x_{k-1})^+ F(x_k)))\|_2 \\
&\quad = \| - F'(x_{k-1})^+ F(x_k) + F'(x_k)^+ F(x_k) - F'(x_k)^+ F(x_k) + F'(x_k)^+ F'(x_{k-1}) F'(x_{k-1})^+ F(x_k)\|_2 \\
&\quad = \| - F'(x_{k-1})^+ F(x_k) + F'(x_k)^+ F'(x_{k-1}) F'(x_{k-1})^+ F(x_k)\|_2 \\
&\quad = \|(I - F'(x_k)^+ F'(x_{k-1})) F'(x_{k-1})^+ F(x_k)\|_2 \\
&\quad = \|F'(x_k)^+ F'(x_k)(I - F'(x_k)^+ F'(x_{k-1})) F'(x_{k-1})^+ F(x_k)\|_2
\end{aligned}$$

since under the assumption of full rank of the Jacobian $F'(x)$, the orthogonal projector satisfies

$$P^\perp = F'(x_k)^+ F'(x_k) = I.$$

This can be further evaluated

$$\|\overline{\Delta x_k} - \Delta x_k + \overline{\Delta}_k\|_2 = \|(F'(x_k)^+ F'(x_k) - F'(x_k)^+ F'(x_k) F'(x_k)^+ F'(x_{k-1})) F'(x_{k-1})^+ F(x_k)\|_2$$

such that applying the third Moore Penrose axiom for generalised inverses, gives

$$F'(x_k)^+ F'(x_k) F'(x_k)^+ = F'(x_k)^+.$$

In the last step, the Lipschitz continuity of the objective function's first derivative is exploited

such that

$$\begin{aligned}\|\overline{\Delta x_k} - \Delta x_k + \overline{\Delta}_k\|_2 &= \|F'(x_k)^+(F'(x_k) - F'(x_{k-1}))F'(x_{k-1})^+F(x_k)\|_2 \\ &\leq \overline{\omega}_k\|x_k - x_{k-1}\|_2\|F'(x_{k-1})^+F(x_k)\|_2 \\ &= \overline{\omega}_k\lambda_{k-1}\|\Delta x_{k-1}\|_2\|F'(x_{k-1})^+F(x_k)\|_2.\end{aligned}$$

Reorganising yields

$$\begin{aligned}&\|\overline{\Delta x_k} - \Delta x_k - \overline{\Delta}_k\|_2 \leq \overline{\omega}_k\lambda_{k-1}\|\Delta x_{k-1}\|_2\|F'(x_{k-1})^+F(x_k)\|_2 \\ \Leftrightarrow\quad &\frac{\|\overline{\Delta x_k} - \Delta x_k - \overline{\Delta}_k\|_2}{\lambda_{k-1}\|\Delta x_{k-1}\|_2\|\overline{\Delta x_k}\|_2} \leq \overline{\omega}_k.\end{aligned}$$

Proposition 4.3.11. *An* a priori *estimate* $[\overline{\omega}_k]$ *for the local Lipschitz constant* $\overline{\omega}_k$ *satisfying*

$$\|F'(x_k)^+(F'(y) - F'(x))v\|_2 \leq \overline{\omega}_k\|v\|_2\|y - x\|_2$$

for $x, y, v \in D_0 \subseteq \mathbb{R}^n$, $\omega_k \leq \overline{\omega}_k < \infty$ *and* $D_0 \subseteq D \subseteq \mathbb{R}^n$ *open and convex, can be obtained by*

$$[\overline{\omega}_k] = \frac{\|\overline{\Delta x_k} - \Delta x_k - \overline{\Delta}_k\|_2}{\lambda_{k-1}\|\Delta x_{k-1}\|_2\|\overline{\Delta x_k}\|_2}. \tag{4.3.19}$$

Annotation 4.3.12. *Since at a later stage, a correction strategy for the damping factor* λ_k *is introduced, the predicted step length will be called*

$$\lambda_k^{(0)}$$

in the following where the upshift index accounts for $\nu = 0$ *corrections performed on the initially predicted step length.*

So far, the adaptive step length approach gave that a descent is taken in terms of the natural level function with

$$T\left(x_k + \lambda_k^{(0)} + \Delta x_k|F'(x_k)^+\right) \leq \left(1 - \lambda_k^{(0)} + \frac{1}{2}(\lambda_k^{(0)})^2 h_k\right)^2 T\left(x_k|F'(x_k)^+\right)$$

and with the available estimate for the Lipschitz constant

$$[\overline{\omega}_k] = \frac{\|\overline{\Delta x_k} - \Delta x_k - \overline{\Delta}_k\|_2}{\lambda_k^{(0)}\|\Delta x_{k-1}\|_2\|\overline{\Delta}_k\|_2}$$

satisfying

$$[\overline{\omega}_k] \leq \overline{\omega}_k.$$

The descent can be maximized, if the factor

$$1 - \lambda_k^{(0)} + \frac{1}{2}\left(\lambda_k^{(0)}\right)^2 h_k$$

is minimized. Since the first derivative with respect to the step length $\lambda_k^{(0)}$ writes

$$h_k\lambda_k^{(0)} - 1,$$

the optimal step length is required to satisfy

$$\lambda_k^{(0)}{}_{opt} = \frac{1}{h_k}. \tag{4.3.20}$$

Combining the above results, let us propose:

Proposition 4.3.13. *The optimal damping factor for the Gauss-Newton method in an affine invariant framework under the above fixed assumptions follows the prediction strategy*

$$\lambda_k^{(0)} = \min\left\{1, \frac{1}{h_k}\right\} \tag{4.3.21}$$

$$= \min\left\{1, \frac{1}{[\overline{\omega}_k]\|\Delta x_k\|_2}\right\} \tag{4.3.22}$$

for all $k = 0, 1, \ldots$.

Note, by the deduced *a priori* estimate for the Lipschitz constant, the proposed quantity above is readily computationally available. Though, the step length prediction strategy requires additional input, namely an initial estimate

$$\lambda_0^{(0)}$$

such that the following damping factors

$$\lambda_1^{(0)}, \ldots, \lambda_k^{(0)}$$

can be determined via the explicit iteration proposed. In case the computed step length in the k^{th} iteration

$$\lambda_k^{(0)}$$

does not satisfy the natural monotonicity test condition

$$\|\overline{\Delta x_{k+1}}\|_2 = \|F'(x_k)^+ F(x_{k+1})\|_2 \leq \overline{\theta}_k \|F'(x_k)^+ F(x_k)\|_2 = \overline{\theta}_k \|\Delta x_k\|_2$$

for $\overline{\theta_k} < 1$ or equivalently in terms of the local level function

$$\|\overline{\Delta x_{k+1}}\|_2 = \| - \nabla T(x|F'(x_k)^+)\big|_{x=x_{k+1}}\|_2 < \| - \nabla T(x|F'(x_k)^+)\big|_{x=x_k}\|_2 = \|\Delta x_k\|_2$$

this is indeed an indicator that the step length as it has been predicted would not ensure a downhill descent. Hence, the need for a correction strategy emerges in the adaptive trust region approach to globalize the convergence behaviour of the Gauss-Newton methods in order to make sure a descent is taken in every iteration. The idea then is simply to incorporate an *a posteriori* estimate for the Lipschitz constant

$$[\overline{\omega_k}].$$

Proposition 4.3.14. *The* ν^{th} *corrected step length*

$$\lambda_k^{(\nu)}$$

for $\nu = 1, 2, \ldots$ *and an* a posteriori *estimate for the Lipschitz constant* $[\overline{\omega_k}]$ *are given by*

$$\lambda_k^{(\nu)} = \min\left\{1, \frac{1}{2}\lambda_k^{(\nu-1)}, \mu_k^{(\nu-1)}\right\} \tag{4.3.23}$$

where it is defined

$$\mu_k^{(\nu-1)} := \frac{1}{2}(\lambda_k^{(\nu-1)})^2 \frac{\|\Delta x_k\|_2}{\left\|\overline{\Delta x_k^{(\nu-1)}} - (1-\lambda_k^{(\nu-1)})\Delta x_k\right\|_2}. \tag{4.3.24}$$

Note that the simplified Gauss-Newton correction with respect to the previous step length is denoted by

$$\overline{\Delta x_k^{(\nu-1)}} = -F'(x_k)^+ F(x_k + \lambda_k^{(\nu-1)} F'(x_k)^+ F(x_k)) = -F'(x_k)^+ F(x_k + \lambda_k^{(\nu-1)} \Delta x_k).$$

If using previous definitions, dependent on the previous step length $\lambda_k^{(0)}$ let us define the estimate

$$[h_k(\lambda_k^{(\nu-1)})] := \frac{2}{(\lambda_k^{(\nu-1)})^2} \frac{\left\|\overline{\Delta x_k^{(\nu-1)}} - (1-\lambda_k^{(\nu-1)})\Delta x_k\right\|_2}{\|\Delta x_k\|_2}$$

Then, it is

$$\begin{aligned}
[h_k(\lambda_k^{(\nu-1)})] &= \frac{2}{(\lambda_k^{(\nu-1)})^2} \frac{\left\|\overline{\Delta x_k^{(\nu-1)}} - (1-\lambda_k^{(\nu-1)})\Delta x_k\right\|_2}{\|\Delta x_k\|_2} \\
&= \frac{2}{(\lambda_k^{(\nu-1)})^2} \frac{\left\|F'(x_k)^+ F(x_k + \lambda_k^{(\nu-1)} F'(x_k)^+ F(x_k)) - (1-\lambda_k^{(\nu-1)}) F'(x_k)^+ F(x_k)\right\|_2}{\|F'(x_k)^+ F(x_k)\|_2} \\
&= \frac{2}{(\lambda_k^{(\nu-1)})^2} \frac{\left\|F'(x_k)^+ F(x_{k+1}) - (1-\lambda_k^{(\nu-1)}) F'(x_k)^+ F(x_k)\right\|_2}{\|F'(x_k)^+ F(x_k)\|_2}.
\end{aligned}$$

Using the estimate

$$\|F'(x_k)^+ F(x_{k+1})\|_2 \le \left(1 - \lambda_k^{(\nu-1)} + \frac{1}{2}(\lambda_k^{(\nu-1)})^2 h_k^{(\nu-1)}\right) \|F'(x_k)^+ F(x_k)\|_2$$

elimination of the local estimate $h_k^{(v-1)}$ for all $k = 0, 1, \ldots$ yields

$$\begin{aligned}
\frac{1}{2}(\lambda_k^{(\nu-1)})^2 h_k^{(\nu-1)} &\ge \frac{\|F'(x_k)^+ F(x_{k+1})\|_2 - (1-\lambda_k^{(\nu-1)})\|F'(x_k)^+ F(x_k)\|_2}{\|F'(x_k)^+ F(x_k)\|_2} \\
&\ge \frac{\|F'(x_k)^+ F(x_{k+1}) - (1-\lambda_k^{(\nu-1)}) F'(x_k)^+ F(x_k)\|_2}{\|F'(x_k)^+ F(x_k)\|_2}.
\end{aligned}$$

Hence,

$$\begin{aligned}
[h_k(\lambda_k^{(\nu-1)})] &= \frac{2}{\left(\lambda_k^{(\nu-1)}\right)^2} \frac{\|F'(x_k)^+ F(x_{k+1}) - (1-\lambda_k^{(\nu-1)}) F'(x_k)^+ F(x_k)\|_2}{\|F'(x_k)^+ F(x_k)\|_2} \\
&\le h_k.
\end{aligned}$$

In the direct consequence, this gives

$$\frac{1}{h_k^{(\nu-1)}} \geq \frac{1}{[h_k(\lambda_k^{(\nu-1)})]}.$$

Choosing the damping factor

$$\lambda_k^{(\nu)} = \min\left\{1, \frac{1}{2}\lambda_k^{(\nu-1)}, \mu_k^{(\nu-1)}\right\}$$

is a combination of a regulatory constraint that the damping factor is bounded from above by 1, and an optimal choice between the previous step length taken and the corrected optimal damping factor. DEUFLHARD (2006) remarks, that depending on the nature of the problem, the correction strategy is mostly not of highest importance to choosing the optimal damping factors (p. 214), while the prediction strategy is crucial to precisely determine λ_k. Note that the estimate

$$[h_k(\lambda_k^{(\nu-1)})]$$

will also be an estimate for the global

$$[h_k^*(\lambda_k^{(\nu-1)})]$$

since $h_k \leq h_k^*$ respectively $h_k(\lambda_k^{(\nu-1)}) \leq h_k^*(\lambda_k^{(\nu-1)})$ is guaranteed.

4.4. Linearly-Implicit Euler Extrapolation for Differential Algebraic Equations

By application of the error-oriented damped Gauss-Newton method, the parameter identification task formulated as a nonlinear least squares problem for parameter identification for the given model reduces to a sequence of linear least squares problems

$$\min_{x \in D} \|F'(x_k)\Delta x_k + F(x_k)\|_2^2$$
$$x_{k+1} = x_k + \Delta x_k$$

for $k = 0, 1, 2, \ldots$. The definition of the residual function $F : D \subseteq \mathbb{R}^n \to \mathbb{R}^m$, implies that the solution to the model has to be computed for a fixed set of parameters $x_k \in \mathbb{R}^n$ for every iteration k. Introduced as a system of ordinary differential equations coupled with two algebraic equations, the model is basically a system of differential algebraic equations.
The solution to this DAE system can be obtained via an one step extrapolation based on linearly-implicit Euler discretisation. Once happened, the residual function can be evaluated and the Jacobian matrix, being the residual function differentiated with respect to the parameter set $x_k \in \mathbb{R}^n$, can be determined. This gives a linear gradient system for the initial minimisation task that can be solved by a customized LU factorization performing forward and backward substitution.

Objecting at briefly summarizing the mathematical background of the linearly-implicit Euler

extrapolation algorithm applied, let us consider a system of differential algebraic equations

$$B(t,y)y' = f(t,y) \qquad (4.4.1)$$
$$y(t_0) = y_0$$

where $B \in \mathbb{R}^{d,d}$ may be singular, $y \in \mathbb{R}^d$ and $y_0 \in \mathbb{R}^d$ a (consistent) initial condition. Possibly, one can add an explicit parameter dependence into the notation for the right hand side, which is omitted for the ease of reading. Any system of ordinary differential equations

$$y' = f(t,y)$$
$$y(t_0) = y_0$$

can be formally transformed to a system of DAEs by taking $B = I$. Due to this, the linearly-implicit Euler extrapolation will be introduced for DAE systems only. In our specific case, the model writes

$$\begin{pmatrix} 1 & 0 & 0 & 0 & 0 & 0 \\ 0 & 1 & 0 & 0 & 0 & 0 \\ 0 & 0 & 1 & 0 & 0 & 0 \\ 0 & 0 & 0 & 1 & 0 & 0 \\ 0 & 0 & 0 & 0 & 0 & 0 \\ 0 & 0 & 0 & 0 & 0 & 0 \end{pmatrix} \begin{pmatrix} y_1'(t) \\ y_2'(t) \\ y_3'(t) \\ y_4'(t) \\ y_5'(t) \\ y_6'(t) \end{pmatrix} = \begin{pmatrix} f_1(t,y) \\ f_2(t,y) \\ f_3(t,y) \\ f_4(t,y) \\ f_5(t,y) - y_5(t) \\ f_6(t,y) - y_6(t). \end{pmatrix} \qquad (4.4.2)$$

The detailed information about the model and the right hand side are given in paragraph 2.3 (p. 10 ff.). Considering the general DAE system (4.4.1), a state discretisation is performed first. Though the stiffness concept is defined only for ordinary systems of differential equations, any equation may be called stiff in case application of implicit methods yield significantly better results than application of explicit methods (Curtis/ Hirschfelder (1952)). An implicit integration method seems adequate for the given nonlinear system of differential equations.

The above stated DAE system (4.4) has a differential index of exactly one, since by differentiation, a pure ODE model is recovered. Justifiable by the DAE system's index of one and the algorithmic robustness of the linearly-implicit Euler extrapolation regarding a possible stiffness of the model equations, Limex was considered an appropriate solver to compute a solution, Limex additionally providing an adaptive step size as well as a local error control. These properties will turn out to be very helpful with regard to predicting potentially fertile windows of a woman's menstrual cycle in chapter 5.3.
Limex is basically a one step extrapolation method based on the linearly-implicit Euler discretisation for the integration of the combined state and sensitivity system. First, only state integration will be considered which is extended to a routine that simultaneously solves the state and sensitivity system following Schlegel/ Marquardt/ Ehrig/ Nowak (2002).
Considering pure state integration, the linearly-implicit Euler discretisation with an initial step size of H gives

$$(B(t,y_k) - HA)(y_{k+1} - y_k) = Hf(t_k, y_k) \qquad (4.4.3)$$

which writes

$$y_{k+1} = y_k + (I - HA)^{-1} Hf(y_k) \qquad (4.4.4)$$

for $k = 1, 2, \ldots$ and

$$A = \frac{\partial}{\partial y} \left(f(y) - By' \right)$$

the Jacobian of the DAE system's residual.
Note that the iteration (4.4.4) corresponds basically to one Newton iteration for the nonlinear system arising through discretisation in the frame of the linearly-implicit Euler extrapolation (Schlegel/ Marquardt/ Ehrig/ Nowak (2002), p. 4 and Deuflhard/ Hairer/ Zugck (1987)).
The extrapolation process starts with the first integration step of length H of a considered integration interval

$$[t_l, t_{l+1}].$$

The solution gives the approximation

$$T_{1,1}$$

for $y(t_l + h)$. Provided an asymptotic H-expansion can be found for one step's global discretisation error, higher order approximations can be obtained through polynomial extrapolation (Deuflhard (1983), p. 400 ff.). Sequential interval diminishment by

$$H_j = \frac{H}{n_j} \tag{4.4.5}$$

yields approximations

$$T_{j,1}.$$

Following Deuflhard (1983), the harmonic sequence

$$\{n_j\} = \{1, 2, 3, \ldots, j_{max}\}$$

proved to be a trustworthy choice.

Recursive extrapolation following the scheme

$$T_{j,k} = T_{j,k-1} + \frac{T_{j,k-1} - T_{j-1,k-1}}{\frac{n_j}{n_{j-k+1}-1}} \tag{4.4.6}$$

defines higher order approximations $T_{j,k}$ for $k = 1, \ldots, j$.
Taking the subdiagonal differences

$$\epsilon_j = \|T_{j,j} - T_{j,j-1}\|_2 \tag{4.4.7}$$

as error estimates (Deuflhard (1987), p. 403 and Schlegel/ Marquardt/ Ehrig/ Nowak (2002), p. 4), any approximation

$$T_{j,j}$$

is accepted as an approximation for

$$y(t_l + H)$$

if for a predefined error tolerance it holds

$$\epsilon_j < TOL. \tag{4.4.8}$$

When terminating, a discrete approximation to the DAE system's solution is obtained.

4.5. Simultaneous State and Sensitivity Analysis

Sensitivity analysis is the study about the influence of changes in the parameter vector on the system or its solution. Sensitivity denotes the extend to which changes in the set of parameters lead to variation in the solution. The absolute sensitivity of the i^{th} solution with respect to the j^{th} parameter is defined as the partial differential quotient

$$s_{i,j} := \frac{\partial y_i}{\partial x_j}(t)$$

for $y \in \mathbb{R}^d$, $x \in \mathbb{R}^n$ and hence $i = 1, \ldots, d$, $j = 1, \ldots, n$. Writing $s_j = (s_{1,j}, \ldots, s_{d,j})^T$, this gives the sensitivity vector for the j^{th} parameter. For n parameters, the sensitivity matrix is defined as

$$S = \begin{pmatrix} s_1 & \ldots & s_n \end{pmatrix} = \begin{pmatrix} s_{1,1} & \ldots & s_{1,n} \\ \vdots & & \vdots \\ s_{d,1} & \ldots & s_{d,n}. \end{pmatrix}$$

Sensitivities only hold in a vicinity of the state determined by $y \in \mathbb{R}^d$ and $x \in \mathbb{R}^n$. The sensitivity analysis of a parameter is therefore local. Sensitivities describe the system around a given set of values for the regarded parameter. Aiming at finding the state's first derivative with respect to a set of parameters, sensitivity analysis and state integration can be performed simultaneously.

For a total number of n parameters, total differentiation of the DAE system with respect to each parameter

$$\frac{\partial}{\partial x}\left[B(t, y(t,x))y'(t,x) = f(t, y(t,x), x)\right]$$

gives by chain rule and interchanging the order of differentiation the right hand side gives

$$\begin{aligned} \frac{\partial}{\partial x_j} f(t, y(t,x), x) &= \frac{\partial f(t, y(t,x), x)}{\partial x_j} + \frac{\partial f(t, y(t,x), x)}{\partial y(t,x)} \frac{\partial y(t,x)}{\partial x_j} \\ &= \frac{\partial f(t, y(t,x), x)}{\partial x_j} + \frac{\partial f(t, y(t,x), x)}{\partial y(t,x)} s_j. \end{aligned}$$

The slightly more complicated total differentiation of the left hand side

$$\begin{aligned} \frac{\partial}{\partial x_j}\left(B(t, y(t,x))y'(t,x)\right) &= \Gamma \frac{\partial y(t,x)}{\partial x_j} + B(t, y(x)) \frac{\partial y'(x)}{\partial x_j} \\ &= \Gamma s_j + B(t, y(x))(s_j)' \end{aligned}$$

where Schlegel/ Marquardt/ Ehrig/ Nowak (2002), p. 3, define the matrix

$$\Gamma := \begin{pmatrix} \sum_{k=1}^{d} \frac{\partial (B(t,y))_{1,k}}{\partial y_1} y'_k & \cdots & \sum_{k=1}^{d} \frac{\partial (B(t,y))_{1,k}}{\partial y_d} y'_k \\ \vdots & & \vdots \\ \sum_{k=1}^{d} \frac{\partial (B(t,y))_{d,k}}{\partial y_1} y'_k & \cdots & \sum_{k=1}^{d} \frac{\partial (B(t,y))_{d,k}}{\partial y_d} y'_k. \end{pmatrix}$$

This gives in the end n sensitivity equation systems of the form

$$B(t,y)s_j' = \frac{\partial f(t,y)}{\partial x_j} + \left(\frac{\partial f(t,y)}{\partial y} - \Gamma\right) s_j \tag{4.5.1}$$

for $j = 1, \ldots, n$, being DAE systems themselves are obtained, depending on the solution of the state system

$$B(t,y)y' = f(t,y).$$

Schlegel/ Marquardt/ Ehrig/ Nowak (2002) underline that the Jacobian matrix of those sensitivity systems is the same as for the state system (p.3). Extending the state DAE system for simultaneous sensitivity analysis, a combined system is set up

$$\begin{pmatrix} B(t,y) & & & \\ & B(t,y) & & \\ & & \ddots & \\ & & & B(t,y) \end{pmatrix} \begin{pmatrix} y' \\ s_1' \\ \vdots \\ s_n' \end{pmatrix} = \begin{pmatrix} f(t,y) \\ \frac{\partial f(t,y)}{\partial x_1} + \left(\frac{\partial f(t,y)}{\partial y} - \Gamma\right) s_1 \\ \vdots \\ \frac{\partial f(t,y)}{\partial x_n} + \left(\frac{\partial f(t,y)}{\partial y} - \Gamma\right) s_n \end{pmatrix}.$$

Provided consistent initial conditions for this coupled DAE system of dimension $(d + nd)$ are given, it can be solved using a linearly-implicit Euler extrapolation. From the algorithmic point of view, transformation of the extended DAE system to a block-diagonal system facilitating any LU factorization that needs to be performed seem favourable, for details the reader may consult Schlegel/ Marquardt/ Ehrig/ Nowak (2002).

Once the sensitivity matrix is computed for a specific state of the DAE system, important information about the eligibility of certain parameters to parameter estimation can be extracted. Analysis of the sensitivity matrix specifically pays attention to individual sensitivities and possible linear dependences among the parameters to be estimated.
The sensitivity matrix S gets singular or numerically singular if it is linearly column dependent. This occurs if parameters exhibit linear dependence, meaning that these parameters affect the solution of the model in a similar way such that the columns of the sensitivity matrix are identical or nearly identical. Linear dependence among parameters makes it impossible to estimate the concerned parameters simultaneously and a more detailed approach must be performed.
In case parameters are not identifiable, the sensitivity is very small or zero, trivially leading to singularity of S also. The corresponding column of the sensitivity matrix gets zero or near to zero.
In anyway, for unidentifiable or linear dependent parameters the sensitivity matrix becomes (numerically) singular.

Using the Euclidean matrix norm

$$\|A\|_2 = \max_{\|\tilde{x}\|_2=1} \frac{\|A\tilde{x}\|_2}{\|\tilde{x}\|_2}$$

appropriate mathematical tools such as the *condition number*, measuring the stability of the sensitivity matrix,

$$\kappa(S) := \frac{\max_{\|\tilde{x}\|_2=1} \|S\tilde{x}\|_2}{\min_{\|\tilde{x}\|_2=1} \|S\tilde{x}\|_2} \in [0, \infty] \tag{4.5.2}$$

for $S \in \mathbb{R}^{d,n}$ the sensitivity matrix, the *subcondition number* and the weighted Euclidean *column norm*

$$\|s_j\| = \sqrt{\frac{1}{d}\sum_{i=1}^{d}(s_{ij})^2}, \tag{4.5.3}$$

the latter giving information about singularities.

First information about the sensitivity matrix S can be obtained through calculating the *column norms*. Through the *column norm*

$$\|s_j\| = \sqrt{\frac{1}{d}\sum_{i=1}^{d}(s_{ij})^2},$$

only singularities or nearly singularities of the sensitivity matrix can be identified with column norms near to zero. If

$$\|s_j\| = 0,$$

all $s_{i,j} = 0$ for $i = 1, \ldots, d$ and if

$$\|s_j\| \neq 0,$$

then the parameter x_j is in principle estimable. Though, S might get singular also by linear dependences among the parameter set. In order to obtain more detailed information about possible linear dependences and sensitivities, a SVD decomposition to estimate the *condition number* or a QR decomposition to estimate the *subcondition number* need to be performed. Rank deficiencies of S can be assessed through this analysis also. While estimating error propagation in the system through the *condition number* requires a SVD decomposition of S, the *subcondition number* solely requires computation of a less costly QR factorization.

The condition number is well defined for non invertible matrices as well as for invertible matrices. In case $S \in \mathbb{R}^{d,n}$ is non-singular and square ($d = n$), another and slightly less general definition writes

$$\kappa(S) = \|S\|_2 \|S^{-1}\|_2$$

while $\kappa(S) := \infty$ for any S singular. Measuring the stability or sensitivity of the linear system the sensitivity matrix represents, it holds

$$\kappa(S) \geq 1.$$

A system whose condition numbers near one is assumed to be well conditioned, while any condition number much greater than 1 indicates an ill-conditioned matrix. Though, there exists no general threshold

$$\kappa_{max},$$

$\kappa(S)$ is not allowed to surmount. With respect to the purpose of the parameter identification problem and the herein performed sensitivity analysis, this threshold can be determined. Widely applied in engineering and biological sciences has been

$$\kappa_{max} \approx 10^4.$$

Under the condition that $S \in \mathbb{R}^{d,n}$ is real, there exists a singular value decomposition

$$S = U\Sigma V^T$$

with $U \in \mathbb{R}^{d,d}$, $V \in \mathbb{R}^{n,n}$ orthogonal and $\Sigma \in \mathbb{R}^{d,n}$ rectangular diagonal matrix. The columns of U and V are called left and right singular vectors, since

$$\Sigma = \begin{pmatrix} \sigma_1 & & & \\ & \sigma_2 & & \\ & & \ddots & \\ & & & \sigma_{\min\{d,n\}} \end{pmatrix}$$

contains the singular values as entries on the diagonal. As a common convention, the singular values are listed in descending order

$$\sigma_1 \geq \sigma_2 \geq \ldots \geq \sigma_{\min\{d,n\}} \geq 0.$$

Then, Σ is uniquely defined by $S \in \mathbb{R}^{d,n}$ while the rotation matrices $U \in \mathbb{R}^{d,d}, V \in \mathbb{R}^{n,n}$ are not. In case S is square, say $S \in \mathbb{R}^{d,d}$ also $\Sigma = diag(\sigma_1, \ldots, \sigma_d)$ and U, V are square of dimension d. The singular value decomposition and the orthogonality of U, V give then with the second definition of the condition number that

$$\kappa(S) = \|U\Sigma V^T\|_2 \|(U\Sigma V^T)^{-1}\|_2 = \frac{\sigma_1}{\sigma_d}$$

since $\|U\|_2 = 1$, $\|V\|_2 = 1$ and $\|\Sigma\|_2 = \max_{\|\tilde{x}\|_2=1} \frac{\|\Sigma\tilde{x}\|_2}{\|\tilde{x}\|_2} = \sigma_1$. Though the condition number gives important information about the estimability of the parameter vector $x \in \mathbb{R}^n$ and the sensitivity of the system to perturbations in $x \in \mathbb{R}^n$, singular value decomposition is computationally expensive. A less theoretically satisfactory way to extract such information is through the *subcondition number* (Deuflhard/ Hohmann (2003)).

Performing a QR decomposition for the rectangular sensitivity matrix $S \in \mathbb{R}^{d,n}$, assuming $d \geq n$ gives

$$S = QR = Q \begin{pmatrix} R_1 \\ 0 \end{pmatrix} = (Q_1 \quad Q_2) \begin{pmatrix} R_1 \\ 0 \end{pmatrix} = Q_1 R_1$$

where $Q_1 \in \mathbb{R}^{d,n}, Q_2 \in \mathbb{R}^{d,(d-n)}$ have orthogonal columns, $R_1 \in \mathbb{R}^{n,n}$ upper triangular matrix. For simplicity, instead of the more general notation Q_1, R_1, let us set $Q := Q_1, R := R_1$. In case the system is underdetermined, i.e. $d < n$, the QR decomposition is identically performed on the transpose

$$S^T = QR.$$

Rearranging the diagonal elements of the upper triangular

$$S\Pi = QR$$

through application of a suitable permutation matrix Π gives

$$R = \begin{pmatrix} |r_{11}| & & & * \\ & |r_{22}| & & \\ & & \ddots & \\ 0 & & & |r_{nn}| \end{pmatrix}$$

with $|r_{11}| \geq \ldots \geq |r_{nn}|$. Having identified the smallest and largest entries of the upper triangular of the previously performed QR decomposition, assuming rank(R)= n, the *subcondition number* is defined by the ratio

$$sc(S) := \frac{|r_{11}|}{|r_{dd}|}. \tag{4.5.4}$$

By its properties $sc(S) \geq 1$, $sc(S) = \infty$ if and only if $S \neq 0$ is singular. By the above stated relation $sc(S) \leq \kappa(S)$, the *subcondition* is a computationally cost effective way to assess the parameters' estimability and potential singularity of the sensitivity matrix.

In the subsequent chapter, the model is analysed. Parameters are estimated through the NLSCON, implemented in the POEM package using the damped Gauss-Newton method. Sensitivity analysis is performed after NLSCON converged to obtain information about the identifiability and sensitivities of certain parameters with the add-on MATLAB software package POEM. The *column norms* are calculated in the first step of the following sensitivity analysis, in order to identify columns with solely zero entries. Knowledge about estimability can be extended through the second step of the sensitivity analysis. POEM performs a QR decomposition, such that more detailed information about the sensitivities, possible linear dependences and the parameter set itself can be extracted.

5. Simulation Results and Evaluation

5.1. Model Analysis and Simulation Results

The proposed model of section 2.3 reads

$$\begin{aligned}
E2'(t) &= p_1^{E2} * H^-(FSH(t), p_5^{E2}, p_6^{E2}) - p_3^{E2} * E2(t) * H^+(LH(t), p_7^{E2}, p_8^{E2}) \\
&\quad + p_2^{E2} * H^+(E_2(t), p_9^{E2}, p_{10}^{E2}) - p_4^{E2} * E2(t) * H^+(P4(t), p_{11}^{E2}, p_{12}^{E2}) \\
P4'(t) &= p_6^{P4} * P4d(t) - p_7^{P4} * P4(t) \\
BBT'(t) &= p_1^{BBT} * P4(t) * (BBT(t) - 35.00) \\
&\quad - p_2^{BBT} * (BBT(t) - 35.00) * H^+((BBT(t) - 35.00), p_3^{BBT}, p_4^{BBT}) \\
P4d'(t) &= p_1^{P4} * H^-(y_4(t), p_3^{P_4}, p_4^{P4}) * LH(t) * P4d(t) - p_2^{P4} * H^+(P4d(t), p_5^{P4}, p_4^{P4})
\end{aligned}$$

with two algebraic functions

$$\begin{aligned}
LH(t) &= p_1^{LH} + p_2^{LH} * \exp\left(-\left(p_3^{LH} \sin\left(\frac{\pi t}{p^{cyclelength}} + p_4^{LH}\right)\right)^2\right) \\
FSH(t) &= p_1^{FSH} + p_2^{FSH} * \exp\left(-\left(p_3^{FSH} \sin\left(\frac{\pi t}{p^{cyclelength}} + p_4^{FSH}\right)\right)^2\right) \\
&\quad + p_5^{FSH} * \sin\left(\frac{\pi t}{p^{cyclelength}} + p_6^{FSH}\right)^4.
\end{aligned}$$

If it is defined

$$y(t) = (E2(t), P4(t), BBT(t), P4d(t), LH(t), FSH(t))^T \in \mathbb{R}^6$$

the model can be written in the form

$$B(t, y)y'(t) = f(t, y)$$

where $B(t, y) \in \mathbb{R}^{6,6}$ is non singular. Specifically, the model gives

$$\begin{pmatrix} 1 & 0 & 0 & 0 & 0 & 0 \\ 0 & 1 & 0 & 0 & 0 & 0 \\ 0 & 0 & 1 & 0 & 0 & 0 \\ 0 & 0 & 0 & 1 & 0 & 0 \\ 0 & 0 & 0 & 0 & 0 & 0 \\ 0 & 0 & 0 & 0 & 0 & 0 \end{pmatrix} \begin{pmatrix} y_1'(t) \\ y_2'(t) \\ y_3'(t) \\ y_4'(t) \\ y_5'(t) \\ y_6'(t) \end{pmatrix} = \begin{pmatrix} f_1(t, y) \\ f_2(t, y) \\ f_3(t, y) \\ f_4(t, y) \\ f_5(t, y) - y_5(t) \\ f_6(t, y) - y_6(t) \end{pmatrix}$$

where the right hand side is just

$$
\begin{aligned}
f_1(t,y) &= p_1^{E2} * H^-(y_6(t), p_5^{E2}, p_6^{E2}) - p_3^{E2} * y_1(t) * H^+(y_5(t), p_7^{E2}, p_8^{E2}) \\
&\quad + p_2^{E2} * H^+(y_1(t), p_9^{E2}, p_{10}^{E2}) - p_4^{E2} * y_1(t) * H^+(y_2(t), p_{11}^{E2}, p_{12}^{E2}) \\
f_2(t,y) &= p_6^{P4} * y_4(t) - p_7^{P4} * y_2(t) \\
f_3(t,y) &= p_1^{BBT} * y_2(t) * (y_3(t) - 35.00) - p_2^{BBT} * (y_3(t) - 35.00) \\
&\quad * H^+((y_3(t) - 35.00), p_3^{BBT}, p_4^{BBT}) \\
f_4(t,y) &= p_1^{P4} * H^-(y_4(t), p_3^{P_4}, p_4^{P4}) * LH(t) * y_4(t) - p_2^{P4} * H^+(y_4(t), p_5^{P4}, p_4^{P4}) \\
f_5(t,y) - y_5(t) &= p_1^{LH} + p_2^{LH} * \exp\left(- \left(p_3^{LH} \sin\left(\frac{\pi t}{p^{cyclelength}} + p_4^{LH} \right) \right)^2 \right) - y_5(t) \\
f_6(t,y) - y_6(t) &= p_1^{FSH} + p_2^{FSH} * \exp\left(- \left(p_3^{FSH} \sin\left(\frac{\pi t}{p^{cyclelength}} + p_4^{FSH} \right) \right)^2 \right) \\
&\quad + p_5^{FSH} * \sin\left(\frac{\pi t}{p^{cyclelength}} + p_6^{FSH} \right)^4 - y_6(t)
\end{aligned}
$$

This six dimensional DAE system involves 33 parameters and an a priori unknown cycle length $p^{cyclelength}$, denoting the length of the current cycle. In a later stage, parameter identification, meaning the fit of the model to any individually available data, concerns only 16 parameters and the cycle length of the running cycle. Of all 33 parameters, the Hill exponents of the 7 Hill functions in the model can be excluded from further parameter estimation. The Hill exponents were adjusted beforehand. Any re-estimation did not yield significant differences, why their estimation seems over all not advantageous. Furthermore, y_5 and y_6 accounting for LH and FSH are modelled via standard curves since no individual measurements are collected here. Due to this fact, all parameters for LH and FSH, 10 in the end, are adjusted beforehand and fixed. Though also P_4 data is not assumed to be accessible in further applications, the concerned parameters should probably not be fixed beforehand in order to enable an adequate solution of the nonlinear least squares problem, especially as E_2 and P_4 closely interact.

The 33 model parameters were estimated simultaneously using the damped Gauss-Newton method implemented in the NLSCON code. All codes perform on MATLAB, MATLAB 2012b was used in this work. The final parameter set estimated for the test data set is shown in table 5.1, which has been obtained after successive re-estimation through NLSCON until it converged. This parameter set is then used to solve the nonlinear least squares problem with the given test data and remains fixed in the following evaluation and sensitivity analysis.

If applying a different data set, as above deduced, the parameter estimation problem reduces from 33 to 16 free parameters – those belonging to E_2, P_4, the P_4 delay and BBT exclusively the involved Hill exponents (even though, they could also be re included). The cycle lengths for the simulation were known from the data and fixed on 29, 26, 28 and 27 days.

	E_2		P_4		LH and FSH		BBT
$p_1^{E_2}$	186.391675192199	$p_1^{P_4}$	0.071476221309	p_1^{LH}	1.332372919499	p_1^{BBT}	0.004924843360
$p_2^{E_2}$	202.263939088376	$p_2^{P_4}$	0.979526047078	p_2^{LH}	110.315843426303	p_2^{BBT}	96.954898958163
$p_3^{E_2}$	4.483306488346	$p_3^{P_4}$	3.844781287017	p_3^{LH}	7.166470180530	p_3^{BBT}	6.942691358857
$p_4^{E_2}$	1.030340524237	$p_4^{P_4}$	4.000000000000	p_4^{LH}	14.104745386110	p_4^{BBT}	6.000000000000
$p_5^{E_2}$	3.415391066868	$p_5^{P_4}$	0.089664953197	p_1^{FSH}	2.980731109637		
$p_6^{E_2}$	4.000000000000	$p_6^{P_4}$	0.884758168213	p_2^{FSH}	6.204468385651		
$p_7^{E_2}$	115.028227706639	$p_7^{P_4}$	0.258961557765	p_3^{FSH}	9.205554706609		
$p_8^{E_2}$	4.000000000000			p_4^{FSH}	67.547726260961		
$p_9^{E_2}$	200.584174200939			p_5^{FSH}	3.103474628950		
$p_{10}^{E_2}$	4.000000000000			p_6^{FSH}	4.267119161284		
$p_{11}^{E_2}$	0.326482174623						
$p_{12}^{E_2}$	4.000000000000						

Table 5.1.: Parameter set applied to fit the model to the given data, consisting of four cycles of different length.

The test data used includes measurements for E_2 (pmol/L), P_4 (ng/mL), LH (UI/L), FSH (UI/L) and BBT (°C) for four cycles of length 29, 26, 28 and 27 days. Measurements for all components except for BBT were available twice a day. The hormonal components E_2, P_4, LH and FSH data were taken from among others recorded *Pfizer* experiments, available at *Konrad-Zuse Zentrum für Informationstechnik Berlin*. Most of these data have been previously plugged into the *GynCycle* model. Since no simultaneous measurements for E_2 and BBT concentrations was acquired, standard BBT curves were taken.
The BBT values displayed a frequency of one measurement per day, such that in order to properly use this data, the BBT measurements were interpolated. The interpolated value between two real BBT measurements is taken as the second BBT value per day and matched best possible to the other components. Due to this, the test data set has to be considered partly artificial even though it seems to properly reproduce the dynamics of an idealized human menstrual cycle. Of course, for final evaluation and assessment of the proposed model, more specific and irregular data is of need.

The complete data set used in this chapter can be found in the appendix (see p. XIII ff.). Using the test data set, the computed solution to the nonlinear least squares model (approximately) represents the key hormonal dynamics of the human menstrual cycle.

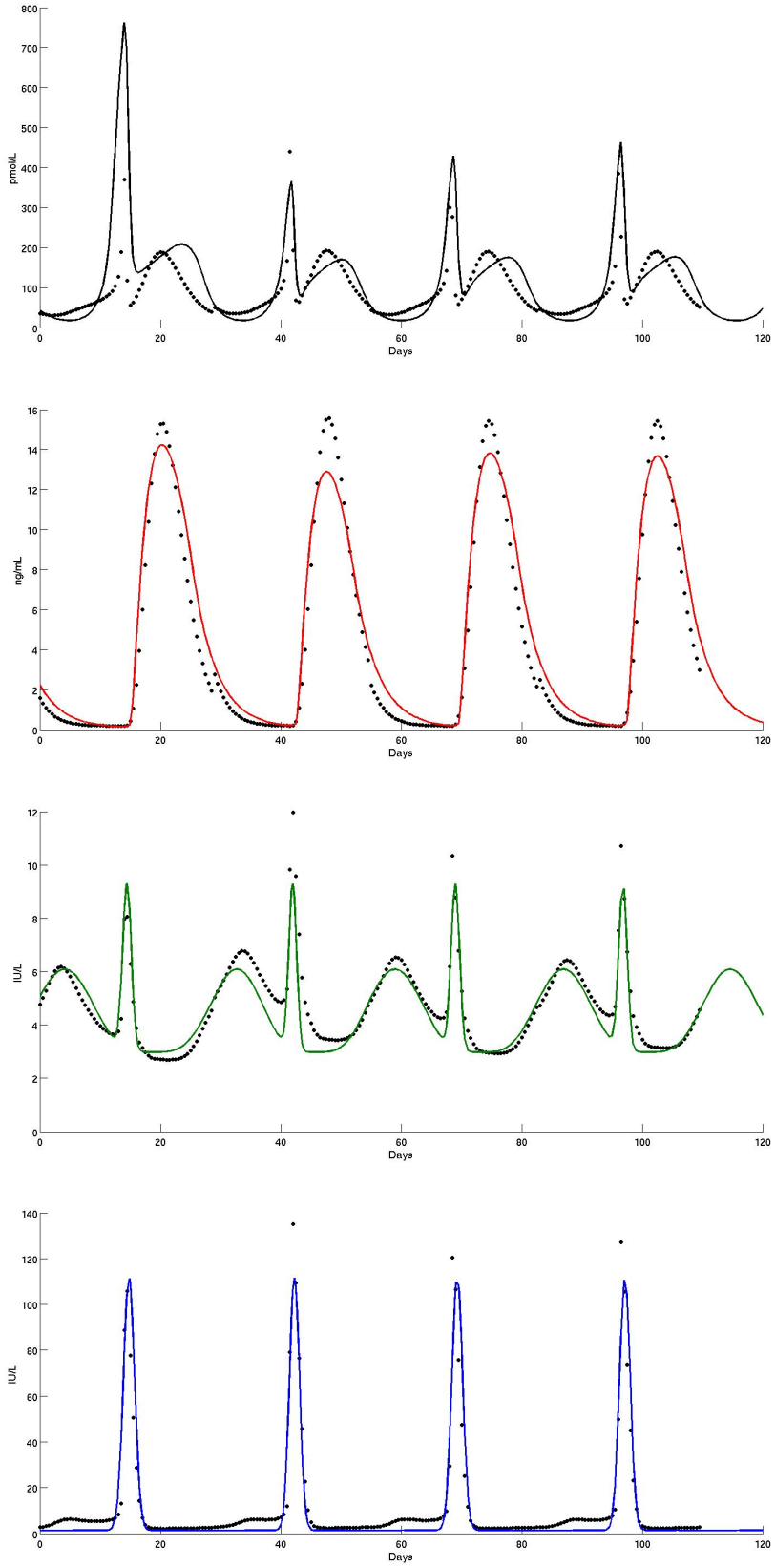

Figure 5.1.: The computed solution of the model to the given test data using the parameter set estimated beforehand gives the above fit to the measurements. Measurement points are plotted as points, the curves are corresponding fits for E_2, P_4, LH and FSH from top to bottom.

As figure 5.1 (p. 82) depictures, the model with the applied parameter set fits quite well the available test data. It obviously takes one to two cycles, before the model can accurately reproduce the change points and the peaks in the different hormone concentrations, which is only due to the chosen initial conditions. Adjustment of these initial conditions leads to a more appropriate representation of the first one to two cycles.
For example, the E_2 fit displays a higher peak than the data in the first cycle as well as a slightly delayed second peak. The height of the peak is not crucial to the final purpose of ovulation prediction though, since absolute values can not be considered anyway. This is because of the fact, that each woman is assumed to have different base and peak levels. P_4 seems to be adequately represented through its model equation. The curves for LH and FSH should not vary over time, as they are modelled as fixed standard curves. The other components should solely represent the best possible fit to the data used over time. Though the corresponding measurements were included in the test data, in future no LH and FSH data will enter the model. Obviously, the sinusoidal exponential functions can give a satisfactory result.

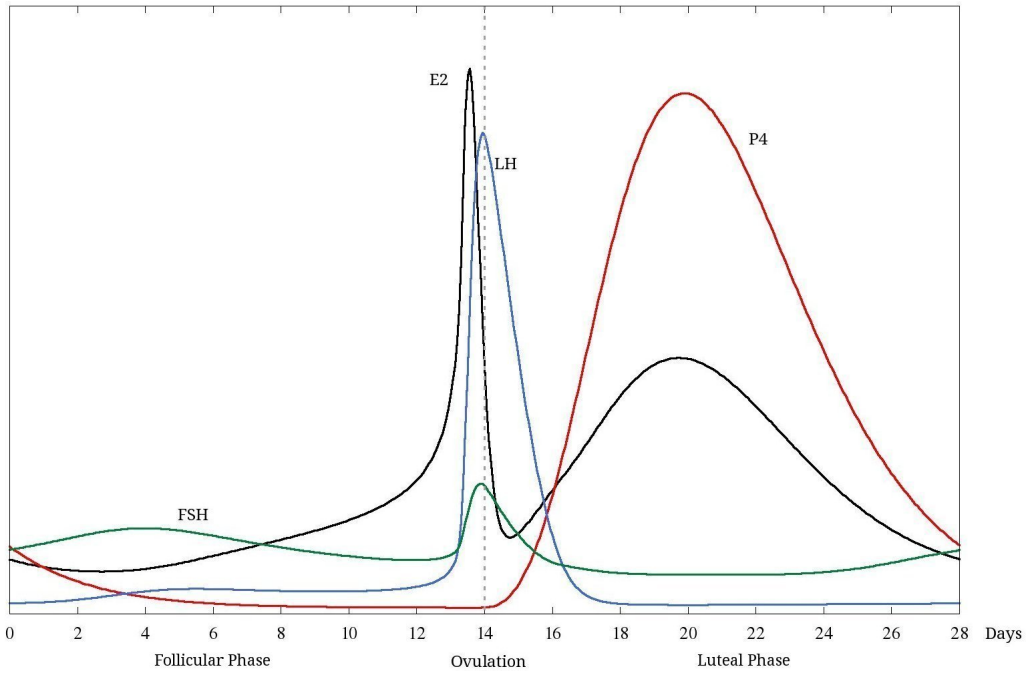

Figure 5.2.: This (scaled) plot was taken as a reference for the endocrinological dynamics of the human menstrual cycle (see also p. 4). It was aimed at reproducing similar dynamics through the proposed model.

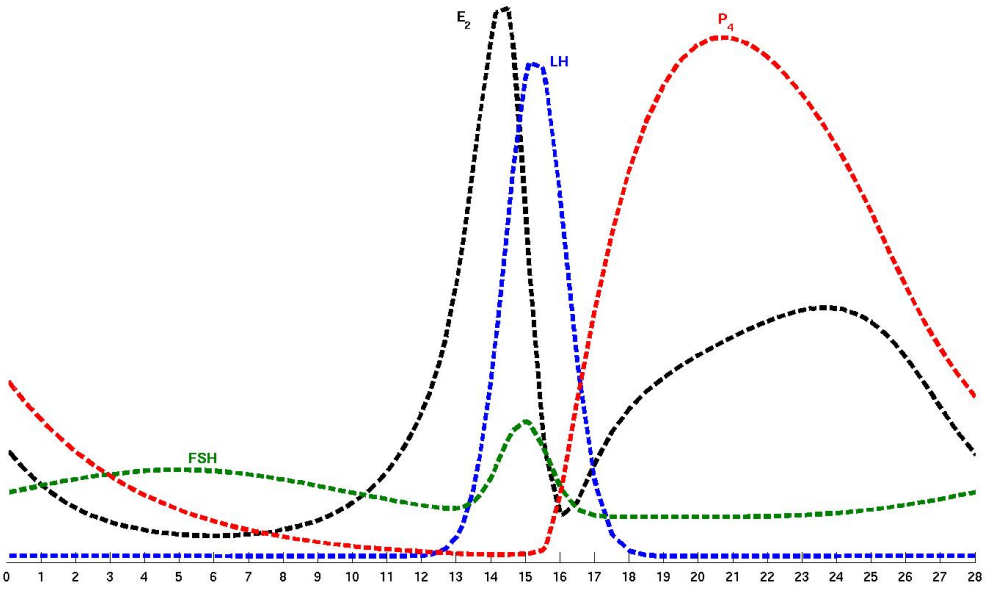

Figure 5.3.: The third cycle of the data set, of length 28 days, was used to reconstruct the endocrinological dynamics in a scaled setting. The dimensionless plots (see figure 2.1, p. 4) are used, and the components scaled with E_2, $25 \cdot P_4$, 3·LH and 10· FSH, since this scaling was applied to the reference figure 5.1 (p. 82). This plot hence gives the scaled endocrinological dynamics displayed by the proposed model for a 28 days test cycle.

A dimensionless comparison of the four endocrinological components is given in figure 5.1 (p. 83). The model's solution for 4 cycles was scaled and only the days $54 - 82$ considered in the further (standard cycle of length 28 days). Figure 5.1 (p. 82), that was already given in section 2.1, was taken as reference to how the model's endocrinological dynamics should look like. For both plots, a the curves were plotted with the scaling E_2, $25 \cdot P_4$, 3·LH and 10· FSH. For both plots, a cycle of 28 days was chosen such that ovulation can be assumed to happen at day 14.
In the model though, the LH peak is slightly delayed compared to the reference plot. LH peak happens around day 14.5, such that ovulation cannot assumed to be happening before day 15. This inaccuracy needs to be mitigated by further model refinements. But still, ovulation his event happens shortly after the peak in LH (blue line) which is in line with theory and the reference plot. E_2 rises previous to the peak in LH. The second peak in E_2 is a bit less pronounced and a little wider in the model. Also, both the peaks in E_2 and LH are less steep in the model, which might lead to a loss in accuracy when detecting the corresponding slope's change points later, in chapter 5.3. FSH seems to be too pronounced in its second peak compared to the reference plot, and less pronounced in its first peak. Though, FSH was fit to the test data and might still be represented correctly. P_4 reacting slower in its dynamics by the model as it is assumed to be, its peak being smoother and wider.

Summarising, the basic hormonal regulation happening during the human menstrual cycle is well represented. The viability of the model's differential equations can unfortunately not be judged finally at this stage, since real data for several individual women might reveal yet unknown inaccuracies. The above comparison is only covering the simulations for the partly artificial data set that was available. Hence, also this comparison might not be representative for more general data. A more detailed evaluation is of need here. For the test data set though, the six dimensional DAE systems appears to provide a suitable approximation. Considerable differences of the model are mostly shown concerning the steepness of the hormonal dynamics as well as their absolute and relative peak heights. The latter is considered less crucial to the modelling process though, as in the end rather the change points than any absolute hormonal levels are crucial to predict ovulation and potentially fertile periods.

5.2. A Sensitivity Analysis for the Model

The study about sensitivities is the analysis of the model's stability and the model response to changes in the parameter set. The six dimensional model contains a total number of 33 parameters. 7 of those are exponents of the occurring Hill functions. The exponents of the Hill functions are fixed beforehand, the Hill functions have the Hill exponents p_6^{E2}, p_8^{E2}, p_{10}^{E2} and p_3^{P4} of 4, while only the Hill function in the BBT differential equation has a different exponent of $p_4^{BBT} = 6$.

Based on the purpose of the model, the parameters were split up into three sets for the sensitivity analysis, that is performed on the solution obtained with the stated parameter values of table 5.1 and the test data set comprising the data for four menstrual cycles. The first parameter set only accounts for the parameters of the LH and FSH functions, consisting of a total number of 10 parameters. Knowledge of those parameters' sensitivities is helpful for further improvements of the LH and FSH curves, but not crucial to the model. These parameters are not re-estimated for new data sets, since the data sets are not assumed to include LH and FSH measurements.

Parameter	Parameter Value	Column Norms
p_1^{LH}	1.332372919499	$8.845 \cdot 10^2$
p_2^{LH}	110.315843426303	$1.357 \cdot 10^4$
p_3^{LH}	7.166470180530	$4.566 \cdot 10^3$
p_4^{LH}	14.104745386110	$1.875 \cdot 10^5$
p_1^{FSH}	2.980731109637	$1.107 \cdot 10^4$
p_2^{FSH}	6.204468385651	$2.849 \cdot 10^2$
p_3^{FSH}	9.205554706609	$9.577 \cdot 10^2$
p_4^{FSH}	67.547726260961	$3.518 \cdot 10^5$
p_5^{FSH}	3.103474628950	$1.941 \cdot 10^3$
p_6^{FSH}	4.267119161284	$2.400 \cdot 10^4$

Table 5.2.: Listing of parameters included in parameter set 1, their values estimated through the Gauss-Newton method in NLSCON and the computed column norms.

The *column norms* $\|s_j\|$ of the sensitivity matrix are a valuable indicator for the comparability of the relative sensitivities. In principle, if for any parameter j it holds

$$\|s_j\| \neq 0,$$

the corresponding parameter is estimable at the considered time and state of the model. Trivially, the column entries of s_j are not all zero and hence S is not singular for this reason. Singularity of S might still occur by possible linear dependences among the considered parameters of set 1. Singularity of S then is only assessable through a more detailed analysis.
If $\|s_j\|$ is large, x_j is a sensitive parameter which means that small perturbations in the parameter lead to large variation in the system or its solution. For nonsensitive parameters, $\|s_j\|$ is small such that small variations in x_j only have a small effect on the system. Reviewing the obtained *column norms* (table 5.2, p. 85), gives that the translation of the sinus argument in the exponential function for FSH on the time axis, p_4^{FSH}, is the most sensitive parameter. The least sensitive parameter is p_2^{FSH}, defining the width of the sinus argument's peak.

To obtain more detailed information on the sensitivity matrix, a QR decomposition is performed in POEM. POEM decomposes S in Q orthogonal and R upper triangular. S is simultaneously

permuted such that

$$R = \begin{pmatrix} |r_{11}| & & & * \\ & |r_{22}| & \ddots & \\ 0 & & & |r_{nn}| \end{pmatrix}$$

with $|r_{11}| \geq \ldots \geq |r_{nn}| \geq 0$. R is also used to determine the *rank* of S, i.e. S is rank deficient if at least the last diagonal entry $|r_{nn}| = 0$.

The decomposition reveals that S_1 for parameter set 1 is rank deficient with $rank(S_1) = 9 < 10$, where 10 is the number of parameters included in this consideration and sensitivity analysis. Obviously, S_1 is by this singular while all its column norms

$$\|s_j^1\| \neq 0.$$

Consequently, linear dependence have to be assumed among the parameters. If S_1 is singular, of course, the obtained *subcondition number* is

$$sc(S_1) = \infty.$$

Generally speaking, the *subcondition number* is defined as

$$sc(S) = \frac{|r_{11}|}{|r_{nn}|}$$

only if S has full rank. Otherwise, $r_{nn} = 0$. Since the *subcondition number* gives an estimate for the error propagation in the system, a *subcondition number* of

$$sc(S) = \infty$$

is definitely not satisfying since no other information than the singularity of S can be extracted.

The notional concept implemented in POEM is based on the reasoning, that successively reducing the set of parameters, being considered in the sensitivity analysis, for the system might yield valuable information. Starting the reduction of the parameter set from bottom to top with those parameters assigned to the last diagonal entries of R, at some stage a non singular system will be recovered provided that not all of the treated parameters are linearly dependent on each other and that all $\|s_j\| \neq 0$. For the user's ease, POEM outputs an ordering of the parameters, where the last parameter displayed is one of possibly more than one parameters causing the singularity of S.

For LH and FSH, the order ending with the *critical parameter* of this sensitivity analysis (since

$rank(S)$ is 9 of 10) provided by POEM writes

$$
\begin{aligned}
&p_4^{FSH}\\
&p_4^{LH}\\
&p_6^{FSH}\\
&p_1^{FSH}\\
&p_2^{LH}\\
&p_3^{LH}\\
&p_5^{FSH}\\
&p_3^{FSH}\\
&p_1^{LH}\\
&p_2^{FSH}.
\end{aligned}
$$

Following this ordering, the system's parameter set is reduced step by step by one parameter, starting with the lowest listed. *Subcondition numbers* are computed for all of the hereby obtained parameter subsets, containing all, all but the last, all except for the two last, etc. parameters referring to the POEM ordering. These *subcondition numbers* for different systems are illustrated in the *Subcondition* plot of e.g. figure 5.2 (p. 91).
From left to right, the *subcondition numbers* are plotted for the system with respect only to the first, to the first two, to the first three, etc. parameters of the ordering. These visualised *subcondition numbers* estimate how strong errors are propagated in the system and its solution. Note, that the *subcondition numbers* are plotted relative to the prescribed *subcondition number* threshold, i.e. in % of 10^4 or with respect to the largest *subcondition number* computed, if this *subcondition number* does not surmount the tolerance of 10^4.

Besides the POEM ordering giving crucial information about the entries of R and hereby information about which parameter make the system over the top sensitive to changes in the parameter's values, the notional concept can also reveal linear dependences in the set's parameters. By successive reduction of the parameters considered together in the sensitivity analysis, sharp decreases in the *subcondition numbers* visualised in the *subcondition plot* (from left to right) – be it decrease in absolute values, in % of 10^4 or in % of the largest absolute *subcondition number* computed – indicate among which of the parameters left out of the consideration (the elimination process still following the POEM ordering) and the subset of remaining parameters dependences occur. Though, it cannot be determined how individual parameters are related or correlated. A more detailed analysis would be required for this purpose.
For LH and FSH, since the upper triangular R is ordered by absolute value, one can say that the solution of the model is obviously most dependent on the parameters p_4^{FSH}, p_4^{LH} which locate the LH and FSH peaks on the time axis. If these peaks are wrongly located over time, the solution will differ significantly. Small variations in p_4^{FSH} and p_4^{LH} lead to large variation in the system. Furthermore, the solution seems to depend more on the FSH base level constituted by p_1^{FSH} than on the corresponding LH base level p_1^{LH}. For the prefactor of the exponential growth term it is the other way around, meaning that the prefactor for LH, p_2^{LH}, seem to be of higher impact to the model's solution that its FSH analogous p_2^{FSH}.
Large variation in the magnitude of the sensitivities, hence the *column norms*, can be appraised only by performing the more detailed analysis involving the QR decomposition of the sensitivity matrix S_1. For the parameter set 1 assigned to LH and FSH, the QR decomposition gave rank

9 of a potential rank of 10. As mentioned above, the *subcondition* of the sensitivity matrix S_1 was estimated via POEM as

$$sc(S_1) = \infty$$

due to the occurring singularity of S_1 if considering all 10 parameters simultaneously in the sensitivity analysis. The *condition number* was not computed for the obtained sensitivity matrix since the SVD decomposition requires a significantly higher computational effort than the QR decomposition necessary to determine the *subcondition number*. Though, for the system and the full parameter set 1, it would also be

$$\kappa(S_1) = \infty.$$

In general, large values for $\kappa(S)$ indicate an ill-conditioned problem. There is no globally prescribed threshold for the *condition number*, but in engineering and biological sciences, usually

$$\kappa_{max} \approx 10^4$$

is applied. Though it holds

$$sc(S) < \kappa(S),$$

both numbers tend to have a comparable size by experience. Hence, also for the *subcondition number*, a maximum of

$$sc_{max}(S) \approx 10^4$$

is widely taken as reference. Of course, the smaller the *condition* and *subcondition number*, the better.

Reducing the set of considered parameters by the last ordered one, meaning that

$$p_2^{FSH}$$

is excluded for further considerations in the sensitivity analysis of parameter set 1, POEM computes the corresponding *subcondition number* as

$$sc(\tilde{S}_1) = 4737.6612 < 10^4$$

the *subcondition number* still is not in the range of the *maximum subcondition number*. Not surmounting the prescribed threshold, one can assume the problem not to be ill-conditioned for parameters set 1 exclusively p_2^{FSH}. Further examination of the *subcondition plot* in the lower plot of figure 5.2 (p. 91) indicates, that at least this parameter p_2^{FSH} has to be left when simultaneously estimate the parameters. From right to left, a nearly exponential decay of the displayed *subcondition numbers* in % of 10^4 can be evidenced. The error propagation hence significantly diminishes from right to left, when first reducing the parameter set 1 by p_2^{FSH} and then also p_1^{LH}. Effectively, the problem to estimate the 9 parameters

$$\{p_1^{LH}, p_2^{LH}, p_3^{LH}, p_4^{LH}, p_1^{FSH}, p_3^{FSH}, p_4^{FSH}, p_5^{FSH}, p_6^{FSH}\}$$

is not ill-conditioned, but even higher stability of the system with respect to error propagation is obtained if only the 8 parameters

$$\{p_2^{LH}, p_3^{LH}, p_4^{LH}, p_1^{FSH}, p_3^{FSH}, p_4^{FSH}, p_5^{FSH}, p_6^{FSH}\}$$

are considered, analysed or estimated through NLSCON simultaneously. Though, further experiments it would be necessary to assess this last relation and the occurring dependences.

Summarising, for set 1 the system is ill-conditioned. Reducing the parameter set by p_2^{FSH} gives a significantly more stable system to perturbations in the parameter vector. All *column norms* and the *subcondition numbers* for the full and successively reduced sets of parameters are graphically summarised in figure 5.2 (p. 91). Hence, if re-estimating the parameters associated with LH and FSH, p_2^{FSH} should be estimated individually or at least not simultaneously with

$$\{p_1^{LH}, p_2^{LH}, p_3^{LH}, p_4^{LH}, p_1^{FSH}, p_3^{FSH}, p_4^{FSH}, p_5^{FSH}, p_6^{FSH}\}.$$

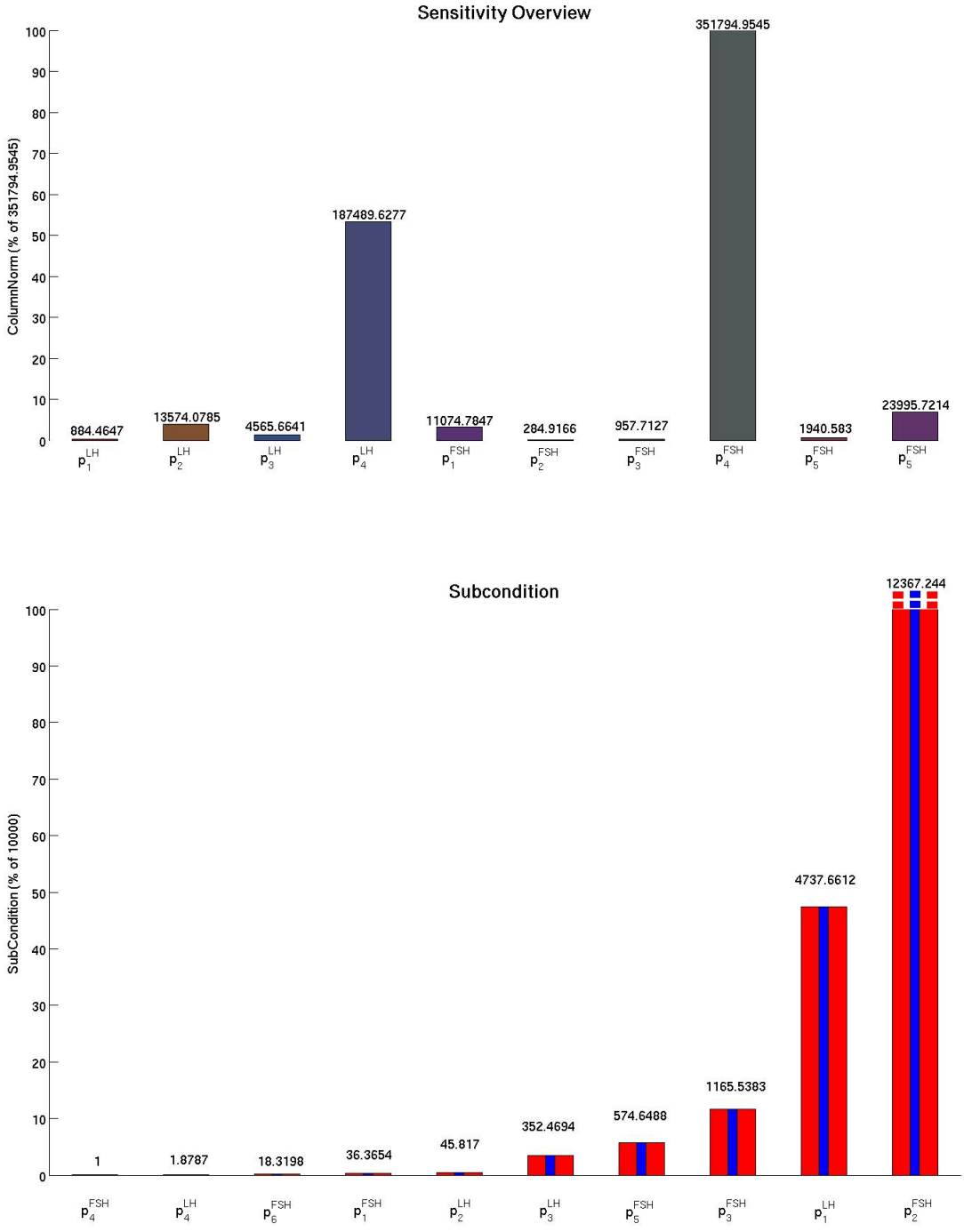

Figure 5.4.: Sensitivity outputs for parameter set 1, i.e. the parameters p_i^{LH} and p_j^{FSH} for $i = 1, \ldots, 4$, $j = 1, \ldots, 6$. The upper plot gives the relative size of each column norm with respect to the largest column norm in %, the absolute value computed of the column norms being showed next to the corresponding bars. The lower plot gives bars for each subset of considered parameters and the associated subcondition number as % of 10000, while the initial parameter set 1 is reduced following the POEM ordering from right to left. The lastly eliminated parameter is written underneath the bar. The absolute associated subcondition number to the system for the particular reduced parameter set considered is written next to the bar. All of the following plots are generated using POEM and edited in MATLAB 2012b with respect to the purpose of this sensitivity analysis.

The second parameter set deals solely with the parameters assigned to the E_2 algebraic differential equation. The second set has been chosen just like this due to the fact, that E_2 data is always assumed to be available and weaknesses concerning the modelling of E_2 are of significant importance for further improvements. The exponents of the Hill functions were left out of the consideration.

Parameter	Parameter Value	Column Norms
$p_1^{E_2}$	186.391675192199	$6.879 \cdot 10^3$
$p_2^{E_2}$	202.263939088376	$4.153 \cdot 10^3$
$p_3^{E_2}$	4.483306488346	$1.387 \cdot 10^3$
$p_4^{E_2}$	1.030340524237	$9.289 \cdot 10^3$
$p_5^{E_2}$	3.415391066868	$1.276 \cdot 10^4$
$p_7^{E_2}$	115.028227706639	$9.279 \cdot 10^3$
$p_9^{E_2}$	200.584174200939	$9.040 \cdot 10^3$
$p_{11}^{E_2}$	0.326482174623	$3.134 \cdot 10^3$

Table 5.3.: Listing of parameter values and the computed column norms for parameter set 2. The relative size of each column norm with respect to the largest column norm in % is given in the upper plot of figure 5.2 (p. 94), the absolute column norms being showed next to the corresponding bars. The subcondition number as % of 10^4 following the POEM ordering are summarised in the lower plot for each parameter. Absolute associated subcondition numbers for the system with respect each successively reduced parameter set (from right to left) are written next to the bars.

For E_2, all parameters included in the sensitivity analysis have a *column norm* not equal zero. Hence, in principle, all parameters are estimable. The most sensitive parameter in the system is $p_5^{E_2}$, while the *column norm* plot (see figure 5.2, p. 94) shows that $p_1^{E_2}, p_4^{E_2}, p_7^{E_2}$ and $p_9^{E_2}$ also have absolute *column norms* of at least 50% of $p_5^{E_2}$. The *column norms* show variations within a range of 1387 to 12786. $p_4^{E_2}$ accounts for the prefactor of the Hill function $H^+(P4(t), p_{11}^{E_2}, p_{12}^{E_2})$ describing the strength or speed of the hormonal interaction between E_2 and its antagonist P_4, p_5^{E2} accounts for the threshold in the Hill function, modelling the inhibitory effect of E_2 to FSH and parameter p_7^{E2} accounts for the threshold in the positive feedback function involving LH. Least sensitivities could be found to be the prefactors $p_1^{E_2}$ and $p_3^{E_2}$ as well as for the threshold $p_9^{E_2}$ of the Hill function describing the stimulatory effect of E_2 to itself. Nevertheless, the plot illustrates that the *column norms* in % of the largest *column norm* $\|s_5\|$ do not deceed the 10 % and all E_2 related parameters included in this analysis can be considered more ore less equally sensitive with individual differences.
Since the QR decomposition gave a rank of 8 out of 8 parameters considered, all parameters are estimable and enter to a certain amount the solution of the system. The QR decomposition in

POEM gave the parameter ordering

$$
\begin{aligned}
&p_5^{E_2}\\
&p_7^{E_2}\\
&p_4^{E_2}\\
&p_{11}^{E_2}\\
&p_2^{E_2}\\
&p_9^{E_2}\\
&p_1^{E_2}\\
&p_3^{E_2}.
\end{aligned}
$$

The computed *subcondition number* amounts to

$$sc(S_2) = 280.1 * 10^2$$

Hence, the problem can be judged not to be ill-conditioned referring to the *subcondition numbers* and the applied threshold of $sc_{max} \approx 10^4$. The *subcondition* plot shows all *subcondition numbers* computed during the sensitivity analysis for the system with respect to the successively extended parameter sets from left to right. Starting with the first parameter of the POEM ordering, i.e. $p_5^{E_2}$, and then successively including following the order

$$p_7^{E_2}, p_4^{E_2}, p_{11}^{E_2}, p_2^{E_2}, p_9^{E_2}, p_1^{E_2}, p_3^{E_2},$$

gives a sharp increase in the *subcondition number* (in % of the largest *subcondition number*) in the last step, where $p_3^{E_2}$ is added to the other parameters. Since the problem to estimate the complete parameter set 2 is well-conditioned, the subsystem's *subcondition numbers* were plotted in % with respect to the largest *subcondition number* (obtained if the full parameter set 2 is considered in the sensitivity analysis). No parameter has to be left out in the estimation process, though some kind of correlation between $p_3^{E_2}$ and the remaining parameters

$$p_5^{E_2}, p_7^{E_2}, p_4^{E_2}, p_{11}^{E_2}, p_2^{E_2}, p_9^{E_2}, p_1^{E_2}$$

has to be assumed since leaving the same out of the analysis, an even less sensitive system can be obtained, where small variation in the parameter set's individual values will only lead to negligible changes in the solution.
The parameters assigned to the E_2 antagonist P_4 were not analysed in detail. Since P_4 measurements are not to be taken in future and P_4 was mainly included as a time dependent component in the model due to the fact that it closely interacts with E_2, the latter being crucial to ovulation prediction, and BBT responds to high P_4 levels by a thermal rise. To a greater degree, the question how sensitive the parameters assigned to BBT are seems interesting.

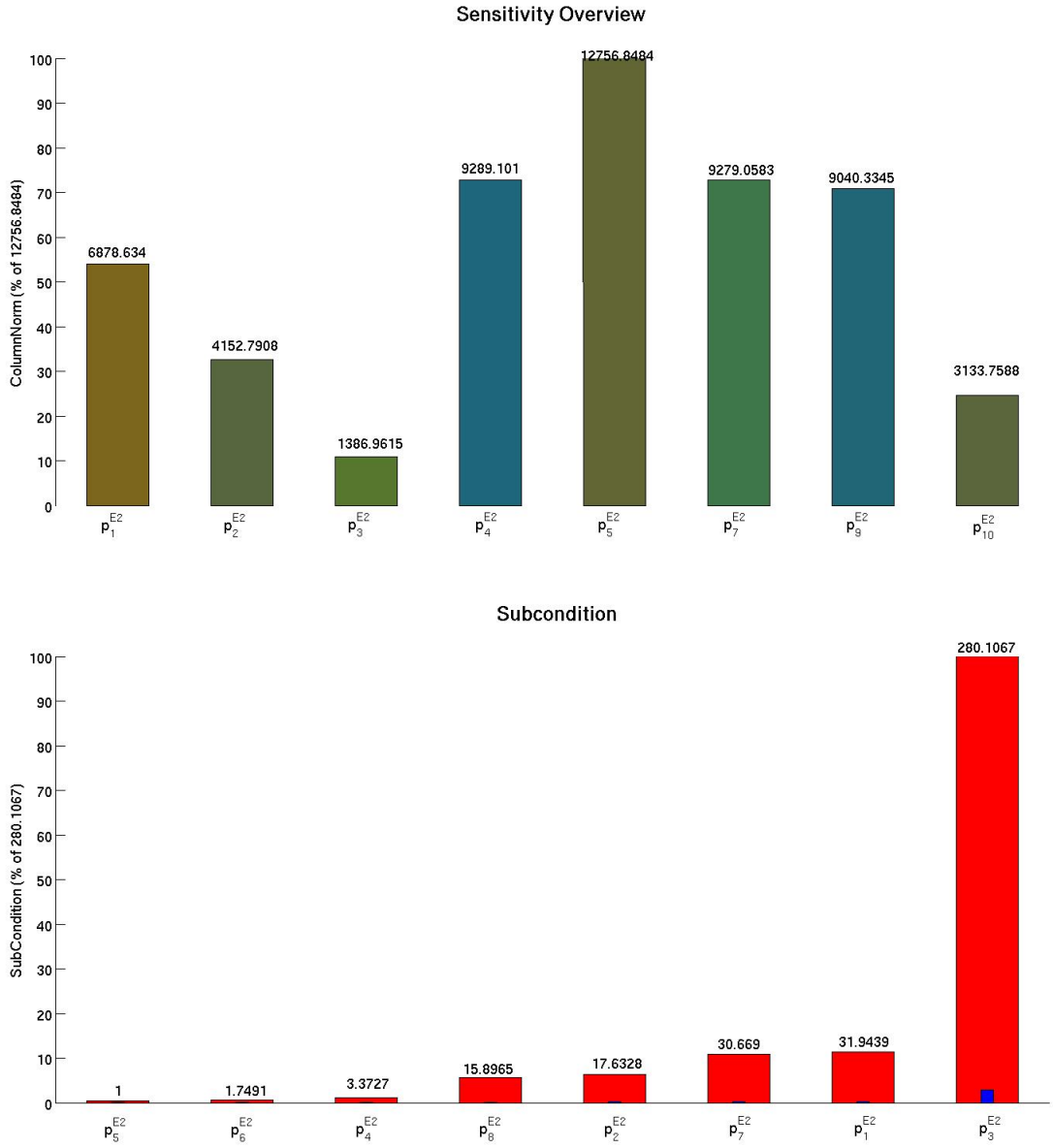

Figure 5.5.: Sensitivity outputs for parameter Set 2, i.e. the parameters $p_i^{E_2}$ for $i = 1, \ldots, 5$ and $p_5^{E_2}, p_7^{E_2}, p_9^{E_2}, p_1 1^{E_2}$. The upper plot gives the relative size of each column norm with respect to the largest column norm in %, the absolute value computed of the *column norms* being showed next to the corresponding bars. The *subcondition* plot gives bars for each subset of considered parameters and the associated *subcondition number* as % of 10^4, while the initial parameter set 2 is reduced following the POEM ordering from right to left. The lastly eliminated parameter is written underneath the bar. The absolute associated *subcondition number* to the system for each particular reduced parameter set considered is written next to the bar.

The third set of parameters is constituted by three parameters since the Hill exponent ($p_4^{BBT} = 6$) of the positive feedback function of BBT to itself was excluded again. In the following tabular (table 5.2, p. 94), the analysed parameters are listed with their values and the corresponding *column norms*.

Parameter	Parameter Value	Column Norms
p_1^{BBT}	0.004924843360	$3.694 \cdot 10^0$
p_2^{BBT}	96.954898958163	$3.986 \cdot 10^0$
p_3^{BBT}	6.942691358857	$2.392 \cdot 10^1$

Table 5.4.: Listing of parameter values and the computed *column norms* for parameter set 3.

Since none of the computed *column norms* equals zero, singularity of the sensitivity matrix for parameter set3, S_3, can be ruled out in the first step. Any other possible singularity, resulting from linear dependences among the considered parameters, has to be identified by performing a more detailed approach in the second step. Computing the QR decomposition of S_3 in POEM gives *rank* 2 of a potential *rank* 3. Assuming that at least one of the regarded parameters is linearly dependent on one or some of the other parameters, the POEM ordering making use of the permuted diagonal entries of the upper triangular R writes

$$\begin{aligned} &p_3^{BBT} \\ &p_1^{BBT} \\ &p_2^{BBT}. \end{aligned}$$

Obviously, p_2^{BBT} is making the whole system very sensitive to variations within the parameter vector such that

$$sc(S_3) = \infty.$$

Carefully reviewing the *subcondition plot* (see figure 5.2, p. 96), reducing the considered parameter set 3 by p_2^{BBT} gave full rank for the corresponding sensitivity matrix $\tilde{S}_3$. Solely regarding the parameter set consisting of

$$\{p_1^{BBT}, p_3^{BBT}\}$$

gives a sensitivity matrix $\tilde{S}_3$ with a *subcondition number* of

$$sc(\tilde{S}_3) = 1.426 * 10^1$$

which is clearly below the prescribed threshold $sc_{max} \approx 10^4$. By the *column norms*, both parameters were estimable while p_1^{BBT} turned out to lead to higher sensitivity in the system. Though the *subcondition number* indicates a pretty stable system when only the parameters p_1^{BBT}, p_3^{BBT} are varied, changes in p_1^{BBT} would lead to larger changes in the well-conditioned problem's solution than p_3^{BBT}. This can also be confirmed through the plot of the percental *subconditions*, see figure 5.2 (p. 96). Summarising, estimating all parameters assigned to BBT simultaneously seems not to be a promising approach, due to detected linear dependences. Considering and estimating only p_1^{BBT} and p_3^{BBT} simultaneously, variations in p_1^{BBT} and p_3^{BBT} seem to only slightly affect the solution of the model.

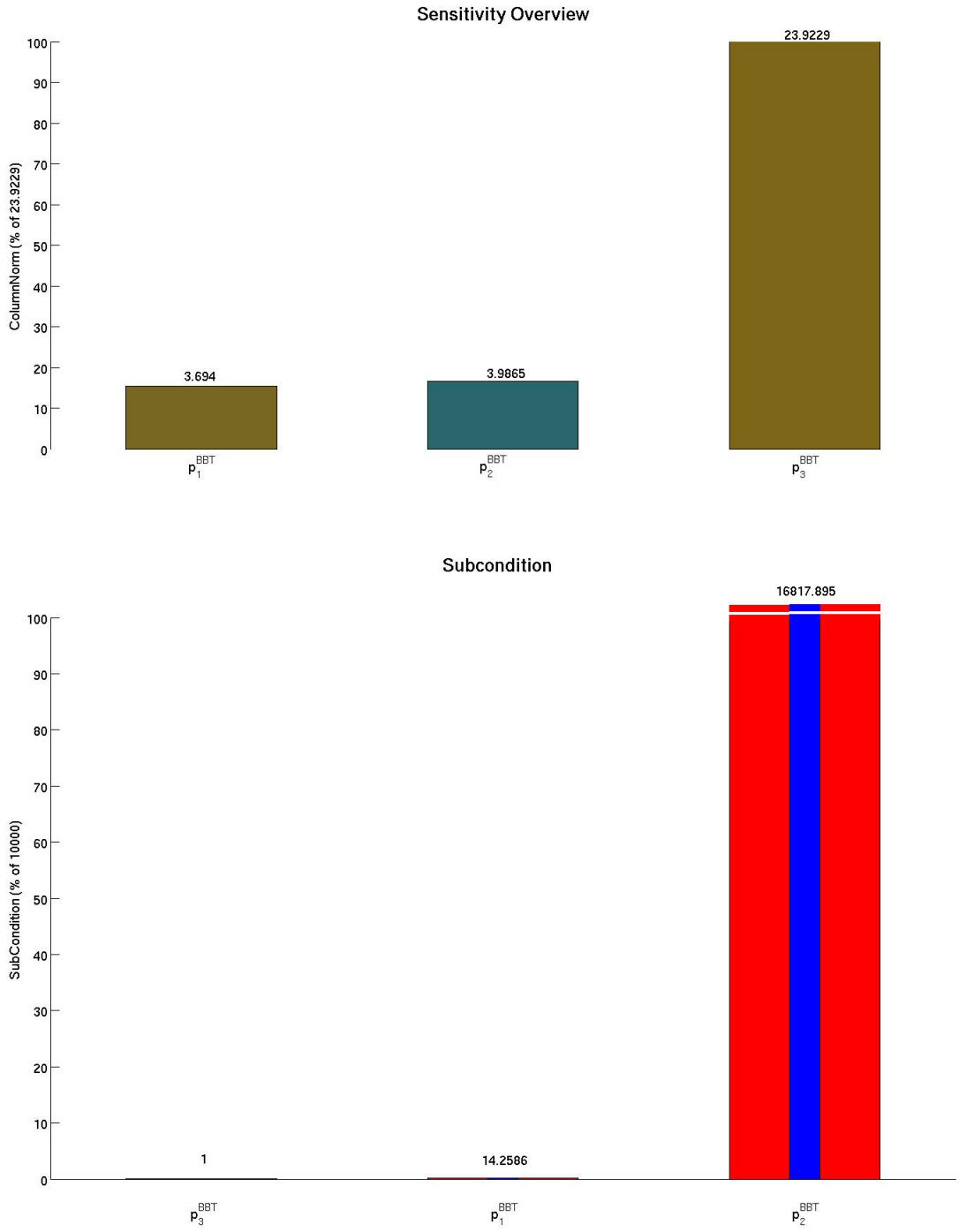

Figure 5.6.: Sensitivity outputs for parameter set 3, i.e. the parameters p_1^{BBT}, p_2^{BBT} and p_3^{BBT}. The relative size of each column norm with respect to the largest *column norm* in % and the *subcondition numbers* as % of 10^4 for each parameter in increasing order are summarised in the above plots. The *subcondition* plot gives bars for each subset of considered parameters and the associated subcondition number as % of 10^4, while the initial parameter set 3 is reduced following the POEM ordering from right to left. The lastly eliminated parameter is written underneath the bar. The absolute *column norms* and *subcondition numbers* computed for each parameter are written next to the corresponding bars.

5.3. Outlook on the Prediction of Potentially Fertile Periods

Following the complex of assumptions and the derived definition of potentially fertile periods of chapter 2, let us now approach the question on how to improve ovulation prediction. Due to the nonavailability of real, simultaneously collected E_2 and BBT measurements, the proposed model could only be validated with a partly artificial test data set. This chapter basically aims at giving an outlook, how ovulation prediction could in future be improved by making use of E_2 data. E_2 measurements will be soon user friendly available through a newly developed saliva utilising tool by *Clue* and *Fraunhofer Institut Potsdam-Golm*.

The proposed model can obviously give an adequate fit to the test data set and the herein shown hormonal dynamics. Using the simulation results obtained for the four cycle long test data of chapter 5.1 and 5.2, the strategy defined in chapter 2.4 is reviewed.
Adopting Carter/ Blight's (1981) Ansatz to obtain an *a priori* estimator for ovulation through a change point in E_2 concentration which is to be completed by an *a posteriori* detection of the rise in basal body temperature (BBT), the step length strategy of the integrator, in this case the linearly-implicit Euler extrapolation, is monitored. The endocrine dynamics of the human menstrual cycle imply, that whatever may disturb this hormonal regulation, in any case E_2 is surging the first of all considered hormonal components of the proposed model provided ovulation happens. The speed, the temporal delays, the base as well as the peak levels might (largely) vary from woman to woman though.
Nevertheless, Adlercreutz/ Lehtinen/ Kairento (1980) conclude in line with research of Baker/ Jennison/ Kellie (1979) that E_2 assays probably give best prediction of human ovulation by the highest mean ratio of peak-to-baseline values such that an earlier hint can be obtained if prediction is based on E_2 values. This implies together with the definition of the potentially fertile period, that the first significant surge in E_2 has to be detected. The potentially fertile period is considered to end with or soon after the thermal shift in BBT.

Let us first restrict to the change point detection for E_2. Out of the simulation results visualised in figure 5.1 (p. 82), again the third cycle was taken as reference cycle. Originally ranging from day 54 to 82, this cycle has a standard length of 28 days. For exactly this time interval, the adaptive step sizes of the linearly-implicit Euler discretisation are monitored. The prescribed accuracy in Limex was set to 10^{-10}. The step lengths performed vary from nearly zero up to more than 1.20. All step length performed in this interval were plotted against time in days. In order to assess if the proposed strategy for E_2 change point detection works out, the simulation of the hormonal components is compared to the step sizes taken during the same cycle. In order to have a more general comparison, the four hormones included in the model are all shown dimensionless in one plot. BBT was excluded from this graphic. The dimensionless plot of the model's endocrine dynamics in a 28 days long cycle was considered advantageous, since not absolute peak heights are of interest but the change points in the hormone concentration.

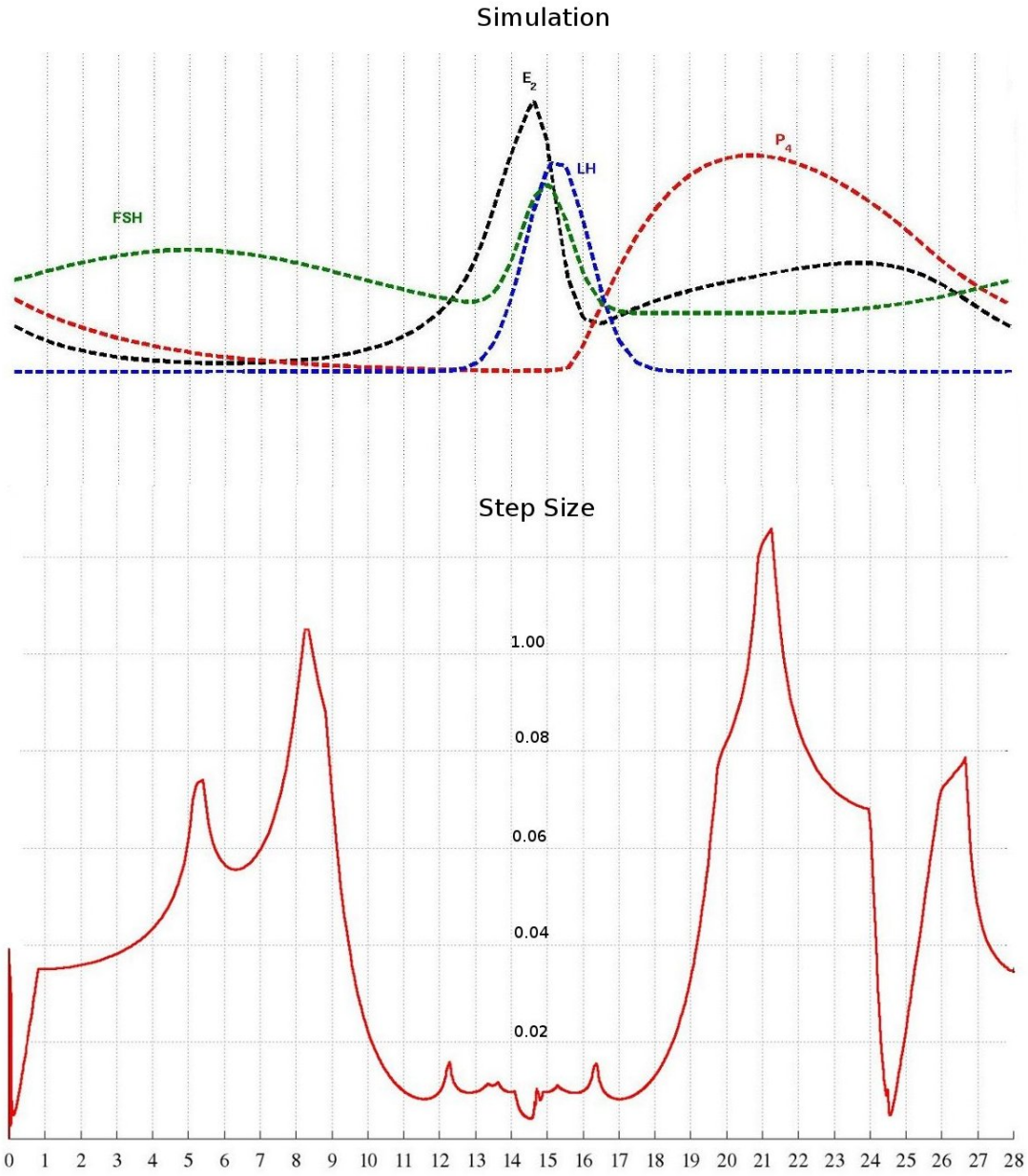

Figure 5.7.: Change point detection for E_2 for a 28 day cycle by monitoring the LIMEX adaptive step sizes with a prescribed accuracy of 10^{-10} and the endocrine dynamics happening during the menstrual cycle as they are displayed by the proposed model.

Obviously, the adaptive step sizes of the integrator first significantly and rapidly decreases around the time, when E_2 is near to rise. The first local minimum is reached shortly after day 11, rather on day 12. The boundaries are left out in the current consideration, since the adaptive step length strategy displays a first sharp decrease from the initial step length guess until it stabilises around day 1. On day 12, E_2 surges. The step lengths oscillate until day 14 is reached. At

this time, E_2 concentration is at its peak, while FSH and LH are near to their peak. Any time, sharp increases or decreases in at least one of the hormonal components can be evidenced, the adaptive step length strategy leads to a reduction in the step size taken in order to adequately perform the integration without surmounting the prescribed accuracy of 10^{-10}. Thus, a global minimum in the step sizes is reached at day 15, when the peak E_2 occurred at day 14.5 and right now, FSH and LH reached their peak levels. For this cycle, ovulation probably occurred at day 15 itself, since the luteal phase in general lasts for 14 days and ovulation is assumed to occur shortly after the peak in LH.
The LIMEX step sizes finally increase when LH and FSH are back to base level, and E_2 is only displaying slow dynamical behaviour and P_4 has passed its change point at day 18. Increasing P_4 levels induce the thermal shift with a certain temporal delay, but most probably the thermal rise in BBT happens also before or around day 19 for the human menstrual cycle.

The adaptive step sizes might decrease again, when E_2 experienced its second, less pronounced peak and BBT as well as P_4 develop back to base level. Due to this, it only seems reasonable to detect the change point in E_2 with the step size monitor provided in the implementation LIMEX of the linearly-implicit Euler extrapolation method for differential algebraic equations. The thermal rise in BBT should probably be monitored with a combined measurement aware, statistical approach. Contrary to the hormonal dynamics, the absolute levels of BBT are crucial to determine the thermal shift. Compromised by stress, sickness, etc. the thermal rise may take up to three days. This rather slow development if the cycle length is of only 28 days might not significantly affect the adaptive linearly-implicit Euler discretisation. Detecting the P_4 change point would be an alternative way to capture the end of the potentially fertile period, but P_4 measurements are not assumed to be available. Hence, the increase in the LIMEX step sizes around day 19 has to be considered with attention.

Parameter	Value (model Fit)	Value (Prediction)	
$p_1^{E_2}$	186.391675192199	116.675	
$p_2^{E_2}$	202.263939088376	224.730	
$p_3^{E_2}$	4.483306488346	4.80258	
$p_4^{E_2}$	1.030340524237	0.643251	
$p_5^{E_2}$	3.415391066868	1.67453	
$p_7^{E_2}$	115.028227706639	120.137	
$p_9^{E_2}$	200.584174200939	211.813	
$p_{11}^{E_2}$	0.326482174623	0.944160	
p_1^{BBT}	0.004924843360		0.00490064
p_3^{BBT}	6.942691358857		6.91679

Table 5.5.: Listing of the adjusted parameters after estimation through the NLSCON for the reduced test data set of 3 cycles in order to give a best possible rudimentary estimation for the fourth cycle.

Summarising, monitoring the adaptive step sizes of the model's differential algebraic equation system' integrator seem a promising and encouraging way to appropriately detect the surge in E_2. For BBT, rather a combined method to detect the thermal shift seems adequate. The review and monitoring of the LIMEX step sizes has not been automated or implemented in a code, since for any further applications, the LIMEX would rather not be the method of choice. For

the purpose of constructing a computational time and cost efficient algorithm for a smart phone *App*, the proposed model defined as a DAE system would rather be transformed into a system of ODEs. Thus, the model should be only treated as a first suggestion. Model refinements and improvements, once real data are available, have to be expected.

Independent from the methodology and the implementation to detect the E_2 change points and the shift in BBT, at any time of a current cycle a fertility or contraception monitor is required to give a best possible estimate about the time of ovulation. For this reason and in order to give an outlook for the prediction the potentially fertile periods of the human menstrual cycle, simulations are run for a reduced test data set. The initial measurements were shortened, only the first three cycles of length 29, 26 and 28 days are included. In line with the perspective, that only E_2 and BBT measurements are on-hand, the nonlinear least squares problem has been solved for the reduced test data set.

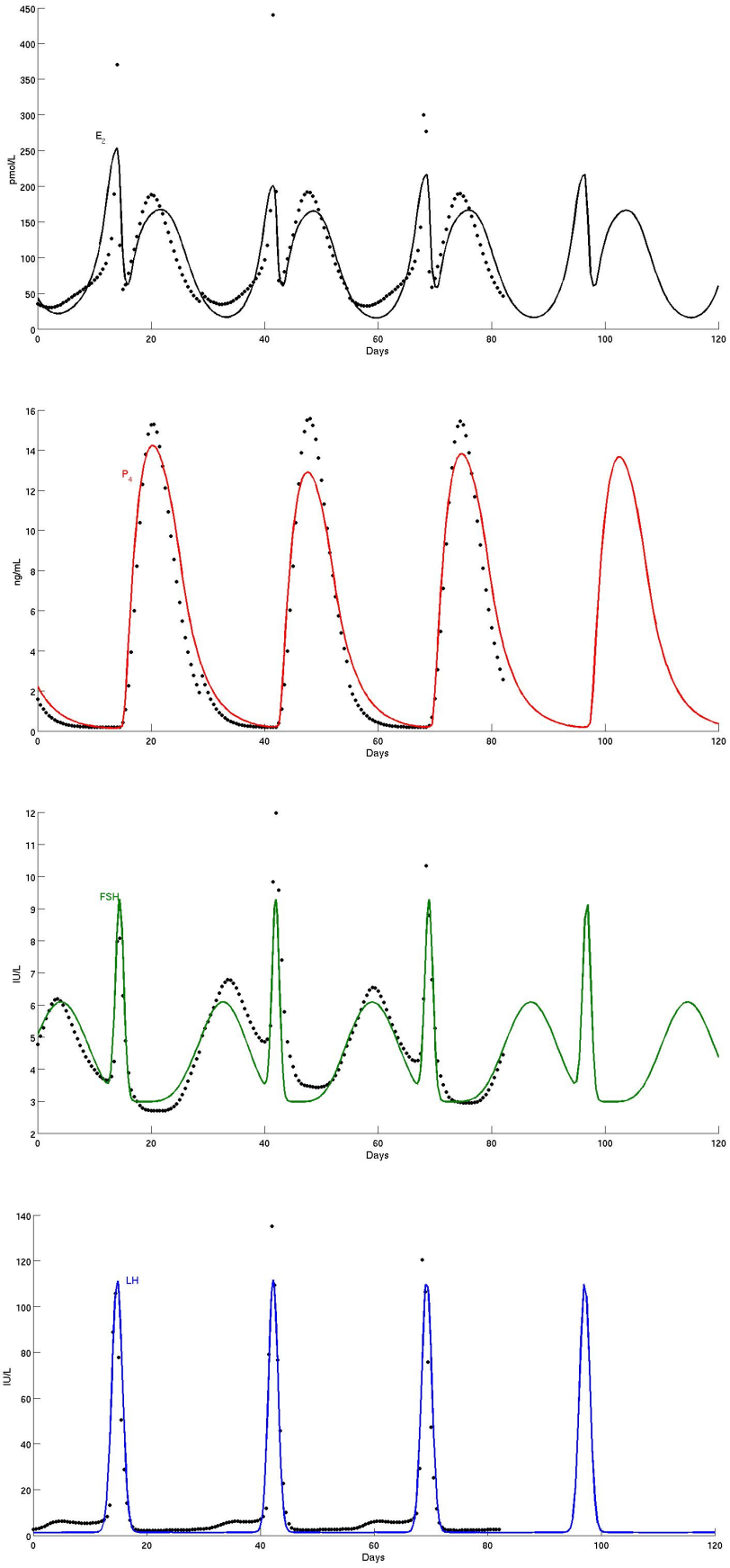

Figure 5.8.: The computed solution of the model to the reduced test data using the parameter set estimated beforehand gives the above fit to the measurements. Measurements end after the third cycle collected. Measurement points are plotted as points, the curve is corresponding fit for E_2, P_4, LH and FSH from top to bottom.

The parameters assigned to E_2 and BBT were re-estimated with the damped Gauss-Newton method in NLSCON. The adjusted parameters are listed in table 5.3 (p. 98). Since the cycle length was known for the three collected cycles, the initial guess for the fourth cycle length

$$p_4^{cyclelength} := \frac{\sum_{i=1}^{3} p_i^{cyclelength}}{3}$$

was chosen as the arithmetic mean of all previous, completed cycle lengths as starting value. This gave an initial guess of $p_4^{cyclelength} \approx 27.67$.
Only considering the *rudimentary* prediction for the fourth cycle by the obtained solution to the nonlinear least squares problem, E_2 and BBT data are compared. Defining the potentially fertile period by the first rise in E_2 and the thermal shift in BBT, the plot gives reason to the assumption that ovulation happens around day 15. The first significant rise in E_2 by the eye would be located around day 10 or 11, the thermal shift around day 19. This would give a predicted total potentially fertile period of 9 days. Of course, this is a very conservative approach but the probability that the effective fertile period is covered through this time interval is quite high.

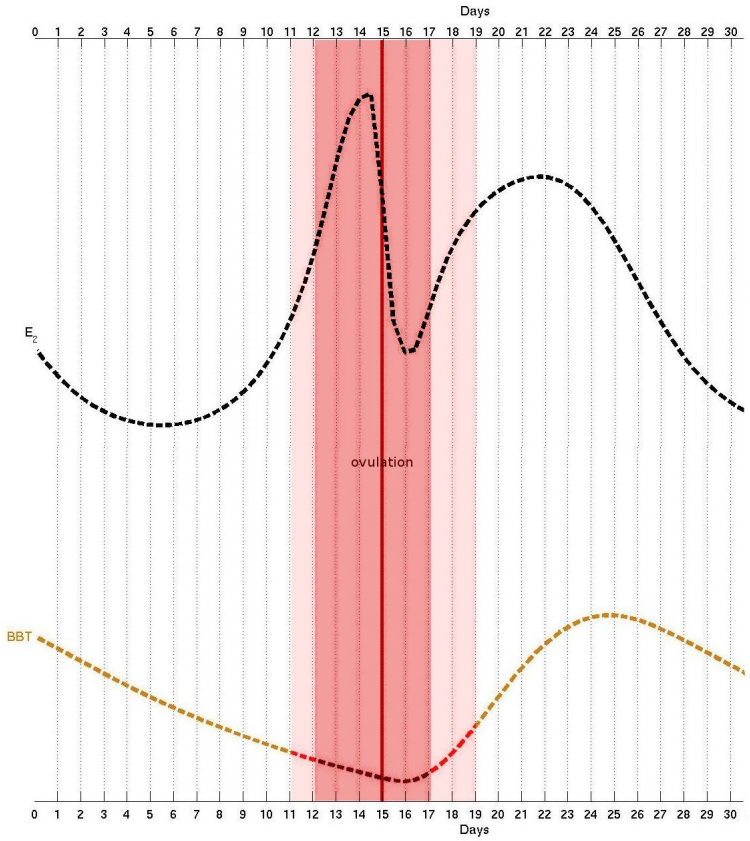

Figure 5.9.: The *rudimentary* prediction for the dynamics of E_2 and BBT for the fourth cycle are plotted against the day numbering of the fourth cycle. Only the time axis is labeled, since not absolute values are of interest here, but rather the change points and surges in E_2 and BBT the reader can observe. This plot is not meant to give precise information but a first impression on how more progressive ovulation prediction could be gained.
The LH peak an ovulation can be assumed for day 15. The detection of the first rise in E_2 with the eye and the step size approach of figure 5.3 (p. 97) would give a first estimate for the potentially fertile time window (light red) from day 11, the first significant rise in E_2, to day 19, the third day of BBT's thermal rise. The strategy defined in chapter 5.3 in contrary would range from day 12 to 17, i.e. from day -3 to $+2$ around the LH peak.

Summarising, two valuable but not final tools to predict potentially fertile periods have been introduced in this outlook. Inserting day by day new measurements, after some days of the new cycle probably way more precise estimations for the day of ovulation and the fertile window could be obtained. Exactly at this point, further experiments and validation of the model with real data are of huge importance. The detection of change points in E_2 through the steepest descent, monitored through a sharp decrease in an adaptive step size strategy, looks promising. The limitations of the proposed model, where refinements and improvements have to be worked out, are given in the following.

5.4. Limitations of the Model

Not solely intra-woman and intra-cycle within-woman variations clearly limit the viability of predictions concerning either the potentially fertile period of the menstrual cycle or the precise time of ovulation.

Concerning the model, LH and FSH are incorporated in the model only through algebraic input functions. Though these functions are constructed referring to the hormonal dynamics displayed by the complex model describing the human menstrual of Röblitz/ Stötzel/ Deuflhard/ Jones/ Azulay/ van der Graaf/ Martin (2011), ameliorated predictions can probably only be obtained if data could be made available for all key hormonal drivers of the menstrual cycle. Due to the business idea of *Clue*, aiming at launching a Smart phone *App* to support women in their fertility management, model reduction seemed appropriate. In the same line, requiring a woman to collect more than two different kind of data would probably compromise the attractiveness of such a fertility monitor. The proposed model and the ovulation prediction strategy applied in the outlook in chapter 5.3 try to best possible detect fertile windows under the restriction of limited available data and a limited model complexity.

Identifying the potentially fertile period through the steepest descent, assessed through changes in the adaptive step length strategy of the applied integrator showed to be encouraging. Accuracy could not be judged by the absence of appropriate data, where on the one hand E_2 and BBT measurements and on the other hand the medical confirmation of ovulation are linked. Also the proposed model could only be appraised through a partly artificial test data set. Improvements and refinement concerning the equations as well as the parameter sets should be approached first. Subsequently, the sketched strategy to ovulation prediction and determination of potentially fertile periods should be worked out. Though, the algorithms applied to solve the arising nonlinear least squares problem Nlscon and Limex might not be the first choice to be implemented in the final *App* from the computational point of view. Transformation of the given DAE system to a ODE system should be considered as well as application of time and cost efficient solvers.

In natural family planning, secondary signs are recorded throughout the menstrual cycle. Especially components like cervical mucus and other body signs can give an aware woman important information about the current state of her cycle. In the final model to be used in such an *App*, incorporation of such secondary sign option should be seriously considered.
Getting back once more to the proposed prediction strategy of potentially fertile periods, according to Royston (1991), it seems appropriate to indicate problematics and show which errors may arise. If the worst case is regarded to apply for the case that no changes in mean analyte levels of E_2 or BBT can be observed throughout the cycle (p. 229), we define:

A type I error occurs if the prediction method wrongly indicated that the woman is fertile.

A type II error occurs if the fertile phase is not detected at all or if the prediction method gives the signal of impending ovulation not early enough.

Contrary to Royston (1991)'s evaluation, the aspiration to support women in getting pregnant makes both error types become less serious as it would be in the context of contraception. Type II error might result in a missed pregnancy opportunity which appears to be more serious than a type I error, excluding wrongly arising personal hopes. Nevertheless, type I error should be tried to minimize as well exactly to prevent a couple from unjustifiable hopes.
As justified subsequent to *Assumption 6*, a predicting a short fertile phase seems adequate.

Though one would normally expect to have low probability of conception at the the limits of the defined fertility interval, by ROYSTON (1991) (p. 237) it can be argued that even two days after the rise in BBT, the conception probability is generally estimated of 0.005. Since the rise in BBT defines the endpoint of our fertility window, one would experience a *Pearl index* of 6.0 assuming 100 woman years with on average 12 menstrual cycles per year. ROYSTON (1991)'s study reveals conception probability to be negligible 4 days after the first rise in BBT, i.e. around 4 days after ovulation.
Concluding, the potentially fertile period of the menstrual cycle as proposed in *Assumption 6* and *8* is rather of pessimistic than optimistic nature; within this timely span, generally a probability of conception of at least 0.05 (i.e. Pearl Index of 60) can be assumed (ROYSTON (1991), figure 5, p. 237).

In the end, the proposed model is a first attempt to model a very complex regulation of the human body. The non-complexity of the proposed model has to pay for accuracy in the system's dynamics. Nevertheless, the model performs astonishing well for the partly artificial test data set. Its performance for real, highly variational and irregular data could not be evaluated at this stage. Only then, a final conclusion can be drawn.

6. Conclusion

The proposed six dimensional model of chapter 2 includes the four hormonal components E_2, P_4, LH and FSH combined with the primary fertility sign BBT. Modelled through four differential equations for E_2, P_4, a delay of P_4 and BBT, coupled with two algebraic input curves accounting for LH and FSH, a total number of 33 parameters is involved. *A priori* unknown, these parameters have been identified through the solution of a nonlinear least squares problem. In the nonlinear least squares problem, the model and partly artificial test data are matched. The given minimization task is solved with a globalisation of the Gauss-Newton method in an affine invariant setting, introduced as the damped Gauss-Newton method in chapter 4. Implemented in the NLSCON code, the gradient system arising through application of the Gauss-Newton method to the minimisation task is evaluated with a linearly-implicit Euler extrapolation (LIMEX).

The test data comprises four cycles with cycle lengths of 29, 26, 28 and 27 days. Parameters were identified with NLSCON, until it converged. The fits obtained are presented as the simulation results in chapter 5.1. A dimensionless comparison of the fit obtained for a 28 days cycle of the test data with a reference plot displaying the key endocrine dynamics gave that the model represents well the temporal relationships as well as the hormonal interaction between E_2, P_4, LH and FSH. Inaccuracies could be found concerning the location of the LH peak and the hereby induced ovulation. Ovulation is assumed to happen around 24 hours after the peak in LH. Thus, luteal phase is at least one day too short in the model and the test data, which contradicts modelling *Assumption 11* of chapter 2.2. *Assumption 4*, that the nadir in BBT coincides with the peak in LH can be represented by the model satisfactorily. In the same way, the data and the model display a thermal shift of $0.2 - 0.5^\circ$ C around 24 hours after the assumed ovulation (*Assumption 5*), as can be evidenced in figure 6. Just as in *Assumption 7*, the first significant rise in E_2 happens around 72 hours prior to the corresponding peak, which itself is located around day 14.

Summarising, the model adequately describes the basic hormonal regulation of the human menstrual cycle. The outlook to ovulation prediction gave in chapter 5.3 together with the definition of potentially fertile period in *Assumption 6* and *8*, that a potentially fertile window is in general determinable. Though, the first time span between the first rise in E_2 and the thermal shift in BBT comprises 9 days for the 28 days cycle of the test data considered. Due to data and model inaccuracies, this potentially fertile window represents a significantly more conservative estimate than initially intended when defining the days -3 to $+2$ around the LH peak as potentially fertile.

Through the model and the solution of the underlying DAE system with a linearly-implicit Euler extrapolation (LIMEX), the first significant rise in E_2 concentration was detectable with the changes in the performed (adaptive) step sizes of the integrator. Using the proposed tools, based on the steepest increase of the E_2 fit, or a simplification of the latter would make improvements concerning ovulation prediction and the hereby constituted fertile period of the human menstrual cycle in future possible.

It remains to state, that by its simplicity, the model cannot be expected to describe the complex hormonal regulation of the human cycle with high accuracy. Due to the absence of *real* data, a

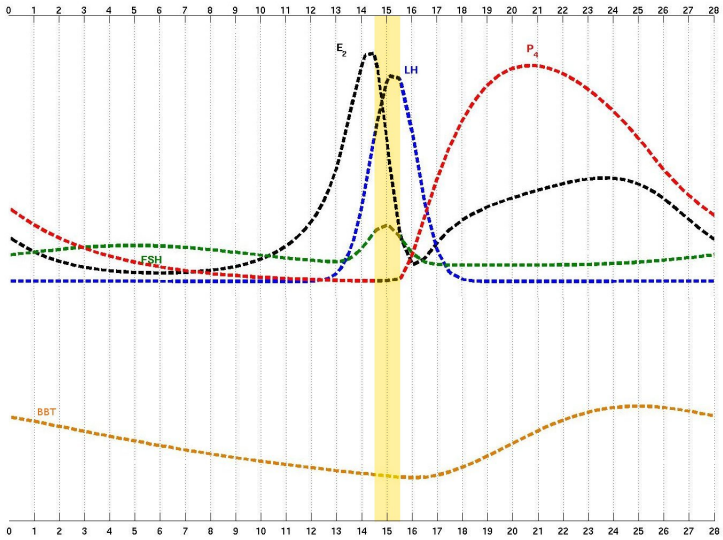

Figure 6.1.: The computed solution of the model to the given test data for a 28 days cycle using the parameter set estimated beforehand gives the above fit to the measurements. The curves are the corresponding fits for E_2, P_4, LH and FSH shown in the upper dimensionless plot, BBT is shown below.

partly artificial test data set has been used throughout the simulations. Results appeared to be satisfactory so far, though no final conclusion towards the general viability of the model can be drawn at this point. Simultaneous acquisition of E_2 and BBT measurements are required for any further evaluation and especially validation of the model. For a smart phone *App*, the proposed model seems to serve the purpose. The change point detection strategy for ovulation prediction as well as the correction strategy, i.e. detection of the rise in BBT, have to be further extended and specified for this purpose. All in all, the business idea of *Clue* as well as the model itself are encouraging to provide women with a reliable, natural family planning fertility monitor or contraception tool in the near future.

References

Adlercreutz, H., T. Lehtinen and A.-L. Kairento, *Prediction of Ovulation by urinary estrogen assays.*, Journal of Steroid Biochemistry, 12, pp. 395–401, 1980.

Arévalo, M., I. Sinai and V. Jennings, *A fixed Formula to define the Fertile Window of the Menstrual Cycle as the Basis of a simple method of Natural Family Planning.*, Contraception, 60 (6), pp. 357-360, 1999.

Arévalo, M., V. Jennings and I. Sinai, *Efficacy of a new method of family planning: The Standard Days Method.*, Contraception, 65 (5), pp. 333-338, 2002.

Baker, T., K. M. Jennison and A. E. Kellie, *The direct radioimmunoassay of oestrogen glucuronides in human female urine.*, Journal of Biochemistry, 151, pp. 369–376, 1979.

Björck, Å., *Numerical Methods for Least Squares Problems.*, SIAM, 1996.

Blackwell, L. F. and J. B. Brown, *Application of time-series analysis for the recognition of increase in urinary estrogens as markers for the beginning of the potentially fertile period.*, Steroids, 57 (11), pp. 554–562, 1992.

Boyd, S. and L.Vandenberghe, *Convex Optimization.*, Cambridge University Press, 2004.

Brown, J. B., P. Harrisson, M. A. Smith, H. Burger, *Correlations between mucus symptoms and the hormonal markers of fertility throughout reproductive life.*, Monograph, Advocate Press Pty., Melbourne, Australia, 1981.

Broyden, C. G., *The convergence of a class of double-rank minimization algorithms.*, Journal of the Institute of Mathematics and its Applications, 6, pp. 76–90 1970.

Carter, R. L. and B. J. N. Blight, *A Bayesian Change-point Problem with Application to the Prediction and Detection of Ovulation in Women.*, Biometrics, 37 (4), pp. 743–751, 1981.

Collins, W. P., *Hormonal Indices of Ovulation and the fertile Period.*, Advanced Contraception, 1, pp. 279–294, 1985.

Collins, W. P., *Biochemical indices of potential Fertility.*, International Journal of Gynecology and Obstetrics, Supplement, 1, pp. 35–44, 1989.

Constantinescu, E. M. and A. Sandu, *Extrapolated Implicit-Explicit Time Stepping.*, Journal of Scientific Computation, SIAM, 31(6), 4452-4477, 2010.

Curtiss, C. F. and J. O. Hirschfelder, *Integration of stiff Equations.*, Proceedings of the National Academy of Sciences, 38 (3), pp. 235–243, 1952.

Dedieu, J. P. and m Shub, *Newton's Method for overdetermined Systems of Equations.*, Mathematics of Computation, 69 (231), pp. 1099–1115, 1999.

Dennis, J. E. Jr. and R. B. Schnabel, *Numerical Methods for Unconstrained Optimization and Nonlinear Equations*, Prentice-Hall Series in Computational Mathematics, 1983.

Deuflhard, P., *Recent Progress in Extrapolation Methods for Ordinary Differential Equations.*, SIAM Review, 27, pp. 505-535, 1985.

Deuflhard, P., E.Hairer and J. Zugck, *One-Step and Extrapolation Methods for Differential-Algebraic Systems.*, Numerical Mathematics, 51 (5), pp. 501-516, 1987.

Deuflhard, P., *Newton Methods for Nonlinear Problems. Affine Invariance and Adaptive Algorithms.*, 2nd edition, Series Computational Mathematics, 35, Springer Verlag, New York, 2006.

Deuflhard, P. and F. Bornemann, *Scientific Computing with Ordinary Differential Equations.*, Texts in Applied Mathematics, 42, Springer Verlag, New York, 2002.

Deuflhard, P. and A. Hohmann, *Numerical Analysis in Modern Scientific Computing. An Introduction.*, Texts in Applied Mathematics, 43, Springer Verlag, New York, 2003.

Dierkes, T., M. Wade, U. Nowak and S. Röblitz, *BioPARKIN – Biology-related Parameter Identification in Large Kinetic Networks.*, ZIB Report, 11-12, Berlin, December 2011.

Ehrig, Reinald, Ulrich Nowak and Peter Deuflhard., *Highly Scalable Parallel Linearly-Implicit Extrapolation Algorithms.*, Technical Report TR 96-11, ZIB, 1996.

Engl, H. W., C. Flamm, P. Kügler, J. Lu and P. Schuster, *Inverse Problems in Systems Biology*, Inverse Problems 25 (12), 2009, pp. 1 – 51.

Fletcher, R., *A New Approach to Variable Metric Algorithms.*, Computer Journal, 13 (3), pp. 317–322, 1970.

Fletcher, R. *Practical methods of optimization.*, 2nd edition, John Wiley & Sons, New York, 1987.

Forster, O., *Analysis 2.*, Vieweg, 2006.

Freundl, G., E. Godehardt, P. A. Kern, P. Frank-Herrmann, H. J. Koubenec and Ch. Gnoth, *Estimated maximum failure rates of cycle monitors using daily conception probabilities in the menstrual cycle.*, Human Reproduction, 18 (12), pp. 2628–2633, 2003.

Geiger, C. and C. Kanzow, *Theorie und Numerik restringierter Optimierungsaufgaben.*, Springer, 1st edition, 2002.

Goldfarb, D., *A Family of Variable Metric Updates Derived by Variational Means.*, Mathematics of Computation, 24 (109), pp. 23–26, 1970.

Häussler, W. M., *A local convergence analysis for the Gauss-Newton and Levenberg-Morrison-Marquardt Algorithms.*, Computing, 31 (3), pp. 231–244, 1983.

Häussler, W. M., *A Kantrovich-type Convergence Analysis for the Gauss-Newton-Method.*, Numerische Mathematik, 48, pp. 119–125, Springer Verlag, Berlin, 1986.

Hairer, E., S. P Nørsett and G. Wanner, *Solving Ordinary Differential Equations I: Nonstiff Problems.*, 1st edition, Springer Series in Computational Mathematics, 8, 1987.

Hairer, E. and G. Wanner, *Solving Ordinary Differential Equations II: Stiff and Differential-Algebraic Problems.*, 2nd edition, Springer Series in Computational Mathematics, 14, 1996.

Harris, L. A., *Differential Equation Models for the Hormonal Regulation of the Menstrual Cycle.*, PhD Thesis, North Carolina State University, ProQuest, 2001.

Johansson, E. D. B., *Preovulatory levels of plasma progesterone and luteinizing hormone in women.*, Acta Endocrinologica, 62, pp. 82–886, 1969.

Johansson, E. D. B. and L. Wide, *Progesterone levels in peripheral plasma during the luteal phase of the normal human menstrual cycle measured by a rapid competitive protein binding technique.*, Acta Endocrinologica, 61, pp. 592–606, 1969.

Jordan, D. W. and P. Smith, *Nonlinear Differential Equations.*, 4th edition, Oxford University Press, 2007.

Kerin, J., *Ovulation Detection in the Human.*, Clinical Reproduction and Fertility, 1(1), pp. 27–54, 1982.

Larsson, S. and V. Thomée, *Partial Differential Equations with Numerical Methods.*, 1st edition, Springer Verlag, 2003.

Levenberg, K., *A Method for the Solution of Certain Problems in Least Squares.*, Quarterly of Applied Mathematics, 2, pp. 164–168, 1944.

Liu, Y., E. B. Gold, B. L Lasley and W. O. Johanson, *Factors affecting menstrual cycle characterisitcs.*, American Journal of Epidemiology, 160 (2), pp. 131–140, 2004.

Marquardt, Donnald, *An Algorithm for Least-Squares Estimation of Nonlinear Parameters.*, SIAM Journal of Applied Mathematics, 11, pp. 431–441, 1963.

Murray, J. D., *Mathematical Biology: I. An Introduction.*, 3rd edition, Springer Verlag, 2007.

Murray, J. D., *Mathematical Biology: II. Spatial Models and Biomedical Applications.*, 3rd edition, Springer Verlag, 2003.

Morris, N. M., L. Underwood and W. Jr. Easterling, *Temporal relationship between basal body temperature nadir and luteinizing hormone surge in normal women.*, Fertility and Sterility, 27 (7), pp. 780 – 783, 1976.

Nitschke-Dabelstein, S., B. J. Hackeloer and G. Sturm , *Ovulation and corpus luteum formation observed by ultrasonography.*, Ultrasound in Medicine & Biology, 7, pp. 33–39, 1980.

O'Connor, K. A., E. Brindle, R. C. Miller, J. B. Shofer, R. J. Ferell, N. A. Klein, M. R. Soules, D. J. Holman, P. K. Mansfield and J. W. Wood, *Ovulation detection methods for urinary hormones: Precision, daily and intermittent sampling and a combined hierarchical method.*, Human Reproduction, 21 (6), pp. 1442–1452, 2006.

Ortega, J. M. and W. C. Rheinboldt, *Iterative Solution of Nonlinear Equations in Several Variables.*, Academic Press, New York, 1970.

Penrose, R., *A generalized inverse for matrices.*, Proceedings of the Cambridge Philosophical Society, 51, pp. 406–413, 1955.

Reinecke, I., and P. Deuflhard, *A Complex Mathematical Model of the Human Menstrual Cycle.*, ZIB Report, 06-18, Berlin, June 2006.

Röblitz, S., C. Stötzel, P. Deuflhard, H. M. Jones, D.-O. Azulay, P. Van Der Graaf and S. W. Martin, *A mathematical Model of the Human Menstrual Cycle for the administration of GnRH analogues.*, Journal of Theoretical Biology, 321, pp. 8–27, 2013.

Schlegel, M., W. Marquardt, R. Ehrig and U. Nowak, *Sensitivity Analysis of linearly-implicit DifferentialAlgebraic Systems by onestep Extrapolation.*, Applied Numerical Mathematics, 48, pp. 83–102, 2004.

Schlosser, P. M. and J. F. Selgrade, *A Model of Gonadotropin Regulation during the Menstrual Cycle in Women: Qualitative Features.*, Environmental Health Perspectives, 108 (5), pp. 873–881, 2000.

Segel, I. H., *Enzyme Kinetics: Behavior and Analysis of Rapid Equilibrium and Steady State Enzyme Systems.*, Wiley and Sons, Interscience, 1975.

Shanno, D. F., *Conditioning of quasi-Newton methods for function minimization.*, Mathematics of Computation, 24 (111), pp. 647–656, 1970.

Soboleva, T. K., A. B. Pleasants, B. T. T. M. van Rens, T. van der Lende and A. J. Peterson, *A dynamic model for ovulation rate reveals an effect of estrogen receptor genotype on ovarian follicular development in the pig.*, Journal of Animal Sciences, 52, pp. 2329–2332, 2004.

Stoer, J. and R. Burlisch, *Numerische Mathematik 1.*, 10th, etdited edition, Springer Verlag , 2007.

Templeton, A. A., *Relation between luteinizing hormone peak, the nadir of the basal body temperature and the cervical mucus.*, British Journal of Obstetrics and Gynaecology, 89, pp. 985–988, 1982.

Weschler, T., *Taking Charge of your Fertility.*, 10th Anniversary Edition: The Definitive Guide to Natural Birth Control, Pregnancy Achievement, and Reproductive Health, William Morrow Paperbacks, 2006.

World Health Organisation, WHO Task Force on methods for the Determination of the Fertile Period, *Temporal Relationship between ovulation and defined changes in the*

concentration of plasma estradiol-17β, LH, FSH and progesterone., American Journal of Obstetrics & Gynecology, 138 (4), pp. 383-390, 1980.

World Health Organisation, WHO Task Force on Methods for the Determination of the Fertile Period, *Temporal Relationships between indices of the fertile Period.*, Fertility and Sterility, 39 (5), pp. 647–655, 1983.

World Health Organisation, WHO Task Force on Methods for the Determination of the Fertile Period, *A prospective multicentre trial of the ovulation method of natural family planning. III. Characteristics of the menstrual cycle and of the fertile phase.*, Fertility and Sterility, 40 (6), pp. 773–778, 1983.

List of Figures

List of Tables

Appendix

A. Test Data Set

Cycle	Time	E_2 (pmol/L)	P_4 (ng/mL)	LH (UI/L)	FSH (UI/L)	BBT (° C)
1	0	35.4756	1.5793	2.6670	4.7659	37.0000
1	0.5000	33.2107	1.3152	2.8425	5.0167	36.9600
1	1.0000	31.5885	1.0973	3.1250	5.2893	36.9200
1	1.5000	30.5750	0.9187	3.5338	5.5667	36.8875
1	2.0000	30.1436	0.7729	4.0583	5.8210	36.8550
1	2.5000	30.2757	0.6545	4.6510	6.0222	36.7925
1	3.0000	30.9705	0.5587	5.2360	6.1464	36.7300
1	3.5000	32.2443	0.4815	5.7313	6.1816	36.7000
1	4.0000	34.0900	0.4196	6.0742	6.1282	36.6700
1	4.5000	36.4195	0.3701	6.2421	5.9992	36.6350
1	5.0000	39.0576	0.3306	6.2561	5.8157	36.6000
1	5.5000	41.8152	0.2993	6.1644	5.6011	36.5950
1	6.0000	44.5657	0.2745	6.0180	5.3753	36.5900
1	6.5000	47.2655	0.2549	5.8559	5.1519	36.5825
1	7.0000	49.9306	0.2394	5.7021	4.9385	36.5750
1	7.5000	52.6051	0.2272	5.5694	4.7391	36.5775
1	8.0000	55.3435	0.2177	5.4638	4.5548	36.5800
1	8.5000	58.2045	0.2102	5.3880	4.3860	36.5900
1	9.0000	61.2531	0.2043	5.3435	4.2323	36.6000
1	9.5000	64.5679	0.1998	5.3327	4.0935	36.5900
1	10.0000	68.2536	0.1962	5.3595	3.9694	36.5750
1	10.5000	72.4642	0.1934	5.4315	3.8607	36.5600
1	11.0000	77.4465	0.1912	5.5630	3.7690	36.5500
1	11.5000	83.6356	0.1895	5.7818	3.6980	36.5375
1	12.0000	91.8946	0.1882	6.1463	3.6556	36.5250
1	12.5000	104.2360	0.1872	6.8006	3.6607	36.5325
1	13.0000	126.6985	0.1864	8.2035	3.7666	36.5400
1	13.5000	189.2778	0.1858	13.1632	4.2332	36.5325
1	14.0000	370.3604	0.1853	88.7983	7.9800	36.5250
1	14.5000	116.9874	0.2015	105.8801	8.0652	36.5100
1	15.0000	55.6992	0.4136	77.7492	6.2867	36.4950
1	15.5000	62.2729	1.0616	50.4817	4.8747	36.4875
1	16.0000	77.8897	2.2480	28.7872	3.8743	36.4800
1	16.5000	94.4197	3.9416	14.2187	3.3512	36.4850
1	17.0000	111.0974	6.0041	6.7295	3.1428	36.4900
1	17.5000	129.3475	8.2310	3.7454	2.9842	36.5425
1	18.0000	147.7467	10.3972	2.7024	2.8550	36.5950
1	18.5000	164.1352	12.2999	2.3468	2.7757	36.6100
1	19.0000	176.8646	13.7906	2.2194	2.7359	36.6250
1	19.5000	184.9784	14.7885	2.1701	2.7174	36.6800

Cycle	Time	E_2 (pmol/L)	P_4 (ng/mL)	LH (UI/L)	FSH (UI/L)	BBT (° C)
1	20.0000	188.1797	15.2765	2.1519	2.7076	36.7350
1	20.5000	186.7094	15.2884	2.1494	2.7010	36.7525
1	21.0000	181.1835	14.8912	2.1568	2.6963	36.7700
1	21.5000	172.4285	14.1696	2.1711	2.6946	36.7875
1	22.0000	161.3407	13.2129	2.1903	2.6979	36.8050
1	22.5000	148.7831	12.1053	2.2129	2.7092	36.8075
1	23.0000	135.5196	10.9206	2.2377	2.7321	36.8100
1	23.5000	122.1803	9.7191	2.2638	2.7710	36.8475
1	24.0000	109.2521	8.5472	2.2903	2.8310	36.8850
1	24.5000	97.0848	7.4380	2.3168	2.9182	36.8975
1	25.0000	85.9080	6.4133	2.3428	3.0386	36.9100
1	25.5000	75.8512	5.4854	2.3681	3.1967	36.8950
1	26.0000	66.9655	4.6591	2.3928	3.3927	36.8800
1	26.5000	59.2435	3.9338	2.4172	3.6186	36.9025
1	27.0000	52.6363	3.3051	2.4421	3.8580	36.9250
1	27.5000	47.0671	2.7658	2.4700	4.0926	36.9275
1	28.0000	42.4443	2.3078	2.5064	4.3145	36.9300
1	28.5000	38.6730	1.9221	2.5627	4.5307	36.9650
2	29.0000	50.0540	2.7596	2.7754	5.0397	37.0000
2	29.5000	45.5934	2.3019	2.8190	5.2633	36.9600
2	30.0000	41.9887	1.9167	2.8830	5.4714	36.9200
2	30.5000	39.1565	1.5949	2.9865	5.6808	36.8875
2	31.0000	37.0326	1.3279	3.1547	5.9037	36.8550
2	31.5000	35.5731	1.1077	3.4117	6.1379	36.7925
2	32.0000	34.7490	0.9271	3.7684	6.3669	36.7300
2	32.5000	34.5389	0.7797	4.2105	6.5653	36.7000
2	33.0000	34.9282	0.6600	4.6972	6.7076	36.6700
2	33.5000	35.9144	0.5631	5.1704	6.7756	36.6350
2	34.0000	37.5040	0.4851	5.5724	6.7625	36.6000
2	34.5000	39.6845	0.4225	5.8641	6.6728	36.5950
2	35.0000	42.3927	0.3725	6.0348	6.5204	36.5825
2	35.5000	45.5180	0.3326	6.1020	6.3250	36.5750
2	36.0000	48.9471	0.3009	6.0991	6.1065	36.5800
2	36.5000	52.6131	0.2758	6.0620	5.8819	36.5900
2	37.0000	56.5172	0.2559	6.0209	5.6632	36.6000
2	37.5000	60.7286	0.2402	5.9986	5.4586	36.5750
2	38.0000	65.3852	0.2279	6.0137	5.2733	36.5500
2	38.5000	70.7169	0.2182	6.0853	5.1115	36.5250
2	39.0000	77.1167	0.2106	6.2410	4.9787	36.5400
2	39.5000	85.3330	0.2046	6.5328	4.8839	36.5325
2	40.0000	97.0383	0.2000	7.0817	4.8476	36.5250
2	40.5000	116.9948	0.1964	8.2516	4.9252	36.5100
2	41.0000	166.2063	0.1935	11.8483	5.3423	36.4950
2	41.5000	440.0284	0.1913	79.1097	9.8253	36.4875
2	42.0000	192.8976	0.1975	135.1576	11.9789	36.4800
2	42.5000	68.0872	0.4010	109.4129	9.5799	36.4850
2	43.0000	64.2980	1.0843	76.5847	7.3975	36.4900
2	43.5000	80.1519	2.2968	45.8371	5.7747	36.5425
2	44.0000	98.2409	3.9813	22.7590	4.8424	36.5950
2	44.5000	114.5520	6.0143	10.1449	4.4017	36.6100

Cycle	Time	E_2 (pmol/L)	P_4 (ng/mL)	LH (UI/L)	FSH (UI/L)	BBT (° C)
2	45.0000	131.7198	8.2183	5.0297	4.0685	36.6250
2	45.5000	149.7023	10.3868	3.2662	3.8001	36.6800
2	46.0000	166.2268	12.3219	2.6847	3.6298	36.7350
2	46.5000	179.4384	13.8695	2.4871	3.5390	36.7525
2	47.0000	188.2268	14.9379	2.4155	3.4935	36.7700
2	47.5000	192.1663	15.4989	2.3899	3.4686	36.7875
2	48.0000	191.3949	15.5767	2.3855	3.4524	36.8050
2	48.5000	186.4577	15.2324	2.3934	3.4406	36.8075
2	49.0000	178.1421	14.5476	2.4096	3.4330	36.8100
2	49.5000	167.3334	13.6110	2.4317	3.4316	36.8475
2	50.0000	154.9039	12.5082	2.4579	3.4396	36.8850
2	50.5000	141.6394	11.3153	2.4867	3.4613	36.8975
2	51.0000	128.1987	10.0955	2.5171	3.5015	36.9100
2	51.5000	115.0981	8.8980	2.5484	3.5663	36.8950
2	52.0000	102.7155	7.7588	2.5798	3.6626	36.8800
2	52.5000	91.3042	6.7018	2.6109	3.7971	36.9025
2	53.0000	81.0130	5.7410	2.6415	3.9747	36.9250
2	53.5000	71.9073	4.8827	2.6715	4.1953	36.9275
2	54.0000	63.9896	4.1272	2.7014	4.4491	36.9300
2	54.5000	57.2163	3.4706	2.7318	4.7154	36.9650
3	55.0000	42.9858	2.2208	2.7233	4.9335	37.0000
3	55.5000	39.4870	1.8506	2.7893	5.1404	36.9600
3	56.0000	36.7310	1.5413	2.9014	5.3569	36.9200
3	56.5000	34.6572	1.2846	3.0888	5.5930	36.8875
3	57.0000	33.2238	1.0728	3.3787	5.8441	36.8550
3	57.5000	32.4025	0.8990	3.7821	6.0909	36.7925
3	58.0000	32.1731	0.7572	4.2807	6.3054	36.7300
3	58.5000	32.5254	0.6420	4.8242	6.4603	36.7000
3	59.0000	33.4665	0.5488	5.3427	6.5359	36.6700
3	59.5000	35.0110	0.4737	5.7671	6.5247	36.6350
3	60.0000	37.1386	0.4135	6.0517	6.4314	36.6000
3	60.5000	39.7511	0.3653	6.1875	6.2717	36.5950
3	61.0000	42.6877	0.3269	6.2000	6.0671	36.5900
3	61.5000	45.7931	0.2964	6.1325	5.8396	36.5825
3	62.0000	48.9751	0.2722	6.0273	5.6066	36.5750
3	62.5000	52.2152	0.2531	5.9161	5.3798	36.5775
3	63.0000	55.5495	0.2381	5.8195	5.1660	36.5800
3	63.5000	59.0488	0.2262	5.7498	4.9687	36.5900
3	64.0000	62.8113	0.2169	5.7154	4.7897	36.6000
3	64.5000	66.9708	0.2096	5.7242	4.6301	36.5750
3	65.0000	71.7229	0.2038	5.7873	4.4911	36.5500
3	65.5000	77.3841	0.1994	5.9238	4.3755	36.5375
3	66.0000	84.5300	0.1959	6.1711	4.2890	36.5250
3	66.5000	94.3675	0.1932	6.6136	4.2441	36.5325
3	67.0000	109.9871	0.1910	7.4798	4.2734	36.5400
3	67.5000	142.3631	0.1894	9.6456	4.4836	36.5325
3	68.0000	300.1625	0.1881	29.3071	6.1916	36.5250
3	68.5000	277.1566	0.1877	120.3877	10.3378	36.5100
3	69.0000	79.9234	0.2614	106.4692	8.7843	36.4950
3	69.5000	58.2605	0.6797	75.7662	6.7896	36.4875

Cycle	Time	E_2 (pmol/L)	P_4 (ng/mL)	LH (UI/L)	FSH (UI/L)	BBT (° C)
3	70.0000	70.5988	1.6087	47.3119	5.2644	36.4800
3	70.5000	87.7347	3.0647	25.2057	4.2576	36.4850
3	71.0000	104.2821	4.9579	11.7204	3.7798	36.4900
3	71.5000	121.3135	7.1206	5.6323	3.5062	36.5425
3	72.0000	139.6417	9.3416	3.4036	3.2817	36.5950
3	72.5000	157.2535	11.4059	2.6514	3.1266	36.6100
3	73.0000	172.1054	13.1347	2.3953	3.0395	36.6250
3	73.5000	182.8267	14.4093	2.3020	2.9955	36.6800
3	74.0000	188.7496	15.1779	2.2664	2.9725	36.7350
3	74.5000	189.8220	15.4469	2.2554	2.9580	36.7525
3	75.0000	186.4620	15.2659	2.2579	2.9472	36.7700
3	75.5000	179.3906	14.7112	2.2694	2.9395	36.7875
3	76.0000	169.4766	13.8705	2.2872	2.9360	36.8050
3	76.5000	157.6109	12.8318	2.3094	2.9393	36.8075
3	77.0000	144.6198	11.6753	2.3346	2.9528	36.8100
3	77.5000	131.2130	10.4694	2.3616	2.9804	36.8475
3	78.0000	117.9602	9.2684	2.3897	3.0270	36.8850
3	78.5000	105.2892	8.1131	2.4179	3.0985	36.8975
3	79.0000	93.4970	7.0316	2.4459	3.2012	36.9100
3	79.5000	82.7684	6.0414	2.4733	3.3407	36.8950
3	80.0000	73.1973	5.1514	2.5000	3.5200	36.8800
3	80.5000	64.8078	4.3638	2.5262	3.7355	36.9025
3	81.0000	57.5723	3.6763	2.5523	3.9741	36.9250
3	81.5000	51.4279	3.0831	2.5798	4.2159	36.9275
3	82.0000	46.2892	2.5765	2.6120	4.4445	36.9300
3	82.5000	42.0613	2.1477	2.6565	4.6582	36.9650
4	83.0000	46.2274	2.4878	2.7196	4.7169	37.0000
4	83.5000	42.2013	2.0727	2.7702	4.9302	36.9600
4	84.0000	38.9806	1.7248	2.8516	5.1410	36.9200
4	84.5000	36.4904	1.4354	2.9886	5.3643	36.8875
4	85.0000	34.6763	1.1962	3.2100	5.6049	36.8550
4	85.5000	33.5020	0.9995	3.5372	5.8525	36.7925
4	86.0000	32.9418	0.8387	3.9702	6.0846	36.7300
4	86.5000	32.9762	0.7078	4.4781	6.2736	36.7000
4	87.0000	33.5970	0.6017	5.0033	6.3960	36.6700
4	87.5000	34.8106	0.5162	5.4774	6.4378	36.6350
4	88.0000	36.6189	0.4474	5.8427	6.3970	36.6000
4	88.5000	38.9760	0.3923	6.0697	6.2830	36.5950
4	89.0000	41.7663	0.3484	6.1639	6.1134	36.5900
4	89.5000	44.8400	0.3134	6.1574	5.9092	36.5825
4	90.0000	48.0759	0.2856	6.0915	5.6899	36.5750
4	90.5000	51.4194	0.2637	6.0030	5.4699	36.5775
4	91.0000	54.8813	0.2464	5.9181	5.2587	36.5900
4	91.5000	58.5218	0.2327	5.8543	5.0617	36.6000
4	92.0000	62.4394	0.2220	5.8235	4.8821	36.5750
4	92.5000	66.7767	0.2136	5.8363	4.7217	36.5500
4	93.0000	71.7477	0.2070	5.9060	4.5826	36.5375
4	93.5000	77.7047	0.2018	6.0547	4.4683	36.5325
4	94.0000	85.3014	0.1978	6.3262	4.3856	36.5400
4	94.5000	95.9497	0.1946	6.8209	4.3498	36.5325

Cycle	Time	E_2 (pmol/L)	P_4 (ng/mL)	LH (UI/L)	FSH (UI/L)	BBT (° C)
4	95.0000	113.4443	0.1922	7.8243	4.4014	36.5250
4	95.5000	152.5575	0.1903	10.5563	4.6856	36.5100
4	96.0000	384.9935	0.1888	49.9023	7.5362	36.4950
4	96.5000	227.2459	0.1901	127.2673	10.7100	36.4875
4	97.0000	71.0548	0.3107	105.4590	8.7290	36.4800
4	97.5000	60.2580	0.8331	73.9419	6.7446	36.4850
4	98.0000	74.2086	1.8790	45.1442	5.2522	36.4900
4	98.5000	91.6249	3.4340	23.2932	4.3346	36.5425
4	99.0000	108.0133	5.3904	10.6514	3.9305	36.5950
4	99.5000	125.1649	7.5721	5.2293	3.6696	36.6100
4	100.0000	143.3744	9.7676	3.2978	3.4499	36.6250
4	100.5000	160.4836	11.7688	2.6513	3.3031	36.6800
4	101.0000	174.5492	13.4084	2.4304	3.2237	36.7350
4	101.5000	184.3343	14.5815	2.3496	3.1849	36.7525
4	102.0000	189.2958	15.2481	2.3193	3.1651	36.7700
4	102.5000	189.4800	15.4238	2.3115	3.1529	36.7875
4	103.0000	185.3710	15.1644	2.3165	3.1442	36.8050
4	103.5000	177.7243	14.5488	2.3301	3.1388	36.8075
4	104.0000	167.4167	13.6650	2.3497	3.1384	36.8100
4	104.5000	155.3285	12.5999	2.3735	3.1461	36.8475
4	105.0000	142.2639	11.4313	2.4001	3.1654	36.8850
4	105.5000	128.9048	10.2247	2.4285	3.2010	36.8975
4	106.0000	115.7924	9.0317	2.4578	3.2583	36.9100
4	106.5000	103.3275	7.8906	2.4872	3.3437	36.8950
4	107.0000	91.7840	6.8271	2.5164	3.4638	36.8800
4	107.5000	81.3277	5.8570	2.5450	3.6240	36.9025
4	108.0000	72.0378	4.9878	2.5729	3.8256	36.9250
4	108.5000	63.9271	4.2207	2.6005	4.0621	36.9275
4	109.0000	56.9603	3.5525	2.6283	4.3166	36.9300
4	109.5000	51.0687	2.9772	2.6582	4.5670	36.9650

Fig. 6.2.: Test data set applied to estimate parameters in the least squares sense. The test data set consists of four cycles of different length, namely 29, 26, 28 and 27 days. Measurements are available twice per day, since the hormonal components E_2, P_4, LH and FSH data was taken from *Pfizer* data available at *Konrad-Zuse Zentrum für Informationstechnik Berlin* that has been previously plugged into the GYN CYCLE model. Since no simultaneous assessment of E_2 and BBT concentrations was accessible, standard BBT curves were taken and matched best possible to the other components. Note, that by this approach, the test data set has to be considered purely artificial why it is not considered apropos to evaluate the model. As far as possible the dynamics and characteristics of the proposed model have been analysed, but real data would be necessary to finally appraise the quality of the model. *Clue* released a *beta* version of their *App* in early 2013 on *www.helloclue.com*, tracking volunatry user's menstrual cycle. Once the E_2 saliva device is released, real data for model evaluation will be available.

B. Erklärung zur Masterarbeit

Hiermit erkläre ich, dass ich die vorliegende Masterarbeitarbeit selbstständig verfasst habe und keine anderen als die angegebenen Quellen und Hilfsmittel benutzt und die aus fremden Quellen direkt oder indirekt übernommenen Gedanken als solche kenntlich gemacht habe.

Die Arbeit habe ich bisher keinem anderen Prüfungsamt in gleicher oder vergleichbarer Form vorgelegt. Sie wurde bisher nicht veröffentlicht.

Berlin, den 9. April 2013 .....

Unterschrift